Finite Scattering Amplitudes In Field Theory

A thesis presented for the degree of

Doctor of Philosophy

by

Gareth Brown

Institute for Particle Physics Phenomenology

University of Durham

February 2007

Durham
University

Abstract

In this thesis we explore the infrared problem perturbatively in massless field theory. We review the current conventional methods and theorems that are applied in the calculation of QCD jet observables and then discuss the formulation of an alternative approach called the Asymptotic Interaction Picture (AIP). The AIP is based on a unitary transformation such that long-ranged interactions are present in the asymptotic Lagrangian and thus the states associated with this picture are no longer free Fock states but are asymptotic states containing soft and collinear interactions.

Under the guidance of the AIP we are led to modifying conventional perturbation theory, cutting up amplitudes in a manner that allows for the construction of infrared finite amplitudes that are in correspondence with the asymptotic states of the AIP. We apply this formalism to several NLO corrections to QCD observables and construct dressed states who's amplitudes are finite in all regions of phase-space. Using these amplitudes we compute several observables and show agreement with the conventional calculations in infrared safe regions. Higher-order calculations are then investigated in ϕ^3 theory and the infrared pole structure is shown to behave as expected such that NNLO corrections to dressed states are obtained. Finally we present part of the NNLO correction to the dressed two-parton amplitude in QCD and show that, with several provisos, this approach may potentially be applied to the precision calculations of observables at the International Linear Collider (ILC). We therefore give a possible alternative to current subtraction methods at NNLO when no initial state radiation is present.

Acknowledgements

I have to start by thanking my supervisor Adrian. Your approachability, optimism and guidance have been instrumental in the completion of this thesis - so thank you! I should also thank Mark and Darren who helped me settle into the research group and were around to answer questions and engage me in some insightful discussions. Another important ingredient to my time at the IPPP has been the office merriment, for which I have to thank Arne, Richard, Steve, Simon and too many more to mention. I should also give a special acknowledgement to Richard who has always had the patience to listen to my incessant ramblings. Well done on that account.

To the rest of the IPPP I wish continued success in their research. Congratulations for cultivating a fantastic research environment that I've had the pleasure of the last three years to be a part of.

Finally I have to mention the unparalleled support from my family and most importantly my parents. Your careful nurturing and encouragement can never be overstated. Thank you for trying to answer why, giving me a paintbrush and showing me the fun in maths.

Declaration

I declare that no material presented in this thesis has previously been submitted for a degree at this or any other university.

The research described in this thesis has been carried out in collaboration with Dr. Adrian Signer, Dr. Darren Forde and Dr. Mark Morley-Fletcher.

Contents

List of Figures

List of Tables

Chapter 1

Introduction

1.1 The S-matrix and physical observables

The goal of particle physics phenomenology is to make quantitative predictions for the vast data collider experiments acquire during their lifespans. Derived from a theory's Lagrangian, the theoretical construct that is central to making such predictions is the S-matrix. This object is used to compute the overlap of an asymptotic state defined at early times with that of an asymptotic state at late times and gives the so-called *amplitude*, $\mathcal{A}$, of the process. Obtaining a prediction amounts to computing $|\mathcal{A}|^2$ and integrating over the phase space of the final state particles, weighted by some function that defines the observable we are interested in.

Asymptotic states should therefore represent physical quantities or particles, with well-defined momentum, charge, spin etc, that an experimentalist can measure at a collider with some known level of precision[1]. Unfortunately the modern quantum field theory of the Standard Model, from which the S-matrix is built, does not

---

[1]More precisely, particles are an irreducible representation of the Poincaré group with nonvanishing mass [1].

permit a direct mapping between the degrees of freedom that are embodied in the Lagrangian to those that are measured by an experimentalist. Mismatching physical states with "theoretical" ones leads to the so-called infrared catastrophe [2] where the S-matrix contains infrared (IR) divergences, terms singular due to the long-ranged exchange of massless particles.

Such a mismatching is evident for all the physical gauge theories of the Standard Model and is apparent at a classical level where Electromagnetism's description of the Coulombic potential is inextricably linked to the charged source that produces it. For the case of Quantum Electrodynamics (QED), the solution is to realise that there is no such thing as "free" charged particle and that an electron must be clothed in a field of photons. Despite this additional complication it is still possible to define what we really mean by a particle and indeed we may, in QED at least, assign such dressed states a physical interpretation [3]. However, in the case of Quantum Chromodynamics (QCD), the problem is complicated significantly by the non-perturbative process of confinement that describes the formation of bound states of constituent quarks that are themselves formed from the quarks and gluons of the Lagrangian. Throughout this thesis, our aim will be to attempt to tackle IR divergences entirely within the context of perturbation theory. The belief is that this can be done consistently for both perturbative non-abelian and abelian theories despite the complication of confinement in QCD.

In order to construct the S-matrix a formal relation between the full states $|\Psi\rangle$ and the asymptotic states $|\Xi\rangle$ must be made

$$
\begin{aligned}
|\Psi_{out}\rangle &= \lim_{t\to\infty} e^{iHt} e^{-iH_A t} |\Xi_{out}\rangle \\
&\equiv \Omega_- |\Xi_{out}\rangle,
\end{aligned}
\tag{1.1}
$$

with an equivalent definition for *in* states at $t = -\infty$. Eq. (1.1) therefore gives us

the Möller operators, $\Omega_{(+/-)}$, that relate the in/out states of the full theory, defined by the Hamiltonian H, to the in/out states of the asymptotic theory, defined by H_A. Known as the adiabatic assumption, the standard approach in field theory is to identify asymptotic states with free-states; H_A is taken to be equal to the free Hamiltonian H_0 so that all interactions are assumed to die out at infinity. Taking this approach free field operators are constructed by imposing canonical equal-time commutation relations and solving the Schrödinger equations of the free Lagrangian [4,5]. This solution to the problem defines the state space to be a Fock space of non-interacting particles and gives the so-called Feynman-Dyson S-matrix, S_{FD}. Transitions between states, or matrix elements of S_{FD}, can then be computed via the Lehmann, Symanzik and Zimmerman (LSZ) formalism that relates scattering to the correlation functions of the full theory.

For massive particles the LSZ reduction formalism can be legitimately applied because the S-matrix is just a set of on-shell momentum-space Green's functions carrying simple poles for each external particle. Massless particles however introduce IR divergences as they alter the simple pole structure of the two-point functions of the theory [6,7]. Essentially there is always the possibility that a state can emit a massless particle of some physically unmeasurable energy; the *spectral density* function of the Källén-Lehmann representation now defines a branch cut running across the entire positive real axis. This type of divergence is called *soft* and, up to the limit of detector resolution, particle number is no longer a good quantum number since there is an indeterminable number of soft particles present in each asymptotic state[2]. *Collinear* divergences also exist for QCD and massless QED, they arise from massless particles degenerate in all quantum numbers and indeed four-momenta. Physically this translates to the fact that it is impossible to distinguish two gluons travelling collinearly with the same total four-momentum as

---

[2]The term *infraparticle* was coined by Schroer [8] to describe the process whereby a particle interacting with a massless field loses its discrete spectrum.

$$|\Xi\rangle \equiv \quad \xrightarrow{\hspace{2cm}} \quad + \quad + \quad + \ldots$$

Figure 1.1: How, in terms of free-states, an asymptotic quark state of QCD might look.

just a single gluon. This statement is of course meaningless in the sense that confinement stops you from ever measuring a gluon. However, QED's fermions and photons are not hidden by confinement and suffer from similar collinear configurations, thus combining this with the perturbative view that the gluon is massless and long-ranged, the IR problem of collinear quarks and gluons of QCD persists. Alternatively you could argue that the final state hadron formed after hadronisation would be the same for the two gluonic states discussed.

A slightly more abstract interpretation of the problem is to realise that the operators $\Omega_{(\pm)}$ must be isometric, requiring a one-to-one mapping of the full states to the asymptotic states of the theory. When we choose the asymptotic basis to be that of the non-interacting theory we end up with degenerate states, such that a given free-particle state will be part of a degenerate sub-space containing states with additional soft and collinear particles. Hence the Möller operators relating the free states to the full ones are not isometric and therefore they are ill-defined.

To summarise, theories with massless particles have a more intricate state-space than that of their massive counterparts. A naive attempt at solving massless gauge theories using a standard Fock space representation will lead to an ill-defined, divergent S-matrix. The true asymptotic states of such theories effectively have all soft and collinear degeneracies absorbed into each state, see Figure 1.1. Thus if we want to perform perturbative calculations free of divergences[3], it is necessary to obtain a better understanding of the true asymptotic dynamics.

---

[3]Of course UV divergences still require regularisation, fortunately UV renormalisation is well understood [9]. In general discussion we assume that our theory has been rendered UV finite.

1.2 The cross-section method

The modern prescription for coping with infrared divergences is to first regulate the S-matrix by employing dimensional regularisation. The act of switching to an unphysical number of dimensions lifts the degeneracy of the free-states and allows perturbative calculations to be performed analytically. The four-dimensional limit can then be regained if we sum incoherent, but physically indistinguishable cross-sections; this is known as the *cross-section* method. For massless gauge theories the method actually relies on two concepts. The first, introduced by Bloch and Nordsieck (BN) [2], says that all soft divergences may be cancelled by summing all cross-sections with indistinguishable final states. Application of this concept renders massive QED infrared finite up to a logarithmic dependence on the detector resolution associated with the observable.

However, massless fermions and self-interacting gluons introduce collinear divergences that significantly complicate the required cancellation of IR poles and also necessitate the consideration of initial-state radiation. The natural extension of the BN theorem is given by the rather general Kinoshita-Lee-Naunberg theorem (KLN) [7, 10] which states that the transition rates of quantum theories will be infrared finite provided all degenerate final and initial states are summed over[4]. In practise however initial state collinear divergences are factorised into the universal parton distribution functions (PDFs) and so practically speaking it is sufficient to only sum over final states for QCD since any remaining IR divergences are defined to cancel when combined with the necessary PDF.

Thus soft and collinear divergences, revealed as poles in the standard dimensional regularisation parameter of ϵ [12], cancel when all the free-state cross-sections that would make up the true asymptotic state cross-section are summed together.

---

[4]It should further be remarked that fundamental questions still remain over the mechanism of IR cancellation with regard to initial-state divergences [11].

Using this approach it is possible to compute any observable that is defined to be *infrared safe* (see Section 2.3).

The downfall of this approach is both aesthetic and practical in nature. Aesthetically speaking we do not have an S-matrix - QCD loop amplitudes in four-dimensions simply do not exist. Practically parts of the calculation have to be performed analytically in order to control the IR divergences. At NLO this is not too much of a problem as general subtraction algorithms do exist [13–15]. For example the general subtraction procedure at NLO is of the form

$$
\begin{aligned}
\sigma_{NLO} &= \int_{m+1} d\sigma^R + \int_m d\sigma^V \\
&= \int_{m+1} (d\sigma^R - d\sigma^A) + \int_{m+1} d\sigma^A + \int_m d\sigma^V \\
&= \int_{m+1} (d\sigma^R - d\sigma^A) + \int_m \left(d\sigma^V + \int_1 d\sigma^A \right),
\end{aligned} \tag{1.2}
$$

where the IR counter-term σ^A is sufficiently simple that it can be analytically evaluated whilst still having identical IR divergent structure to that of the real cross-section σ^R. Observing the last line of Eq. (1.2) the first integral over $m + 1$ partons is explicitly finite and may be performed numerically, the second piece over m partons involves a cancellation of poles in ϵ before numerical integration of the phase-space can be implemented[5].

As we anticipate the need for precision physics at future colliders it is clear that the bottle-neck associated with performing horrendously complicated loop and phase-space integrals at NNLO will become severe. Despite the looming need, development of a general subtraction algorithm [18, 19] at NNLO is slow and whilst several analytic and semi-numerical methods for evaluating loop and phase-space integrals do exist [20–26], they all suffer from placing serious demands on com-

---

[5]Soper [16, 17] has developed a procedure applicable to numerical integration of the virtual piece.

putational resources. Since numerical methods have to be employed for exclusive processes it appears that the analytic route offers little benefit at higher orders or indeed leading radiative corrections to multi-parton final states. Thus a completely numerical approach should be investigated, since it would ultimately obviate the need for large scale analytic calculations. The main obstacle for doing this is the presence of IR divergences in amplitudes and phase-space integrals.

To overcome the shortcomings of the cross-section method we should therefore look for a new way to describe asymptotic dynamics in massless gauge theories. Ultimately we want to be able to write down relatively simple amplitudes well defined in four-dimensions and finite in all regions of phase-space. Such an achievement would in principle allow for an efficient automation of high order perturbative corrections.

1.3   An infrared finite theory of Coulomb scattering

Before re-examining the asymptotic dynamics of massless gauge theories it is instructive to look at a simpler theory. Consider the non-relativistic scattering of an electron off a Coulomb potential [27, 28], the Hamiltonian for such a system can be written as

$$H = \frac{\vec{p}^2}{2m} + \frac{g}{|\vec{r}|} = H_0 + V. \tag{1.3}$$

If we consider the interaction representation, then the asymptotic behaviour of $V(t)$ is given by

$$\lim_{t \to \pm\infty} V(t) = \frac{mg}{|\vec{p}||t|} + O\left(|t|^{-2}\right), \tag{1.4}$$

where we have made use of $\vec{r}(t) = \frac{\vec{p}t}{m} + \vec{r}$ and $\vec{p}(t) = \vec{p}$ at asymptotic times. This potential, with respect to time, is not integrable at infinity and so the dynamics

7

of the system at infinity cannot be described solely by H_0, indeed

$$H_A = H_0 + \frac{mg}{|\vec{p}||t|}. \tag{1.5}$$

Using this definition for the asymptotic Hamiltonian, the Schrödinger equation can be solved for the wave-packet Ψ_S to give

$$\begin{aligned} \Psi_S(t) &= U_A(t, t_0)\, \Psi_S(t_0) \\ &= e^{-iH_0(t-t_0)} \exp\left\{ -i\frac{mg}{|\vec{p}|} \operatorname{sign} t\, \ln \frac{|t|}{t_0} \right\} \Psi_S(t_0), \end{aligned} \tag{1.6}$$

with t_0 being some constant of integration. Explicitly we see that the evolution of the asymptotic theory is supplemented by a Coulomb phase factor missed by the free state solution. It can then be shown [28] that Eq. (1.1) holds as a strong operator limit for this choice of asymptotic Hamiltonian, i.e that the Möller operator is truly isometric,

$$\Omega_{(\pm)} = \lim_{t \to \mp\infty} e^{iHt} U_A(t), \tag{1.7}$$

and that the S-matrix,

$$S = \Omega_-^\dagger \Omega_+, \tag{1.8}$$

does exist.

1.4 Infrared finite approaches to QCD

Following the previous section, a possible approach to constructing an infrared finite S-matrix for QCD is apparent. The first step is to identify what interactions of the Lagrangian remain at asymptotic times and then to solve the corresponding Schrödinger equation. For massive QED this was achieved by P.P. Kulish and L.D. Faddeev (KF) in 1970 [27]. They obtained the asymptotic interaction by

simply inserting the free-field expansions of the fermion and photon field operators into the interaction part of the QED Lagrangian and then observing which terms could be neglected at large times. It has since been shown [29] that this simple prescription actually fails when applied to scalar ϕ^4 theory. The apparent mistake is the reliance on strong operator convergence, strictly analysis of the dynamics should be performed at the weaker level of matrix elements, however this is not a problem for massive QED.

KF showed that the terms non-vanishing at infinity gave rise to an asymptotic current operator that could be viewed as a relativistic generalisation of Eq. (1.4). Solving the Schrödinger equation for this operator led KF to a finite theory at the expense of changing the state space to a Fock space of charged particles combined with a non-separable von Neumann space of photons. This so-called *coherent* state basis [30, 31] essentially gave states with multiple soft photon emission summed to all orders in the coupling. The S-matrix was also found to be modified by "phase factors" with respect to S_{FD}, but these factors where shown to drop out of calculations. Many authors have attempted to generalise this approach to the more intricate problem of QCD (a non-exhaustive list being [6, 32–43]), however the construction of coherent states becomes very complicated once collinear singularities are included and all-order resummations appear intractable. This is no surprise, after all a solution would correspond to the extremely hard task of obtaining the full hadronic spectrum of the theory!

A different approach to this problem can also be found in the works of [3, 29, 44, 45] where individual charged fields are constructed via a dressing that maintains gauge invariance of the field whilst violating Lorentz invariance and locality. This ultimately leads to a description of a charged particle at the cost of a less direct relationship to the fields producing it. Having regained a simple pole structure for the propagators of the theory, finite perturbative calculations can be performed

by applying the LSZ formalism.

Within the context of this thesis we propose to sidestep the problem of confinement and all order resummations by adopting an entirely perturbative viewpoint and placing the emphasis on a practical method for computing infrared finite amplitudes. Since today's colliders work in the high energy regime we take this limit and set all fermion masses to zero, embracing the full infrared divergent behaviour of gauge theory. We do not intend to treat collinear and soft divergences differently or indeed distinguish them in any way as such, therefore for the remainder of the thesis we will consistently consider all infrared divergences as soft with the understanding that we include collinear configurations.

Using this philosophy a first attempt at a practical method is described in [46] where it is successfully applied to the calculation of $e^+e^- \to$ hadrons at NLO. Here the free states are dressed up to a given order in time dependent perturbation theory with infrared finite matrix elements computed using the standard S_{FD} [47]. Unfortunately the time-ordered Hamiltonian approach taken in [46] results in a proliferation of non-covariant diagrams with differing energy delta-functions. Besides significantly increasing the complexity of the calculation, the differing energy arguments made the translation to the cross-section ambiguous due to the need to "square" the amplitude. In an attempt to circumvent this problem an entirely covariant approach has since been developed [48, 49] using the asymptotic interaction picture [6, 42].

1.5   Overview of thesis

For the rest of this thesis we discuss the theory and practical implementation of the asymptotic interaction picture for calculations of jet observables using infrared finite amplitudes. Chapter 2 briefly reviews the central concepts of perturbative

QCD, including renormalisation, infrared safety and factorisation. This is then followed by a technical chapter discussing how perturbative calculations are actually performed, in particular we describe the modern methods of Mellin-Barnes transformations and sector-decomposition.

In Chapter 4 we introduce the general theory underlying the Asymptotic Interaction Picture (AIP) [49], highlighting its differences with respect to the standard interaction picture. We discuss how the conventional Feynman rules are modified and how infrared finite amplitudes may be constructed. The precise separation of the Lagrangian of QCD into hard and soft sectors is described and the merits of both non-analytic and analytic separation functions are detailed. In order to obtain an improved understanding of the formalism we advocate the use of a separation function amenable to standard perturbative methods and in the following chapters we test the theory using this function.

Chapter 5 describes several jet calculations exemplifying the practicalities and utility of the asymptotic interaction picture. A new $e^+e^- \to$ hadrons at NLO calculation is presented and is followed by a NLO correction to a three-jet observable, the N_F part of the C-parameter. Problems with the gauge structure of QCD will then lead us to Chapter 6, where topologies at $O(\alpha^3)$ are investigated within the context of ϕ^3 theory. Finally the NNLO corrections, proportional to N_F, for e^+e^- to $q\bar{q}$ are discussed in Chapter 7.

Chapter 8 concludes the thesis and discusses the need for further development of the theory of the asymptotic interaction picture coupled with the development of a completely numerical approach that dispenses with costly analytic calculations.

Chapter 2

Perturbative Quantum Chromodynamics

2.1 The Lagrangian and Feynman rules of QCD

Before discussing how the asymptotic interaction picture should modify conventional perturbation theory, we start by briefly summarising the theory of perturbative QCD. We describe the Feynman rules and discuss the fundamental theorems of renormalisation, infra-red safety and factorisation critical to making quantitative predictions [5, 9, 50–52].

The Lagrangian of QCD describes the interactions of the bare quark fields, q_i^a, of flavour i, transforming in the fundamental representation of $SU(3)$ colour space, with bare gluon fields, A_μ^A transforming in the adjoint representation. It may be written as

$$\mathcal{L}_{\text{QCD}} = -\frac{1}{4} F_{\mu\nu}^A F_A^{\mu\nu} + \sum_i^n \bar{q}_i^a (i\slashed{D} - m_i)_{ab} q_i^b - \frac{1}{2\xi} \left(\partial^\mu A_\mu^A \right)^2 + \mathcal{L}_{\text{ghost}}, \qquad (2.1)$$

where $\not{D} = \gamma_\mu D^\mu$, with γ_μ defined by the Clifford algebra

$$\{\gamma^\mu, \gamma^\nu\} \equiv \gamma^\mu \gamma^\nu + \gamma^\mu \gamma^\nu = 2\, g^{\mu\nu}. \tag{2.2}$$

D^μ denotes a covariant derivative in colour space (we denote generators of the algebra as t_{ab}^α) and $F_{\mu\nu}^A$ is the field strength tensor defined by

$$
\begin{aligned}
D_{ab}^\mu &= \partial^\mu\, \delta_{ab} - i\, g\, A_A^\mu\, t_{ab}^A \\
-i\, g\, t^A\, F_{\mu\nu}^A &= [\, D_\mu, D_\nu\,].
\end{aligned}
\tag{2.3}
$$

The coupling of QCD is denoted by g and $\mathcal{L}_{\text{ghost}}$ introduces ghost fields necessary to maintain a covariant description with a physical state space.

The Feynman rules describe the perturbative expansion of an n-particle Green's function of the theory. They are obtained from the Green's function by first transforming into the interaction picture and expanding in the coupling g. Wick's theorem is then applied to reduce the expansion to products of two-point functions (or propagators) with vertices created at the space-time points of overlapping propagators [4]. In momentum space the Feynman rules for QCD are given as

$$
\begin{aligned}
&= iS^0(p) &&= \frac{i\,(\not{p} + m\,)}{p^2 - m^2 + i0^+} \\
{}_a^\mu \,\text{〜〜〜〜}\, {}_b^\nu \;\; &= -i\delta^{ab} D_{\mu\nu}^0(p) &&= \frac{-i\,\delta^{ab}}{p^2 + i0^+}\left(g^{\mu\nu} - (1-\xi)\frac{p^\mu p^\nu}{p^2}\right) \\
{}_a\, \text{- - ▸ - -}\, {}_b \;\; &= i\delta^{ab} G^0(p) &&= \frac{i\,\delta^{ab}}{p^2 + i0^+},
\end{aligned}
$$

for the propagators, and the vertices, where momentum must be conserved, are given by

$$= i g \gamma^\mu t^a$$

$$= g f^{abc} [g^{\mu\nu}(k - p)^\rho + g^{\nu\rho}(p - q)^\mu + g^{\rho\mu}(q - k)^\nu]$$

$$= -g f^{abc} p^\mu$$

$$= -i g^2 [f^{abe} f^{cde}(g^{\mu\rho} g^{\nu\sigma} - g^{\mu\sigma} g^{\nu\rho})$$
$$+ f^{ace} f^{bde}(g^{\mu\nu} g^{\rho\sigma} - g^{\mu\sigma} g^{\nu\rho})$$
$$+ f^{ade} f^{bce}(g^{\mu\nu} g^{\rho\sigma} - g^{\mu\rho} g^{\nu\sigma})].$$

Additional rules are the integration over undetermined loop momenta, symmetry factors, a factor of -1 for each fermion loop and representations for external states, see for example [4, 50].

We note that the gluon propagator depends on the gauge-fixing parameter ξ, this parameter is obtained from the gauge-fixing term, $-\frac{1}{2\xi} \left(\partial^\mu A^A_\mu \right)^2$, of the Lagrangian of QCD. Its presence is necessary to ensure that the operator corresponding to the gluon field's equation of motion may be inverted. ξ may be chosen arbitrarily, but consistently, for a perturbative calculation of all diagrams contributing to a gauge-invariant subset of the amplitude. This also implies that, for QCD and other gauge theories, there is no point in speaking about the "value" of an individual graph, as this value depends in general on our choice of the gauge parameter. Only in the sum of graphs over a gauge-invariant set does this dependency on the gauge parameter cancel. The most economical choice is $\xi = 1$, which is called Feynman

gauge.

2.2   Renormalisation

The gauge theories comprising the Standard Model (SM) all suffer from ultra-violet divergences; this is nothing but a reflection of our ignorance of a more fundamental theory. We can parameterise our ignorance via a redefinition of the bare fundamental fields and couplings of the corresponding Lagrangian. With this re-parameterisation implemented the Feynman rules gain additional counter-terms (propagators and vertices) that are defined through physical renormalisation conditions [50]. The counter-terms then remove all ultraviolet divergences leaving only the infrared divergences that are the subject of this thesis.

In order to keep the coupling of the perturbative expansion dimensionless the renormalisation scale parameter μ must also be introduced. This necessarily breaks the scale invariance of massless QCD and thus the theory will exhibit qualitatively different behaviours at varying energies. Physical observables and bare parameters of the Lagrangian cannot depend on the actual value chosen for μ, therefore *renormalisation group equations* may be derived that describe how the perturbative expansion must change in order to maintain the physicality of predictions. We define the renormalised coupling constant, α_s, of QCD in terms of the bare coupling, g, to be

$$\alpha_s = \frac{g^2}{4\pi} \, Z_g^{-2} \, (\mu^2)^{-\epsilon},$$

(2.4)

where Z_g is the multiplicative renomalisation factor for the coupling [50]. Insisting that g cannot depend on μ leads us to an integral equation that determines how the coupling constant changes with the energy scale μ, we find that

$$\int_{\alpha_s(\mu_0^2)}^{\alpha_s(\mu^2)} \frac{d\alpha}{\beta(\alpha)} = \ln\left(\frac{\mu^2}{\mu_0^2}\right),$$

(2.5)

which is obtained from the beta-function as $\beta(\alpha) \equiv \mu \frac{\partial}{\partial \mu} \alpha$. If we assume that the coupling at both scales presented in Eq. (2.5) is small enough, then a perturbative solution to this integral equation may be found. This leads us to the critical property of QCD known as *asymptotic freedom*, which states that at high energies quarks and gluons may be treated as weakly interacting particles justifying a perturbative expansion[1].

For the calculations presented in this thesis we shall adopt the $\overline{MS}$ prescription of subtracting only the UV poles plus the attendant Euler-Mascheroni constant and factor of $\ln(4\pi)$, thus we define

$$\frac{1}{\bar{\epsilon}} \equiv \frac{1}{\epsilon} e^{-\gamma_E \epsilon} (4\pi)^{\epsilon}. \tag{2.6}$$

For the remainder of the thesis we shall exclusively use Feynman rules with counterterms and thus the fields are no longer the bare fields as shown in Eq. (2.1).

2.3 Infrared safety

To understand the necessity of computing only infrared safe observables in QCD we consider the next-to-leading (NLO) correction to the process $e^+e^- \to \bar{q}q$. Using the notation of cut diagrams [50, 51] we can draw the contributing Feynman diagrams shown in Figure 2.1. We note that including the non-amputated diagram presented in Figure 2.1 is equivalent to the more standard approach of computing only with amputated Green's functions and multiplying by external wave function renormalisation factors[2].

Anticipating the presence of IR divergences in the amplitude for this process we

---

[1]This comes with the caveat that the number of quark species must be less than 17.

[2]This representation is particularly useful for visualising the cancellation of IR singularities across cuts of the same topology.
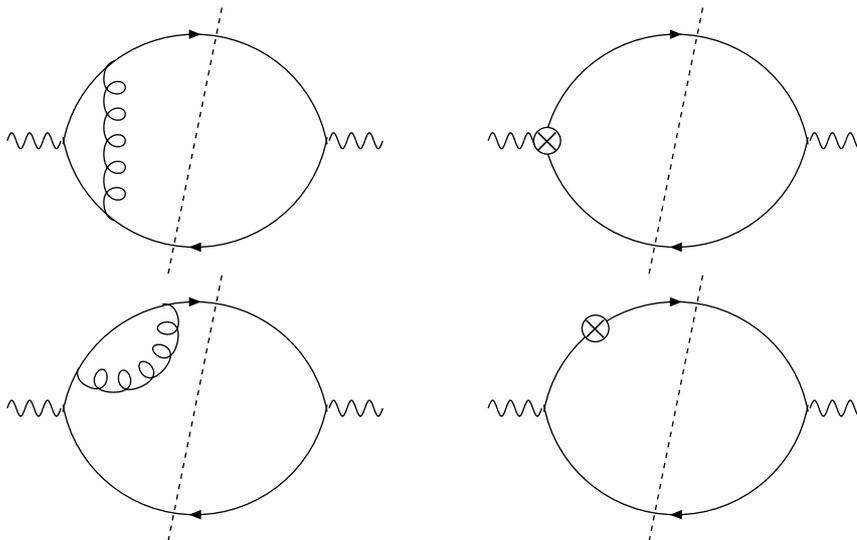
Figure 2.1: Cut diagrams contributing to the amplitude-squared for the final state $|\bar{q}\,q\rangle$. Note that the crossed circles denote counter-terms and that the anti-quark leg also requires external leg renormalisation, conjugate diagrams must also be included.

regulate with a gluon mass[3], m, suppressing technical calculations we find that the NLO cross-section for $e^+e^- \to \bar{q}q$ is given by

$$\sigma_{\text{NLO}}^{\text{virtual}} = \sigma_0 \left(1 + \frac{3\,C_F \alpha_s}{2\,\pi} \left[\ln^2 \frac{m^2}{s} + 3 \ln \frac{m^2}{s} - \frac{\pi^2}{2} + \frac{7}{2} + \mathcal{O}(m_s^2) \right] \right), \qquad (2.7)$$

where σ_0 gives the tree-level cross-section. We see immediately that taking $m \to 0$ will give an infinite answer for this cross-section, this tells us that we have not actually computed a physically observable cross-section. Indeed, as discussed, the free quark final states can always be accompanied by other collinear and soft massless free particles that are not resolved.

To construct a physically measurable observable we realise that an experiment, with some finite resolution, will be unable to detect partons that are soft and collinear with respect to the $\bar{q}q$ final state. The BN/KLN theorem is nothing but a more precise statement of this fact. To the order we are working, such diagrams

---

[3]The use of a gluon mass to regulate non-abelian gauge theories breaks down at higher orders because it introduces non-physical external states [5].

including the necessary soft and collinear kinematics correspond to making a cut of Figure 2.1 that crosses the gluon propagator and gives a three-particle final state. Were we to add these *real* emission diagrams to the *virtual* ones we have just presented we would see a complete cancellation of the logarithmic mass divergences. The simplest observable that we may compute in this way is the fully *inclusive* total rate of $\sigma(e^+e^- \rightarrow \text{hadrons})$, this observable is described as infrared safe because it is completely insensitive to soft processes. The statement of insensitivity to soft processes is equivalent to insensitivity to long ranged interactions, which from the running of the coupling of QCD correspond to process that perturbation theory cannot be reliably applied to i.e. confinement. Thus the statement of an observable being infrared safe really means that perturbative methods will succeed in making predictions for it.

Within this thesis we shall seek to perturbatively construct infrared finite amplitudes, this means that the corresponding NLO cross-section for Eq. (2.7) will be without logarithmic mass divergences[4] and therefore the limit of $m \rightarrow 0$ would be well defined. However this does *not* make the infrared finite prediction for $\sigma_{\text{NLO}}^{\text{virtual}}$ infrared safe. To see this we realise that the argument of a detector having a finite resolution still holds and therefore, despite $\sigma_{\text{NLO}}^{\text{virtual}}$ being finite, it would still be sensitive to long-range physics.

Total cross-section rates, particularly at the Large Hadron Collider (LHC), are generally difficult to measure, therefore it is important to define exclusive observables that may be reliably computed in perturbation theory. An infrared safe exclusive observable can be obtained by simply ensuring that the cancellation of mass divergences is maintained. This means that the defining observable function $O(p_i)$ must, in the singular limits of phase-space, behave the same as when fewer

---

[4]For the remainder of the thesis will shall use dimensional regularisation to regulate all IR divergences.

external particles are defined in the amplitude. More precisely we have

$$\lim_{p_n \to 0} O(p_1, \ldots, p_{n-1}, p_n) = O(p_1, \ldots, p_{n-1})$$

$$\lim_{p_n \to z p_{n-1}} O(p_1, \ldots, p_{n-1}, p_n) = O(p_1, \ldots, p_{n-1} + p_n). \qquad (2.8)$$

2.4 Factorisation

When the initial state consists of massless particles the problem of infrared divergences becomes more acute. KLN theorem would suggest that we should sum over initial states, as well as final, with all possible soft processes attached, this would quickly become very complicated at increasing orders in perturbation theory. Such an investigation has been carried out by the authors of [11], however the results of this pose fundamental questions over the validity of the KLN theorem and a satisfactory theoretical solution to the problem has yet to be formulated.

An additional obstruction for QCD is that our external states are hadrons and mesons, it is therefore not at all obvious how we can correctly represent these states using perturbation theory. Instead the fundamental theorem of factorisation is applied, we factorise the calculation into a hard scattering, $\hat{\sigma}$, calculable in perturbation theory, and a parton distribution function (PDF), f, defined by parameters that are determined experimentally. Explicitly, for an electron scattering off a proton, we have

$$\sigma(e\,p \to X) = \sum_a \int_0^1 d\eta \, f_a(\eta, M) \, \hat{\sigma}(e\,a \to X, M), \qquad (2.9)$$

where a denotes a sum over all different partons of QCD. The PDF, $f_a(\eta, M)$, gives the probability of a parton of species a with momentum fraction η of the proton interacting with the incoming electron. The significance of the mass scale

19

M refers to the fact that a renormalisation has been performed. The bare hard scattering, $\hat{\sigma}^B(e\,a \to X)$ would carry IR divergences associated with initial state radiation, similarly the bare PDF, $f_a^B(\eta)$, is defined to carry exactly the IR divergences necessary to cancel those of $\hat{\sigma}^B(e\,a \to X)$. If we are using dimensional regularisation then a soft scale M is required to make the coupling dimensionless and to allow finite expressions for $\hat{\sigma}$ and f_a. As in the case of ultraviolet renormalisation, renormalisation group equations exist that describe how the PDFs evolve as the scale M is altered. These equations are known as the Dokshitzer-Gribov-Lipatov-Altarelli-Parisi (DGLAP) equations [52].

Chapter 3

Modern Techniques for Perturbative Calculations

3.1 Integral parameterisations

In order to perform the calculations presented in this thesis a variety of techniques for evaluating loop and phase-space integrals have been employed. This chapter briefly reviews some of the tools available for perturbative calculations and concentrates on two more advanced methods necessary for the higher-order calculations. Throughout this thesis we shall perform analytic calculations using dimensional regularisation [5,9,12], where the space-time dimension of the integral is analytically continued to either $d = 4 - 2\epsilon$ or $d = 6 - 2\epsilon$.

The determination of a physical observable requires first the evaluation of the appropriate amplitudes or Green's functions contributing to the process, followed by their integration over the phase-space of the final state partons. Thus we need to compute both loop and phase-space integrals, this requires a suitable parameterisation of the physical parameters, i.e. the momenta and masses of the

interacting particles, that is amenable to analytic or semi-analytic methods[1]. In the following sub-sections we outline the parameterisations used.

3.1.1   Scalar loop integrals

We define the most general, d-dimensional, scalar loop integral to be

$$I_n^{(d)} = \left(\prod_{l=1}^{n} \int \frac{d^d k_l}{i\,\pi^{\frac{d}{2}}} \right) \prod_{j=1}^{m} \frac{1}{P_j^{\nu_j}}, \qquad P_j = \left(\sum_{l=1}^{n} c_{jl} k_l - p_j \right)^2 - m_j^2 + i0^+ \qquad (3.1)$$

where p_j denotes external momenta, m_j the external masses, ν_j and c_{jl} are complex numbers and $i0^+$ denotes the causal prescription.

To evaluate Eq. (3.1), the propagators, P_i, are rewritten into one denominator using Feynman parameters [4, 5]

$$\prod_{i=1}^{n} \frac{1}{(-P_i)^{\nu_i}} = \frac{\Gamma(\nu)}{\prod\limits_{i=1}^{n} \Gamma(\nu_i)} \int_0^1 \left(\prod_{i=1}^{n} dx_i \, x_i^{\nu_i - 1} \right) \frac{\delta\left(1 - \sum\limits_{i=1}^{n} x_i \right)}{\left(-\sum\limits_{i=1}^{n} x_i P_i \right)^{\nu}}, \qquad (3.2)$$

where $\nu = \sum_{i=1}^{n} \nu_i$. The integral over the single denominator is then evaluated by completing the square in the loop momentum, k_i, and using the identity

$$\int \frac{d^d k}{i\pi^{\frac{d}{2}}} \frac{1}{[-\mathcal{U}k^2 + \mathcal{F}]^{\nu}} = \frac{\Gamma(\nu - \frac{d}{2})}{\Gamma(\nu)} \frac{\mathcal{U}^{-\frac{d}{2}}}{\mathcal{F}^{\nu - \frac{d}{2}}}, \qquad (3.3)$$

once for every loop integral. What remains is a generally non-trivial integral over Feynman parameters of the functions $\mathcal{U}$ and $\mathcal{F}$. The vanishing of $\mathcal{U}$ is associated with ultra-violet sub-divergences whilst the vanishing of $\mathcal{F}$ is the root cause of infrared divergences in loop integrals. $\mathcal{F}$ differs from $\mathcal{U}$ in the sense that its zeroes are dependent on the kinematics and not just the topology of the Feynman dia-

---

[1]If the integral is explicitly finite then entirely numerical methods may be employed.

gram. It is this dependence on kinematics which makes it hard to develop general theorems on the IR divergences of Feynman diagrams when compared with UV divergences.

For any Feynman diagram the functions $\mathcal{F}$ and $\mathcal{U}$ may be derived directly from the topology and choice of external kinematics, see for example [53, 54].

3.1.2 Tensor loop integrals

Gauge theories contain tensor structure that complicates the evaluation of loop integrals. The most popular method for dealing with such structures is known as Passarino-Veltman reduction [55]. This simple approach basically relies on equating the integral to the most general tensor structure possible, i.e. in terms of all possible combinations of the integral's external four-momenta p_i^μ and the metric tensor $g^{\mu\nu}$, multiplied by unknown coefficients. The determination of the coefficients amounts to solving a system of equations that are themselves obtained by contracting the general tensor structure with all independent combinations of p_i^μ and $g^{\mu\nu}$. However there are problems with this approach. The first difficulty is the so-called Gram determinant problem where the coefficients become singular in certain kinematic limits. The second affects multi-loop integrals; in this case the presence of irreducible numerators forces the consideration of more complicated scalar integrals and this makes the approach less effective [56].

An alternative method for reduction of tensor integrals to scalar integrals was devised by Davydychev [57] and refined by Tarasov [54] in terms of *Tensor operators*. For multi-loop problems the tensor operator must be constructed on a case by case basis, however a general expression at one loop does exist [58] and is given by

$$I_{\mu_1\ldots\mu_r}^{(d)} = T_{\mu_1\ldots\mu_r}(\{p_i\}, \{\partial_j\}, \mathbf{d}^+) I_1^{(d)}, \tag{3.4}$$

where $\mathbf{d}^+ I^{(d)} \equiv I^{(d+2)}$, $\partial_j \equiv \frac{\partial}{\partial m_j^2}$ and

$$
T_{\mu_1\dots\mu_r}(\{p_i\},\{\partial_j\},\mathbf{d}^+) = \frac{1}{i^r} \prod_{j=1}^{r} \frac{\partial}{\partial a_{\mu_j}} \exp\left[i\left(\sum_{k=1}^{n-1}(ap_k)\alpha_k - \frac{1}{4}a^2\right)\rho\right]\Bigg|_{\substack{a_j=0 \\ \alpha_j=i\partial_j \\ \rho=i\mathbf{d}^+}} .
$$
(3.5)

The result of applying this tensor operator to some scalar integral is a set of tensorial structures dependent on the external momenta and the metric tensor times new scalar integrals. These integrals are generally in higher space-time dimensions, as a result of the $\mathbf{d}^+$ operator, with the powers of the propagators also raised, as a result of the ∂_j operator. An implementation of this one-loop tensor operator can be found in the program TIRA (see Appendix C).

3.1.3 Representations of phase-space

For the purposes of analytic calculations presented in this thesis we shall outline the representations of phase-space for e^+e^- annihilation to massless two, three and four parton final states. We shall use l_1 and l_2 to denote the four-momenta of the initial electron and positron respectively and we will use p_i to represent final state momenta. We shall describe the representations found in [21], they are chosen due to their suitability for the application of plus-distributions, as defined in Section 3.4.2.

The two-parton final state phase-space is absolutely constrained, the fully integrated phase-space of the two massless particles, $\mathcal{R}_2$, is given by

$$
\mathcal{R}_2 = \frac{s^{\frac{d-4}{2}}}{(2\pi)^{d-2}} \frac{\Omega_{d-1}}{2^{d-1}},
$$
(3.6)

where s is the centre of mass energy squared of the colliding electron and positron

and Ω_d is the solid angle in d dimensions,

$$\Omega_d = \frac{2\pi^{\frac{d}{2}}}{\Gamma(\frac{d}{2})}. \tag{3.7}$$

For the three-parton massless final state phase-space the kinematics of the final state is fully described by the invariant masses s_{12}, s_{13}, and s_{23}, (with $s_{ij} = 2\, p_i \cdot p_j$) they satisfy the constraint $s_{12} + s_{13} + s_{23} = s$. Integrating over the trivial angular dependence, the three particle phase-space can be written as

$$\int [\mathrm{d}p_1][\mathrm{d}p_2][\mathrm{d}p_3]\ (2\pi)^d \delta^{(d)}(l_1 + l_2 - p_1 - p_2 - p_3) =$$

$$= \frac{1}{(4\pi)^{d/2}} \frac{\mathcal{R}_2\, s^{\frac{d-2}{2}}}{\Gamma(3 - \frac{d}{2})} \int_0^1 \mathrm{d}\lambda_1 \mathrm{d}\lambda_2\, \lambda_1^{\frac{d-4}{2}}(1 - \lambda_1)^{\frac{d-4}{2}} \lambda_2^{\frac{d-4}{2}}(1 - \lambda_2)^{d-3}, \tag{3.8}$$

where $[\mathrm{d}p_i] = d^{d-1}p_i/(2\pi)^{d-1}p_i^0$. The invariant masses have the following expressions in terms of the Feynman parameters λ_1 and λ_2

$$s_{12} = s\,(1 - \lambda_2)(1 - \lambda_1), \quad s_{13} = s\,(1 - \lambda_2)\lambda_1, \quad s_{23} = s\,\lambda_2. \tag{3.9}$$

Finally the massless four parton phase-space is given by

$$\int [\mathrm{d}p_1][\mathrm{d}\bar{p}_2][\mathrm{d}p_3][\mathrm{d}p_4](2\pi)^d \delta^{(d)}(l_1 + l_2 - p_1 - p_2 - p_3 - p_4) = \mathcal{N}_4 \int_0^1 \mathrm{d}\lambda_1 \mathrm{d}\lambda_2 \mathrm{d}\lambda_3 \mathrm{d}\lambda_4 \mathrm{d}\lambda_5$$

$$\times [\lambda_1\,(1 - \lambda_1)\,(1 - \lambda_2)]^{d-3}\, [\lambda_2 \lambda_3\,(1 - \lambda_3)\, \lambda_4\,(1 - \lambda_4)]^{\frac{d-4}{2}}\, [\lambda_5\,(1 - \lambda_5)]^{\frac{d-5}{2}}, \tag{3.10}$$

where the overall normalisation is

$$\mathcal{N}_4 = s^{d-2}\, \mathcal{R}_2 \left[\frac{\Gamma(3 - \frac{d}{2})}{(4\pi)^{d/2}}\right]^2 \left[\frac{\Omega_{d-1}}{2^{d-1}}\right]^2 \frac{(4\pi)^d}{(2\pi)^{2d-2}} \frac{\Gamma^2(d-2)\Gamma(d-3)}{\Gamma^2(3 + \frac{d}{2})\Gamma^4(\frac{d-2}{2})\Gamma^2(\frac{d-3}{2})}, \tag{3.11}$$

and the invariant masses have the following expressions in terms of the λ_i

$$
\begin{aligned}
s_{234} &= s\,\lambda_1, & s_{34} = s\,\lambda_1\lambda_2, & \qquad s_{23} = s\,\lambda_1\,(1-\lambda_2)\,\lambda_4, \\
s_{134} &= s\,\lambda_2 + s\,\lambda_3\,(1-\lambda_1)\,(1-\lambda_2), & s_{13} = \lambda_5\left(s_{13}^+ - s_{13}^-\right) + s_{13}^-, & \qquad (3.12)
\end{aligned}
$$

with

$$
s_{13}^\pm = s\,(1-\lambda_1)\left[\lambda_3\lambda_4 + \lambda_2\,(1-\lambda_3)\,(1-\lambda_4)\right] \pm \cdots
$$
$$
2\,s\,(1-\lambda_1)\,\sqrt{\lambda_2\lambda_3\,(1-\lambda_3)\,\lambda_4\,(1-\lambda_4)}. \quad (3.13)
$$

3.2 Reduction of integrals

Another important feature of analytic calculation is the use of reduction algorithms. Often the number of integrals that need to be evaluated is very large and it becomes necessary to reduce this number to a manageable number of master integrals. Loop and phase-space integrals generally obey various identities[2] that relate integrals of differing space-time dimension and index power (the power that a propagator is raised to). The best known type of relation is integration by parts (IBP) [60], it is based on the fact that the integral of a total derivative is zero. The IBP identities are generated via

$$
\int \frac{d^d k_i}{i\pi^{d/2}} \frac{\partial}{\partial k_i^\mu} v^\mu f(k_i, p_j) = 0, \qquad (3.14)
$$

where the four-momentum, v^μ, may either be a loop momentum, k_i^μ, or an external momentum p_j^μ. Other identities include Lorentz identities (LI), derived from invariance due to infinitesimal Lorentz transformations [61], and recurrence relations

---

[2]Note that the relations for phase-space integrals are generated by first re-writing them as loop integrals [59].

with respect to the space-time dimension [54].

Since each relation generated using these methods is linear in the scalar integrals, Gauss elimination can be used to reduce the set of integrals that need to be evaluated to a basis of master integrals. Several reduction algorithms are in existence using several different approaches in addition to Gauss elimination [58, 62–64].

3.3   Mellin-Barnes representations

Having obtained representations for master integrals in terms of integrals over Feynman parameters, the remaining steps are to analytically evaluate the integrals and obtain their expansions in the regulator ϵ. Only the simplest cases allow direct evaluation of the integral, so the past thirty years since the inception of perturbative calculations [12, 65, 66] have looked at more advanced ways of computing the integral and ultimately its expansion. One of the most successful methods for doing this lies in the use of the Mellin-Barnes identity [67], followed by an automated analytic continuation in the parameter ϵ [22, 23, 68, 69].

3.3.1   The integral identity

The starting point for Mellin-Barnes calculations is the formula

$$\frac{1}{(A_1 + A_2)^\alpha} = \frac{1}{2\pi i} \int_{c-i\infty}^{c+i\infty} dw A_1^w A_2^{-\alpha-w} \frac{\Gamma(-w)\Gamma(\alpha + w)}{\Gamma(\alpha)}, \qquad (3.15)$$

where c denotes a complex contour separating the poles of $\Gamma(-w)$ and $\Gamma(\alpha + w)$ and the condition $|arg(A_1) - arg(A_2)| < \pi$, must be satisfied. Closing the contour to the right, i.e picking up the poles in the positive half-plane, we obtain the Taylor expansion for $|A_1/A_2| < 1$. If we close to the left then we obtain the

complementary Taylor expansion for $|A_2/A_1| < 1$, thus giving us a simultaneously valid representation for both possibilities.

The usefulness of this transformation is that integrals in terms of Feynman parameters can always be reduced to the form

$$\int_0^1 \left(\prod_{i=1}^n dx_i \, x_i^{\alpha_i} \, (1 - x_i)^{\beta_i} \right) = \prod_{i=1}^n \left(\frac{\Gamma(\alpha_i + 1)\Gamma(\beta_i + 1)}{\Gamma(\alpha_i + \beta_i + 2)} \right), \qquad (3.16)$$

through successive applications of Eq. (3.15). Having performed the trivial integrations of Eq. (3.16), the Feynman integral has been reduced to a multi-dimensional contour integral over gamma functions or rather a multiple infinite sum of residues of gamma functions. In some simple cases it is possible to compute the infinite sum or contour integral using Barnes' lemmas, however this problem is generally very difficult.

3.3.2 Analytic continuation

Instead of directly computing the multi-dimensional contour integral, a more effective route is to first perform the Taylor expansion in ϵ, then the resulting contour integrals are significantly simpler and also amenable to numerical evaluation. Before performing the Taylor expansion, the contour integral must first be analytically continued so that the representation is valid at $\epsilon = 0$. This is done by accounting for poles that lie on the wrong side of the contour when $\epsilon = 0$; automated algorithms exist for this process and can be found in the work of [22, 23].

The idea is to first start with a value for $\epsilon = \epsilon_0$ where the representation, $\mathcal{R}(\epsilon)$, is valid, then we find the maximum allowable value for ϵ, say this occurs at $\epsilon = \epsilon_1$, see Fig 3.1. If there is only one such pole obstructing a valid representation at ϵ_1,
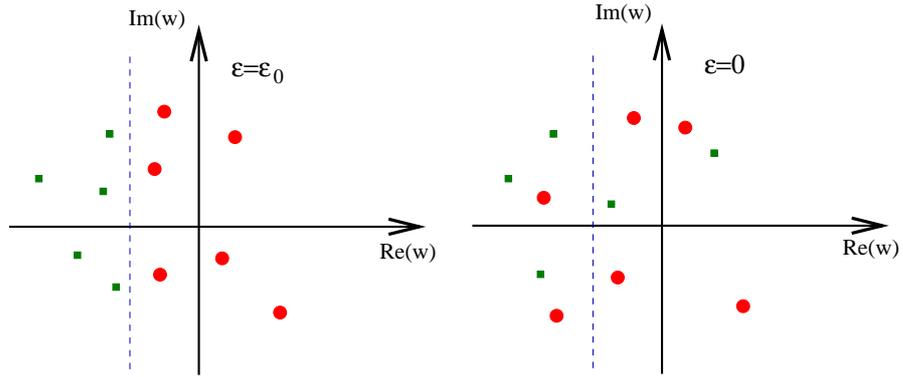
Figure 3.1: Red dots denote poles belonging to $\Gamma(\alpha + w)$ and green belong to $\Gamma(-w)$ of Eq. (3.15). For $\epsilon = \epsilon_0$ the Mellin-Barnes representation, $\mathcal{R}(\epsilon_0)$, is valid. However, taking $\epsilon \to 0$, poles migrate over the contour of integration such that $\mathcal{R}(0)$ is not valid (Figure taken from [23]).

then we can account for this by writing

$$\mathcal{R}(\epsilon_1) = \mathcal{R}(\epsilon_0) \pm Res(\mathcal{R}), \tag{3.17}$$

where $Res(\mathcal{R})$ says to take the residue in one of the contour integral variables, w_i, at the position of the obstructing pole and the sign depends on the direction the pole was travelling. This procedure may be applied iteratively until a valid representation for $\mathcal{R}(0)$ is reached.

3.3.3 Evaluating coefficients of the expansion

Once the expansion in ϵ has been performed, the resulting integrals may be solved using Barnes Lemmas or evaluated numerically for specific choices of kinematics invariants [22]. Alternatively the contour integrals may be re-written as infinite sums and then evaluated using summation identities[3], see for example [70, 71].

---

[3]Many of the results presented in Chapters 6 and 7 are obtained from such calculations.

3.4   Sector decomposition

A very powerful method for evaluating the ϵ expansion of Feynman integrals is sector decomposition. The basic idea is to take the Feynman parameterisation of some integral and then apply various changes of variables such that all overlapping singularities of the starting integrand are factorised. Once this has been achieved plus distributions may be applied and an expansion in ϵ obtained [20, 21, 53]. In general the coefficients of the expansion cannot easily be evaluated analytically. However, for Euclidean choices of kinematics, Monte-Carlo integration routines can efficiently compute the expansion.

3.4.1   Overlapping divergences and changing variables

To illustrate the technique consider the simple integral of

$$I = \int_0^1 dx\, dy\, x^{-1-\epsilon} y^{-1-\epsilon} \left(x + y\right)^{-\epsilon}. \tag{3.18}$$

Eq. (3.18) has an overlapping divergence that we remove by first splitting the integral into two parts

$$I = \left(\int_0^1 dx \int_0^x dy + \int_0^1 dy \int_0^y dx \right) x^{-1-\epsilon} y^{-1-\epsilon} \left(x + y\right)^{-\epsilon}. \tag{3.19}$$

If we consider the first term of I and make the change of variables $y' = y/x$, and correspondingly the transformation $x' = x/y$ for the second term, we obtain

$$
\begin{aligned}
I &= \int_0^1 dx\, dy \left(x^{-1-3\epsilon} y^{-1-\epsilon} \left(1 + y\right)^{-\epsilon} + y^{-1-3\epsilon} x^{-1-\epsilon} \left(1 + x\right)^{-\epsilon} \right) \\
&= 2 \int_0^1 dx\, dy\, x^{-1-3\epsilon} y^{-1-\epsilon} \left(1 + y\right)^{-\epsilon}
\end{aligned}
\tag{3.20}
$$

Using similar transformations to those described in the previous example, it is

always possible to re-write any divergent multi-dimensional Feynman parameter integral, $f(x_i)$ into a sum of m factorised terms of the form

$$\int_0^1 \left(\prod_{i=1}^n dx_i\right) f(x_i) = \sum_{j=1}^m \int_0^1 \left(\prod_{i=1}^n dx_i\right) x_i^{n_{ij}+c_{ij}\epsilon} \, \tilde{f}^j(x_i), \qquad (3.21)$$

where c_{ij} and n_{ij} are integers and $\tilde{f}^j(x_i)$ is finite over the entire region of integration. With all singularities of the integral factorised, Eq. (3.21) is now amenable to the application of plus-distributions.

3.4.2   Plus distributions

Observing Eq. (3.21) we note that an expansion in ϵ, before integration, would be valid if the singular regions of integration space could be subtracted out. If we consider the example of a factorised one-dimensional integral, then the expansion in ϵ can be obtained via the subtraction of $\tilde{f}(0)$:

$$\int_0^1 dx \, x^{-1+\kappa\epsilon} \, \tilde{f}(x) = \frac{1}{\kappa\epsilon} \, \tilde{f}(0) + \int_0^1 dx \, x^{-1+\kappa\epsilon} \left[\tilde{f}(x) - \tilde{f}(0)\right]. \qquad (3.22)$$

Such a subtraction is equivalent to making the substitution

$$x^{-1+\kappa\epsilon} = \frac{1}{\kappa\epsilon}\delta(x) + \sum_{n=0}^\infty \frac{(\kappa\epsilon)^n}{n!} \left[\frac{\ln^n(x)}{x}\right]_+, \qquad (3.23)$$

where a plus distribution is defined via

$$\int_0^1 dx \left[\frac{\ln^n(x)}{x}\right]_+ f(x) = \int_0^1 dx \ln^n(x) \left[\frac{f(x) - f(0)}{x}\right]. \qquad (3.24)$$

The generalisation to the multi-dimensional case and the necessary substitutions for $x^{-n+\kappa\epsilon}$ can be straightforwardly implemented.

Chapter 4

Theory of the Asymptotic Interaction Picture

4.1   An infrared finite perturbation theory

It is generally possible to infer Feyman rules directly from any field theories Lagrangian, thus allowing the computation of perturbative corrections to physical observables [4]. However, as discussed in the introduction, the usual on-shell Green's functions for massless theories suffer from infrared divergences that hamper the determination of higher-order corrections. For such massless theories[1] it is therefore desirable to develop an alternative method for performing perturbative calculations that does not suffer from infrared divergences and is well defined in four space-time dimensions[2].

For the rest of this chapter we will analyse the standard approach to generat-

---

[1]Massive theories may also suffer from large corrections due to logarithms of some mass-scale over the centre-of-mass energy, in such cases new approaches to perturbative calculations are also desirable.

[2]Renormalisation can be performed using subtractions at the integrand level (e.g Bogoliubov-Parasiuk-Hepp-Zimmerman (BPHZ) renormalisation) without violating any of the symmetries of the theory.

ing Feynman rules and advocate an alternative to this - namely the Asymptotic Interaction Picture (AIP) [42]. Within this new approach the usual unitary transformation of the interaction picture is replaced by a transformation in which the states are no longer free Fock states, but are defined through the asymptotic Hamiltonian where soft interactions are still present. Thus the usual Hamiltonian, H, is divided as

$$
\begin{aligned}
H = H_0 + H_I &= H_0 + H_S + H_H \\
&= H_A + H_H,
\end{aligned} \tag{4.1}
$$

where $H_H = H_I - H_S$ and H_S is defined to carry all the soft interactions of the theory such that the states of the theory are determined by $H_A = H_0 + H_S$. Explicitly the usual interaction picture is defined by the transformation

$$
\Phi(t, \vec{x}) = U^\dagger(t, t_0) \, \Phi_I(t, \vec{x}) \, U(t, t_0), \tag{4.2}
$$

where t_0 denotes a definite choice of Schrödinger picture and the Heisenberg field, Φ, is related to the interaction picture field, Φ_I, via the unitary operator

$$
U(t, t_0) = e^{iH_0(t-t_0)} e^{-iH(t-t_0)}. \tag{4.3}
$$

In the standard interaction picture the operator Φ_I's time evolution is determined by commutation with H_0 and the Fock states evolve according to $H_I(t)$, the interaction part of the Lagrangian given in the interaction picture. Instead, the AIP is obtained by the unitary transformation

$$
U_A(t, t_0) = e^{i \, H_A(t-t_0)} e^{-iH(t-t_0)}, \tag{4.4}
$$

so that Φ_I's time evolution is now determined through H_A and the asymptotic

states, $|\Xi\rangle$, evolve in time according to the hard interaction operator, $H_H(t)$, in the asymptotic interaction picture. Thus $H_H(t)$ is given by

$$H_H(t) = e^{i H_A (t-t_0)} H_H e^{-i H_A (t-t_0)}. \qquad (4.5)$$

Using this picture we would then wish to diagonalise the Hamiltonian, H_A, and solve for a complete set of eigenstates $|\Xi\rangle$ of H_A. Such states would be characterised by a complete set of quantum numbers commuting with H_A, in this situation we can no longer expect free-parton particle number to be conserved. Instead $|\Xi\rangle$s will be a superposition of free-parton states with differing numbers of free particles; the free-parton IR divergences "carried" by these superpositions would cancel within the state $|\Xi\rangle$. Thus scattering amplitudes of the form $\langle \Xi_i | S_A | \Xi_j \rangle$ would always be IR finite, with S_A only carrying hard interactions.

Moreover such an approach justifies the use of perturbation theory, since we define all interactions to be hard and therefore the coupling is always small and an expansion in this parameter is valid. Unfortunately the main obstacle to this direct approach is that no exact solution to such an asymptotic Schrödinger equation is in existence, when we implement this transformation we shall ultimately have to use the standard interaction picture to understand the states of H_A. Thus in the following sections we shall determine how the standard Feynman rules should be modified and describe how calculations in the following Chapters will be performed.

4.2 Asymptotic fields

4.2.1 The adiabatic assumption

The critical starting point in the development of calculational tools for field theory, and the root cause of infrared divergences, is the adiabatic assumption[3]:

$$\lim_{t \to \pm\infty} \langle \alpha | \Phi(x) | \beta \rangle = \lim_{t \to \pm\infty} Z_A^{1/2} \langle \alpha | \Phi_A(x) | \beta \rangle. \tag{4.6}$$

Eq. (4.6) is a weak operator limit and effectively says that, at remote times in the past and future, the quantum field of some theory, Φ, has the same kinematics as the asymptotic field, Φ_A, such they are effectively identical up to a normalisation factor $Z_A^{1/2}$. We might hope that this relation is well defined, so that Z_A is finite taking on some value between zero and one.

In the usual approach the asymptotic fields are taken to evolve freely, described by the free Lagrangian of Φ with all interaction terms removed[4]. For massless gauge theory, $Z_A = Z_p$ (where Z_p is called the *pole-scheme* wave function renormalisation factor), it is calculated as the on-shell residue of a free external state. Using conventional perturbation theory this corresponds to a scaleless integral and we find that the unrenormalised $Z_p = 1$ to all orders (using dimensional regularisation). This result for the unrenormalised Z_p is interpreted as a complete cancellation of IR and UV poles; including counter-terms we are left with only the IR divergences and some finite part[5].

The appearance of IR poles in Z_A for massless gauge theories in four-dimensions indicates that long-ranged interactions pertain at asymptotic times and the adi-

---

[3]Where the operators $\Phi(x)$ and $\Phi_A(x)$ correspond to measurable renormalised fields.

[4]Throughout this thesis we shall use Φ to denote a field that evolves with some interactions defined in its Lagrangian and ϕ to denote the same field but with no interactions present in its Lagrangian.

[5]This evidently depends on the choice of renormalisation scheme and we shall use $\overline{MS}$ renormalisation throughout.

abatic assumption breaks down unless regulated. To avoid the introduction of infrared divergences we instead attempt to use a different set of asymptotic states that have the asymptotic interactions of massless field theories included in their descriptions. Assuming this can be achieved, Eq. (4.6) becomes well defined in four-dimensions and Z_A will be finite after ultra-violet renormalisation.

4.2.2   Creation and annihilation

We start examination of the AIP by comparing the usual free fields with fields containing interactions in massless scalar field theory. Our aim is to include only the soft interactions that do not die off at infinity, so we define the asymptotic field, Φ_A, to evolve according to the soft Lagrangian $\mathcal{L}_S$. In the non-interacting case the Lagrangian, $\mathcal{L} = \frac{1}{2}(\partial_\mu \phi)^2$, implies that the scalar field satisfies the classical Klein-Gordon equation of

$$\frac{\partial^2 \phi(x)}{\partial t^2} = \nabla^2 \phi(x), \qquad (4.7)$$

where ϕ denotes a free field. Supposing we now add some form of interaction into the Lagrangian then the equations of motion can be re-written as

$$\Box_x \Phi_A(x) = \frac{\partial \mathcal{L}_S}{\partial \Phi_A(x)}, \qquad (4.8)$$

with Φ_A denoting the interacting field and $\mathcal{L}_S$ denotes all long-ranged interactions of the theory[6]. We also define $\mathcal{L}_H$ to describe all the remaining short-ranged interactions, thus $\mathcal{L}_I = \mathcal{L}_H + \mathcal{L}_S$.

In both free and interacting cases we quantise the theory by promoting the field,

---

[6]In writing Eq. (4.8) we make the standard assumption that the interaction, $\mathcal{L}_I$ has no derivative terms. We continue this assumption throughout the thesis.

Φ_A, and its conjugate momenta

$$\Pi_A(x) = \partial_0 \Phi_A(x), \tag{4.9}$$

to operators and impose the usual equal-time commutation relations of

$$[\Phi_A(t, \vec{x}), \Pi_A(t, \vec{y})] = i\delta^{(3)}(\vec{x} - \vec{y}),$$

$$[\Phi_A(t, \vec{x}), \Phi_A(t, \vec{y})] = 0 \ , \ [\Pi_A(t, \vec{x}), \Pi_A(t, \vec{y})] = 0. \tag{4.10}$$

The next step is to expand the fields in terms of asymptotic creation and annihilation operators defined as

$$\lim_{t \to \infty} \langle \Theta | \, a_a(t, \vec{k}) \, \sqrt{2E_k} \equiv \, _{out}\langle \Xi(\vec{k})| \qquad \lim_{t \to -\infty} \, \sqrt{2E_k} \, a_a^\dagger(t, \vec{k}) |\Theta\rangle \equiv |\Xi(\vec{k})\rangle_{in}$$

$$\lim_{t \to \infty} \langle \Theta | \, a_a^\dagger(t, \vec{k}) \equiv 0 \qquad\qquad \lim_{t \to -\infty} \, a_a(t, \vec{k}) |\Theta\rangle \equiv 0. \tag{4.11}$$

E_k is an energy normalisation factor associated to the Fourier mode k, $|\Theta\rangle$ is the vacuum of the interacting field and $|\Xi\rangle$ denotes an asymptotic state of the theory. Evidently the free field case gives us the free vacuum, $|0\rangle$, the standard creation and annihilation operators and the usual Fock basis of non-interacting states i.e. $|\Xi\rangle \to |\phi\rangle$. Ultimately, for the AIP, we want to take the interacting field, Φ_A, to be precisely the true asymptotic field so that the form for the interaction part of Lagrangian remains the same at all times.

The expansion of the field Φ_A, in the Heisenberg picture, gives

$$\Phi_A(t, \vec{x}) = \int \frac{d^3k}{(2\pi)^3 \sqrt{2E_k}} \left(a_a(t, \vec{k}) \, e^{i\vec{k}.\vec{x}} + a_a^\dagger(t, \vec{k}) \, e^{-i\vec{k}.\vec{x}} \right), \tag{4.12}$$

and using Eq. (4.9) we write

$$\Pi_A(t, \vec{x}) = \int \frac{d^3k}{(2\pi)^3\sqrt{2E_k}} \left(\partial_0 a_a(t, \vec{k}) \, e^{i\vec{k}.\vec{x}} + \partial_0 a_a^\dagger(t, \vec{k}) \, e^{-i\vec{k}.\vec{x}} \right)$$

$$= i \int \frac{d^3k}{(2\pi)^3\sqrt{2E_k}} \left(\left[H_A, a_a(t, \vec{k}) \right] e^{i\vec{k}.\vec{x}} + \left[H_A, a_a^\dagger(t, \vec{k}) \right] e^{-i\vec{k}.\vec{x}} \right). \quad (4.13)$$

If we take the case of a non-interacting scalar field then $H_A = H_0$, the Hamiltonian describes a simple harmonic oscillator and may be written in diagonal form as

$$H_0 = \int \frac{d^3k}{(2\pi)^3} \, \omega_k \left(a^\dagger(\vec{k}) a(\vec{k}) + \frac{1}{2} \left[a(\vec{k}), a^\dagger(\vec{k}) \right] \right), \quad (4.14)$$

with $\omega_k = |\vec{k}|$ and the usual commutation relations of

$$\left[a(t, \vec{k}), a^\dagger(t, \vec{k}') \right] = (2\pi)^3 \delta^{(3)}(\vec{k} - \vec{k}')$$

$$\left[a(t, \vec{k}), a(t, \vec{k}') \right] = 0 \; , \; \left[a^\dagger(t, \vec{k}), a^\dagger(t, \vec{k}') \right] = 0, \quad (4.15)$$

hold. We shall now try to extend these relations to the case where an interaction term is present and the Hamiltonian cannot be diagonalised. To do this we assume that Eq. (4.15) is valid also for any asymptotic creation/annihilation operator i.e. we re-write Eq. (4.15) with a replaced by a_a. Then we substitute Eq. (4.12) and Eq. (4.13) into the relation $[\Phi_A(t, \vec{x}), \Pi_A(t, \vec{y})] = i\delta^{(3)}(\vec{x} - \vec{y})$, this gives

$$i \int \frac{d^3k}{(2\pi)^3\sqrt{2E_k}} \frac{d^3k'}{(2\pi)^3\sqrt{2E_{k'}}} \Big([a_a(t, \vec{k}), [H_A, a_a(t, \vec{k}')]] \, e^{i\vec{k}.\vec{x}} e^{i\vec{k}'.\vec{y}}$$

$$+ [a_a(t, \vec{k}), [H_A, a_a^\dagger(t, \vec{k}')]] \, e^{i\vec{k}.\vec{x}} e^{-i\vec{k}'.\vec{y}} + [a_a^\dagger(t, \vec{k}), [H_A, a_a(t, \vec{k}')]] \, e^{-i\vec{k}.\vec{x}} e^{i\vec{k}'.\vec{y}}$$

$$+ [a_a^\dagger(t, \vec{k}), [H_A, a_a^\dagger(t, \vec{k}')]] \, e^{-i\vec{k}.\vec{x}} e^{-i\vec{k}'.\vec{y}} \Big) = i\delta^{(3)}(\vec{x} - \vec{y}), \quad (4.16)$$

which implies

$$[H_A, a_a^\dagger(t, \vec{k})] = E_k \, a_a^\dagger(t, \vec{k}) \qquad [H_A, a_a(t, \vec{k})] = -E_k \, a_a(t, \vec{k}), \quad (4.17)$$

in direct analogy with the free field calculation obtained using Eq. (4.14) and Eq. (4.15). If we use Eq. (4.17) combined with the Heisenberg picture relation,

$$a_a(t, \vec{k}) = e^{iH_A t} a_a(\vec{k}) e^{-iH_A t}, \tag{4.18}$$

we can write the asymptotic creation and annihilation operators as

$$\sqrt{2E_k}\, a_a(\vec{k}) = \int d^3x\, e^{ik.x} (E_k\, \Phi_A(t, \vec{x}) + i\Pi_A(t, \vec{x}))\big|_{k^0 = E_k}$$

$$\sqrt{2E_k}\, a_a^\dagger(\vec{k}) = \int d^3x\, e^{-ik.x} (E_k\, \Phi_A(t, \vec{x}) - i\Pi_A(t, \vec{x}))\big|_{k^0 = E_k}. \tag{4.19}$$

What remains is to relate E_k to the momentum of the mode $\vec{k}$. Due to the nature of interactions such a relation is very hard to determine, instead we note that, in order to maintain covariance of the states, Φ_A must transform under displacements as the full field Φ, therefore

$$[P^\mu, \Phi_A(x)] = -i\frac{\partial\, \Phi_A(x)}{\partial x_\mu}. \tag{4.20}$$

Now if we consider an arbitrary eigenstate

$$P^\mu |n\rangle = p^\mu |n\rangle \tag{4.21}$$

and form the following matrix element with the free vacuum, $|0\rangle$,

$$-i\frac{\partial}{\partial x_\mu} \langle n|\, \Phi_A(x)\, |0\rangle = \langle n|\, [P^\mu, \Phi_A(x)]\, |0\rangle = p_n^\mu\, \langle n|\, \Phi_A(x)\, |0\rangle, \tag{4.22}$$

using Eq. (4.8) we see that

$$\Box_x\, \langle n|\, \Phi_A(x)\, |0\rangle = -p_n^2\, \langle n|\, \Phi_A(x)\, |0\rangle = \langle n|\frac{\partial\mathcal{L}_S}{\partial\, \Phi_A(x)}|0\rangle. \tag{4.23}$$

Eq. (4.23) implies that the asymptotic states are not massless but depend on the interactions of the asymptotic Lagrangian. If we take the interaction to only be those parts that would lead to infrared divergences in perturbation theory, then the asymptotic states no longer consist solely of the original parton, but include a cloud of soft and collinear partons as perceived from the Fock basis of non-interacting states. We therefore define the invariant mass of such an asymptotic state to be given as

$$k^2 = E_k^2 - \vec{k}^{\,2} = M_A^2, \tag{4.24}$$

where M_A^2 is a function of the soft Lagrangian $\mathcal{L}_S$.

4.3 Green functions and LSZ reduction

4.3.1 LSZ reduction

The first step to obtaining quantitative predictions for observables is to relate S-matrix elements to time-ordered correlation functions[7] via the LSZ formalism [4,5], for a simple scalar field theory the standard expression is

$$
\begin{aligned}
{}_{out}\langle p_1, \ldots, p_n | q_1, \ldots, q_m \rangle_{in} = \\
(iZ_p)^{-\frac{n+m}{2}} \int d^4x_1 \ldots d^4x_m \, d^4y_1 \ldots d^4y_n \; e^{i\sum p_i \cdot y_i} e^{-i\sum q_i \cdot x_i} \; \times \cdots \\
K_{y_1} \ldots K_{y_n} K_{x_1} \ldots K_{x_m} \langle \Omega | \, T\left\{ \Phi(y_1) \ldots \Phi(y_n) \Phi(x_1) \ldots \Phi(x_m) \right\} | \Omega \rangle, \quad (4.25)
\end{aligned}
$$

where $|\Omega\rangle$ is the vacuum of the full theory[8], K_i denotes the Klein-Gordon operator and Z_p is the pole-scheme wave function renormalisation obtained by calculating

---

[7]Correlation functions of the form $\langle \Omega | \, T\left\{ \Phi(z_1) \ldots \Phi(z_r) \right\} | \Omega \rangle$ are also known as r-particle Green's functions.

[8]We shall always take the approach of [4] and denote $|\Omega\rangle$ as the vacuum of the full interacting field and $|0\rangle$ to denote the vacuum for a free field.

the on-shell self-interaction of the field. The Klein-Gordon operator removes the propagators of the external legs of the S-matrix element and we see that we need to compute the multi-pole residue of the $r = m + n$ Green's function. Eq. (4.25) can be extended to include, for example QCD, where the tensor structure of the fields does not alter the general procedure of the LSZ reduction formalism; for spinor fields, K_i is replaced by the Dirac operator D_i.

For the AIP we must determine the corresponding reduction formalism for asymptotic creation operators acting on the vacuum. This proceeds along the same lines of the standard derivation that can be found in [5]. We start by extracting an asymptotic creation operator from the initial state

$$
\begin{aligned}
\mathcal{A} &= {}_{out}\langle p_1, \ldots, p_n | q_1, \ldots, q_m \rangle_{in} \\
&= \lim_{t \to -\infty} {}_{out}\langle p_1, \ldots, p_n | \sqrt{2E_{q_1}}\, a_{in}^\dagger(\vec{q_1}) | q_2, \ldots, q_m \rangle_{in},
\end{aligned} \qquad (4.26)
$$

where $a_{in}^\dagger(q_1)$ is an asymptotic creation operator $a_a^\dagger$ as defined in Eq. (4.11). Using Eq. (4.19) we obtain

$$
\begin{aligned}
&\lim_{t \to -\infty} {}_{out}\langle p_1, \ldots, p_n | \sqrt{2E_{q_1}}\, a_{in}^\dagger(\vec{q_1}) | q_2, \ldots, q_m \rangle_{in} \\
&= \lim_{t \to -\infty} \int d^3x\, e^{i\,\vec{q_1} \cdot \vec{x}} \langle p_1, \ldots, p_n | E_{q_1} \Phi_A(t, \vec{x}) - i\Pi_A(t, \vec{x}) | q_2, \ldots, q_m \rangle,
\end{aligned} \qquad (4.27)
$$

where we have dropped the *in* and *out* labels from the *in* and *out* states. In the asymptotic limit we can then write

$$
\begin{aligned}
e^{-iE_k t} \left(E_k \Phi_A(t, \vec{x}) - i\Pi_A(t, \vec{x}) \right) &= -i \left(e^{-iE_k t} \overset{\leftrightarrow}{\partial_0} \Phi_A(t, \vec{x}) \right) \\
&= -i\, Z_A^{-1/2} (e^{-iE_k t} \overset{\leftrightarrow}{\partial_0} \Phi(t, \vec{x})),
\end{aligned} \qquad (4.28)
$$

Eq. (4.27) then becomes

$$\lim_{t \to -\infty} (-i) \, Z_A^{-1/2} \int d^3x \, e^{-i \, q_1.x} \, \overleftrightarrow{\partial_0} \, \langle p_1, \ldots, p_n | \, \Phi(x) \, | q_2, \ldots, q_m \rangle, \qquad (4.29)$$

where $q_1^2 = M_A^2$ as a consequence of the soft interactions included in the asymptotic field. Following the standard approach we add and subtract

$$\lim_{t \to \infty} \, {}_{out}\langle p_1, \ldots, p_n | \, \sqrt{2E_{q_1}} \, a_{out}^\dagger(q_1) \, | q_2, \ldots, q_m \rangle_{in}, \qquad (4.30)$$

and use the result

$$\left(\lim_{t \to \infty} - \lim_{t \to -\infty} \right) \int d^3x \, F(x,t) = \lim_{t_f \to \infty, t_i \to -\infty} \int_{t_i}^{t_f} dt \frac{\partial}{\partial t} \int d^3x \, F(x,t), \qquad (4.31)$$

to write Eq. (4.29) as

$$iZ_A^{-1/2} \int d^4x \, \partial_0 \left(e^{-iq_1.x} \, \overleftrightarrow{\partial_0} \, \langle p_1, \ldots, p_n | \, \Phi(x) \, | q_2, \ldots, q_m \rangle \right)$$
$$+ \lim_{t \to \infty} \, {}_{out}\langle p_1, \ldots, p_n | \, \sqrt{2E_{q_1}} \, a_{out}^\dagger(q_1) \, | q_2, \ldots, q_m \rangle_{in}. \quad (4.32)$$

The second term of Eq. (4.32) is either zero, in the case where q_1 is not an element of the set $\{p_1, \cdots, p_n\}$, or it represents a disconnected piece. The disconnection represents an event where the initial state particle of momentum, q_1, takes no part in scattering and simply becomes one of the final state momenta. In the usual LSZ formalism we drop such terms from our calculations since they do not contribute to $\mathcal{A}$ as it is defined[9]. However, since asymptotic states may interact softly, it is no longer clear that they do not contribute to the $\mathcal{A}$ of interest and therefore they cannot be ignored as in the usual approach. For the remainder of the LSZ derivation we shall drop these "disconnected" pieces and remember that they are

---

[9]These terms are actually of importance when considering initial state radiation described by coherent states [30]. Only the conventional use of PDFs circumvents the consideration of such disconnected diagrams.

still to be accounted for. Expanding the first term of Eq. (4.32) and using the relation

$$\partial_0^2 \, e^{-iq_1 x} = \left(\nabla^2 - M_A^2\right) e^{-iq_1 x}, \tag{4.33}$$

we obtain

$$iZ_A^{-1/2} \int d^4x \, \langle p_1, \ldots, p_n| \left\{ e^{-iq_1 \cdot x} \, \partial_0^2 \, \Phi(x) - \cdots \right.$$
$$\left. \left[\left(\nabla^2 - M_A^2\right) e^{-iq_1 \cdot x}\right] \Phi(x) \right\} |q_2, \ldots, q_m\rangle. \tag{4.34}$$

Applying integration by parts to Eq. (4.34) gives

$$iZ_A^{-1/2} \int d^4x \, e^{-iq_1 \cdot x} \langle p_1, \ldots, p_n| \, A_x \, \Phi(x) \, |q_2, \ldots, q_m\rangle, \tag{4.35}$$

with $q_1 = (E_{q_1}, \vec{q}_1)$ and the operator A_x is defined by the relation

$$A_x \, \Phi_A(x) = \Box_x \, \Phi_A(x) - \frac{\partial \mathcal{L}_S}{\partial \Phi_A(x)} = 0. \tag{4.36}$$

The extraction of all the *in* and *out* states proceeds to give the generalisation of the usual LSZ reduction formalism

$$_{out}\langle p_1, \ldots, p_n | q_1, \ldots, q_m \rangle_{in} =$$
$$(iZ_A)^{-\frac{n+m}{2}} \int d^4x_1 \ldots d^4x_m \, d^4y_1 \ldots d^4y_n \, e^{i\sum p_i \cdot y_i} e^{-i\sum q_i \cdot x_i} \times \cdots$$
$$A_{y_1} \ldots A_{y_n} A_{x_1} \ldots A_{x_m} \langle \Omega| \, T \left\{\Phi(y_1) \ldots \Phi(y_n)\Phi(x_1) \ldots \Phi(x_m)\right\} |\Omega\rangle, \tag{4.37}$$

remembering that we will have to consider all combinations of disconnected pieces as well. Comparing Eq. (4.25) with Eq. (4.37) we see two differences, the first is that Z has been replaced by the IR finite Z_A, secondly the external legs of the process are now being operated on by A_x as opposed to the Klein Gorden operator.

We would naively expect that this operation basically removes the propagators of the external asymptotic states and puts them on-shell, i.e. with some mass M_A. Unfortunately, since we cannot directly solve for these asymptotic states, it is far from clear how such a process can be implemented. Instead we shall have to use perturbative methods based in the usual interaction picture to try to understand these asymptotic states and their propagators; the following sections describe how we do this.

4.3.2 Expanding Green's functions

Sticking with the case of a scalar field theory, the next step to formulating Feynman rules is to use the interaction picture to relate the full fields of the theory, Φ, to the free ones, ϕ, the standard relation takes the form

$$\langle\Omega|\, T\{\Phi(x_1)\dots\Phi(x_n)\}|\Omega\rangle = \frac{\langle 0|\, T\{\phi(x_1)\dots\phi(x_n)\exp\left(-i\int_{-\infty}^{\infty}d^4x\,\mathcal{L}_I\right)\}|0\rangle}{\langle 0|\, T\{\left(-i\int_{-\infty}^{\infty}d^4x\,\mathcal{L}_I\right)\}|0\rangle}.$$
(4.38)

The derivation of Eq. (4.38) is in fact a general result for any unitary transformation. Thus instead of using the transformation given by Eq. (4.3) we use instead Eq. (4.4) and obtain the result

$$\langle\Omega|\, T\{\Phi(x_1)\dots\Phi(x_n)\}|\Omega\rangle = \frac{\langle\Theta|\, T\{\Phi_A(x_1)\dots\Phi_A(x_n)\exp\left(-i\int_{-\infty}^{\infty}d^4x\,\mathcal{L}_H\right)\}|\Theta\rangle}{\langle\Theta|\, T\{\left(-i\int_{-\infty}^{\infty}d^4x\,\mathcal{L}_H\right)\}|\Theta\rangle},$$
(4.39)

where $|\Theta\rangle$ denotes the vacuum of the asymptotic field Φ_A and $\mathcal{L}_H$ denotes the part of the interaction Lagrangian, $\mathcal{L}_I$, that only contains hard interactions not leading to IR divergences. For now we shall resist defining how precisely the split of the interaction Lagrangian into hard and soft parts is performed. Since we cannot solve for the asymptotic theory exactly, we will attempt to make a reasonable

approximation for the division of the hard and soft parts of the Lagrangian in the following sections.

Obtaining the usual Feynman rules from Eq. (4.38) involves a perturbative expansion in the coupling of the theory. Wick's theorem then allows a dramatic simplification of the expansion in terms of time-ordered two-point functions or the propagators of free field theory. For every point in space-time that several propagators meet a vertex can be associated to it and we are able to build a set of rules associated to a diagrammatic representation for any term in the expansion.

For the AIP we start again by performing a perturbative expansion in the coupling and then applying Wick's theorem. Since this theorem relies solely on the creation and annihilation operator's commutation relations that are identical for the asymptotic and non-interacting theories, we can immediately generalise Wick's theorem to obtain the result

$$
\langle\Theta|\, T\left\{\Phi_A(x_1)\ldots\Phi_A(x_n)\right\}|\Theta\rangle
$$
$$
= \begin{cases} 0 & : \text{odd n} \\ \sum_P \langle\Theta|\, T\left\{\Phi_A(x_1)\Phi_A(x_2)\right\}|\Theta\rangle \ldots \langle\Theta|\, T\left\{\Phi_A(x_{n-1})\Phi_A(x_n)\right\}|\Theta\rangle & : \text{even n} \end{cases}
$$

where P is a sum over all permutations of the x_i with $\langle\Theta|\, T\left\{\Phi_A(x_1)\Phi_A(x_2)\right\}|\Theta\rangle$ and $\langle\Theta|\, T\left\{\Phi_A(x_2)\Phi_A(x_1)\right\}|\Theta\rangle$ counted as a single term.

Wick's theorem allows us to simplify the perturbative expansion of the AIP's Green's functions into asymptotic two-point functions and interaction vertices that explicitly prevent soft momentum configurations from developing. In comparison to the usual free-field expansion we see that all the IR divergent structure has effectively been resummed into the asymptotic propagators leaving us with an IR finite perturbative series. Another pleasant feature of this expansion is that we expect the coupling to always be small since we are now exclusively dealing with

hard processes.

Unfortunately we do not have an exact solution for the asymptotic propagator and we are forced to relate this object to a perturbative expansion using the interaction picture, thus we have

$$\langle\Theta|\,T\{\Phi_A(x_1)\Phi_A(x_2)\}|\Theta\rangle = \frac{\langle 0|\,T\{\phi(x_1)\phi(x_2)\exp\left(-i\int_{-\infty}^{\infty}d^4x\,\mathcal{L}_S\right)\}|0\rangle}{\langle 0|\,T\{\left(-i\int_{-\infty}^{\infty}d^4x\,\mathcal{L}_S\right)\}|0\rangle}. \quad (4.40)$$

4.3.3 Amputation of the external legs

Within the usual prescription of the LSZ the Klein-Gorden operators remove the external free-field propagators and put these fields on-shell. Since we do not have an exact solution for the asymptotic propagators we instead consider the effect of the asymptotic operator A_x on the perturbative expansion of the asymptotic propagator given in Eq. (4.40), this gives

$$A_x\langle\Theta|\,T\{\Phi_A(x)\Phi_A(y)\}\,|\Theta\rangle =$$
$$\left(K_x - \frac{\partial\mathcal{L}_S}{\partial\,\Phi_A(x)}\,\Phi_A(x)^{-1}\right)\langle 0|\,T\{\phi(x)\phi(y)\exp\left(-i\int_{-\infty}^{\infty}d^4z\,\mathcal{L}_S(z)\right)\}\,|0\rangle, \quad (4.41)$$

where we have suppressed the denominator of this expression. The operation of K_x on the perturbative expansion of the asymptotic propagator would correspond to taking the residue of the pole as in the usual free field case, the only modification is the presence of a soft self-energy diagram attached to the external leg. Such a modification would only change the overall constant multiplying the free-propagator, so this corresponds to a relatively minor alteration to the formalism. The effect of the operator $\frac{\partial\mathcal{L}_S}{\partial\,\Phi_A(x)}\,\Phi_A(x)^{-1}$ is far harder to quantify. The presence of several fields at the same space-time point seems to indicate that parton number will not be a good quantum number, since both free quark and gluons will be included in

a state $|\Xi\rangle$. This operator also contains powers in the coupling and, for a perturbative expansion, is suppressed relative to the leading order contribution that comes from the Klein-Gorden operator. Such soft interactions in principle permit the exchange of soft particles between external states and can interact softly with the disconnected pieces found in the derivation of Eq. (4.37). Whilst conceptually speaking such effects are to be expected, the correct theoretic treatment is far from clear. However, we may still use our qualitative understanding of the asymptotic external states to construct infrared finite amplitudes and we shall describe this in the next section.

4.4 An alternative approach to the AIP

4.4.1 Slicing up conventional amplitudes

The basic idea of the AIP is to split the interactions of the theory into two sectors - soft and hard. The soft sector should describe the evolution of the asymptotic states and therefore defines the vector space of asymptotic states. The hard sector defines all the short-ranged interactions of the theory, for these interactions the use of perturbation theory is valid because we can say that the coupling is small for such processes. Unfortunately solving the asymptotic equations of motion proves too difficult and we have found that a perturbative treatment of the soft sector is unavoidable - the cost of doing this is that we are left trying to interpret Eq. (4.41). However, since we expand both the soft and hard regions and we must ultimately work in a Fock basis of free states, it is conceivable that the perturbatively expanded AIP should map straight onto the conventional amplitudes and cross-sections of normal perturbative field theory. The crucial difference is that we have still split up the Lagrangian and therefore a vertex may either be

hard or soft. In order to obtain the same results as in the conventional approach we must therefore sum all combinations of hard and soft vertices.

The utility of splitting up the vertices into hard and soft is that we can change the manner in which we group amplitudes. In the conventional approach amplitudes are grouped according to the number of final state partons, this is necessary since the phase-space integration must generally be performed numerically. In this alternative approach we group amplitudes according to the number of "resolved" partons.

4.4.2   A simple example
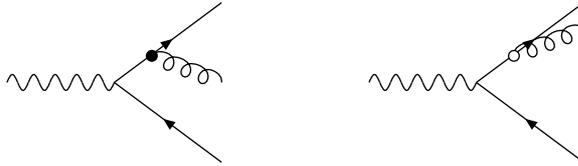
Figure 4.1: The emission of a hard (dark circles) gluon contributes to the dressed state $|\{\bar{q}\,q\,g\}\rangle$, whereas the emission of a soft (open circles) gluon contributes to the dressed state $|\{\bar{q}\,q\}\rangle$.

To make this more concrete we shall sketch the basic idea for e^+e^- annihilation to hadrons at $\mathcal{O}(\alpha_s)$. If we just consider the real emission of a gluon as illustrated in Fig 4.1, then if the vertex is hard, we expect it to contribute to the asymptotic or dressed three-parton state $|\bar{q}\,q\,g\rangle_H \equiv |\{\bar{q}\,q\,g\}\rangle$, else if it is soft then the amplitude should contribute to the two-parton dressed state $|\bar{q}\,q\rangle + |\bar{q}\,q\,g\rangle_S \equiv |\{\bar{q}\,q\}\rangle$. We note that no hard or soft vertex is placed at the photon vertex since we are explicitly assuming it to be off-shell and not leading to IR divergences. The point here is that integration over the three-parton phase space of the amplitude-squared of $|\{\bar{q}\,q\,g\}\rangle$ is explicitly finite. Contrary to the conventional amplitude $|\bar{q}\,q\,g\rangle$, which diverges
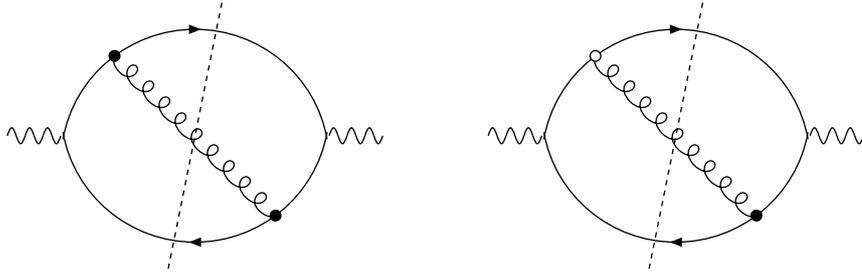
Figure 4.2: Cut diagrams contributing to an amplitude squared for the final state $|\{\bar{q}\,q\,g\}\rangle$ (left) and $|\{\bar{q}\,q\}\rangle$ (right).

in the two-jet regions of phase-space, the dressed three-parton amplitude-squared simply vanishes in this region.

The amplitude $|\{\bar{q}\,q\}\rangle$ now corresponds to an amalgamation of the IR divergent loop correction to the tree-level two-jet amplitude, plus the IR divergent phase space integral over the soft gluon of Fig 4.1. Combining these IR divergent "sub-amplitudes" gives rise to the infrared finite amplitude $|\{\bar{q}\,q\}\rangle$ at $\mathcal{O}(\alpha_s)$. Regarding the IR divergent phase space integral, the important point to note is that, because the gluon is not resolved, we may be completely inclusive in the integration over its phase-space. Therefore the idea would be to factorise the three-parton phase space into a two-parton phase-space times a fully inclusive, divergent, one-parton phase-space integral that cancels the IR divergences of the loop integral.

Keeping with the simple example we have so far discussed, we see an additional complication to this approach in Fig 4.2. It is clear that we must actually consider individual cut diagrams before deciding whether or not a contribution should be part of the dressed three or two-parton final state. In the case where all vertices are hard we expect all final state free-partons to be resolved and therefore the diagram on the left must contribute to $|\{\bar{q}\,q\,g\}\rangle$. The diagram on the right is a contribution to $|\{\bar{q}\,q\}\rangle$, we can see that this must be true since the left hand side of the cut belongs to a dressed state with a reduced final state particle content. Physically this cut contribution corresponds to the kinematic situation where a

gluon is emitted co-linearly with respect to the quark field. We further note that, due to the hard vertex, the limit of vanishing gluon energy should set this amplitude to zero.

4.4.3 Summary of alternative approach

Adopting this alternative approach we see that basically the conventional Feynman rules remain unchanged. The only difference is that each vertex will now either be multiplied by a hard factor, that will set an amplitude to zero if a soft momentum configuration flows through it, or a soft factor where the inverse condition holds. We can consider the amplitude for some process where all vertices are hard, $\mathcal{A}_{\mathrm{H}}(\{\phi_{p_1} \ldots \phi_{p_n}\})$, this can be considered a contribution to the infrared finite expansion of Eq. (4.39). The presence of soft vertices gives contributions to the amplitude, collectively grouped as $\mathcal{A}_{\mathrm{S}}(\{\phi_{p_1} \ldots \phi_{p_n}\})$, that we associate with modifications to the usual LSZ reduction formula. Having outlined the basic idea for constructing such amplitudes, what remains is to define a suitable split of the Lagrangian into hard and soft sectors, to check that amplitudes $\mathcal{A}_{\mathrm{H}}(\{\phi_{p_1} \ldots \phi_{p_n}\})$ are indeed infra-red finite and to then make explicit constructions.

To summarise, we expect amplitudes in this alternative approach to take the form

$$\mathcal{A}_{\mathrm{AIP}}(\{\phi_{p_1} \ldots \phi_{p_n}\}) = \mathcal{A}_{\mathrm{H}}(\{\phi_{p_1} \ldots \phi_{p_n}\}) + \mathcal{A}_{\mathrm{S}}(\{\phi_{p_1} \ldots \phi_{p_n}\}), \qquad (4.42)$$

where $\mathcal{A}_H$ is IR finite and is obtained by taking the conventional amplitude and inserting hard factors at every vertex. $\mathcal{A}_S$ denotes an IR finite sum of conventional Feynman diagrams with various combinations of hard and soft factors, this term is associated to the perturbative expansion of asymptotic propagators and the required modifications of the LSZ formalism.

4.5 Splitting the Lagrangian

4.5.1 The soft scale Δ

The next step in development of this theory is to actually determine how to split the interaction part of the Lagrangian $\mathcal{L}_I$ into hard and soft sectors. Ideally we would choose $\mathcal{L}_S$ so that it has precisely the asymptotic dynamics of the field theory, i.e. the asymptotic limit of $\mathcal{L}_I$. Since we do not know how to compute this limit, instead we simply ensure that $\mathcal{L}_S$ has all long-ranged interactions plus a portion of the short-ranged interactions defined by the soft scale Δ. Thus, roughly speaking, the limit $\Delta \to 0$ shrinks the soft region to zero and recovers the conventional perturbative field theory, whereas the limit $\Delta \to \infty$ should correspond to solving the AIP with full states of the theory.

Essentially Δ acts as a resolution parameter and determines to what extent we may resolve any jets that appear in our calculations; the work of [46] takes this view where an explicit split is introduced for the Hamiltonian rather than the Lagrangian. We expect that, providing the scale Δ is smaller than any experimental resolution parameter and there is some hard scale present, we should recover the same results for a jet observable as obtained using conventional methods.

Indeed, were we not to use perturbation theory, we might expect that the asymptotic matrix elements are completely independent of Δ, consider

$$
\begin{aligned}
\langle \Xi_\beta(\Delta)|S_A(\Delta)|\Xi_\alpha(\Delta)\rangle &= \langle \Xi_\beta(\Delta)|\Omega_d^{(-)\dagger}\Omega_d^{(-)}S_A(\Delta)\Omega_d^{(-)\dagger}\Omega_d^{(-)}|\Xi_\alpha(\Delta)\rangle \\
&= \langle \Xi_\beta(2\Delta)|S_A(2\Delta)|\Xi_\alpha(2\Delta)\rangle
\end{aligned}
\tag{4.43}
$$

where $\Omega_d^{(-)}$ is a unitary operator which relates the two pictures. We know that $\Omega_d^{(-)}$ is unitary since the two different pictures should only differ by a finite amount. Evidently Eq. (4.43) implies that the actual matrix elements do not depend on Δ,

despite the fact that working to a finite order in perturbation theory will invoke a dependence.

4.5.2 Separation requirements

Any function that separates the hard and soft parts of the Lagrangian effectively must satisfy a number of criteria which will now be outlined. We discuss only the requirements for f_s, since $f_h = 1 - f_s$, and we will only consider three-leg vertices, as this is all we require for the calculations presented in this thesis. In principle the criteria presented can be straightforwardly implemented for four-leg vertices as well. Denoting p_1, p_2 and p_3 as the momenta entering a three-leg vertex, we might require that f_s tends to one if a soft configuration develops, say $p_3 = \lambda p_1$. However, it is known that preventing the soft emission of partons from external lines is sufficient to construct infrared finite amplitudes [72, 73]. Taking this into account we arrive at the following conditions -

1. $f_s \Rightarrow 1$ for all momenta on-shell.

2. $f_s \Rightarrow 0$ for any momenta tending to infinity.

3. f_s is symmetric with respect to all p_i.

4.5.3 The Theta-function split

Having defined the requirements of the splitting function in Section 4.5.2 we shall now specify an appropriate choice for f_s. Many choices are possible, each with their own merits. If we were to implement a completely numerical evaluation, which is our ultimate goal, a simple choice would be that of a theta-function type

separation

$$f_s(p_1, p_2, p_3) \equiv \prod_{i=1}^{3} \Theta(\Delta - |p_i^2|), \quad f_h(p_1, p_2, p_3) \equiv 1 - f_s(p_1, p_2, p_3), \qquad (4.44)$$

where $\Delta > 0$ and defines the scale at which hard/soft separation occurs.
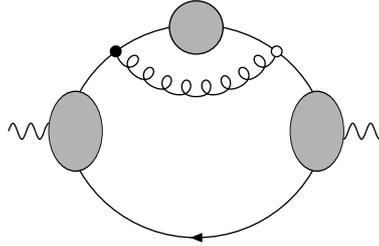
Figure 4.3: For the theta-function split, conflicting hard and soft insertions will set any possible cut of a self-energy diagram to zero. Grey blobs denote any subdiagram.

The great advantage of this separation function is that it sets many cut diagrams to zero immediately. For example any self-energy cut-diagrams with mixed hard and soft vertices will always be zero as depicted in Fig 4.3.
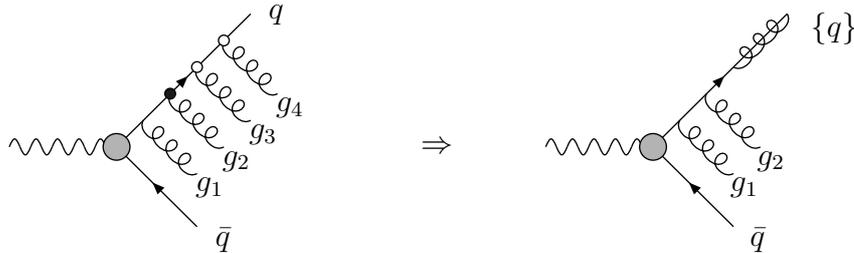
Figure 4.4: Contribution of a conventional Feynman diagram with soft and hard vertices to a Feynman diagram corresponding to dressed external states.

The theta-function also ensures a specific ordering of momentum for real emission processes. If we consider the situation of a soft emission from an external free quark shown in Fig 4.4, we see that the first hard vertex signals the end of any further soft emission since $(q + g_1 + g_2 + g_3 + g_4)^2 \geq (q + g_2 + g_3 + g_4)^2$ for massless external states. Such an observation suggests that, in this situation, we do not need to consider the

division of the vertex of g_1 into hard and soft. The conventional amplitude on the left therefore reduces to an apparent four-parton dressed-state $|\{\bar{q}\, q\, g_1\, g_2\}\rangle$. If we consider cut diagrams then we see that soft configurations where, say g_2 becomes collinear to either g_1 or $\bar{q}$, may still occur and therefore the state also contributes to the dressed states $|\{\bar{q}\, q\, g\}\rangle$ and $|\{\bar{q}\, q\}\rangle$.

4.5.4   A separation for perturbative calculations

Whilst Eq. (4.44) may be a good choice for a numerical approach, it is bad if we want to have analytic control over infrared finite amplitudes. Ultimately we want to avoid analytic calculations all together, however at this stage in the development of the theory it is important to have analytic insight into this new approach. Thus we shall now use a definition practical from the viewpoint of perturbative calculations

$$f_s(p_1, p_2, p_3; \Delta) \equiv \prod_{i=1}^{3} \left(\frac{\Delta}{p_i^2 + \Delta} \right)^N, \tag{4.45}$$

where we take N to be some positive integer. The advantage of this choice is that conventional reduction methods can immediately be applied, albeit at the cost of large algebraic expressions. For example, in practical calculations dependent denominators will appear and these can be trivially simplified as

$$\frac{1}{p_i^2} \frac{\Delta}{p_i^2 + \Delta} = \frac{1}{p_i^2} - \frac{1}{p_i^2 + \Delta}. \tag{4.46}$$

Generalisations of this identity always allow us to return to terms with the same number of denominators as the conventional amplitude, the difference being that the denominators may now carry the imaginary mass term given by Δ.

Taking $N = 1$ in Eq. (4.45) would correspond to the simplest form computationally speaking, since larger values of N would inevitably lead to more reduction and larger analytic expressions. However, it has been empirically discovered that the

choice $N = 1$ appears to lead to an unsatisfactory separation of hard and soft sectors. In Chapter 5 we adopt the the choice $N = 2$ since it gives good agreement with the standard QCD results in the perturbative regime (see Section 5.2.3). In Chapter 6, where we look at higher order corrections in ϕ^3, $N = 1$ is preferred since we are only interested in the pole structure of various amplitudes and do not really care about the finite part.

Finally we note that this choice of split will not have the nice properties of the non-analytic split defined in the previous section where certain contribtutions could immediately be set to zero. Instead such contributions will only be suppressed by the ratio Δ over some hard scale.

4.6   Finiteness of hard diagrams

A crucial ingredient for the consistency of calculations using hard and soft vertex factors, and the construction of dressed states, is that Feynman diagrams with exclusively hard vertices are always free of IR divergences. This is a necessary condition since an infrared finite amplitude at leading-order can have no contributions from diagrams with soft factors. Unfortunately, whilst power-counting arguments exist for Euclidean four-momenta [51], the generalisation to the case of Minkowski space has yet to be achieved. Without a complete framework for showing finiteness of the amplitude we resist discussing the problem in detail and instead refer to the previous work of [48, 49].

The conclusions drawn from [49] essentially rest in Euclidean space and state that possible IR divergences that develop at higher orders in perturbation theory will be removed by the asymptotic gluon generating a mass through soft resummations. However such an argument requires the mixing of different orders in perturbation theory and it is less clear how this may be implemented from a practical point of

view. A way out of this is to redefine how we split up the gluon propagator so that it maintains its transverse structure, see Section 4.7.5. Doing this keeps the gluon massless to all orders in perturbation theory, but also improves the IR behaviour of the perturbatively expanded asymptotic gluon propagator such that the theory appears to be finite when hard factors are present at all vertices.

Less can be said about finiteness in Minkowski space. However, if we observe the hard vertex defined by the non-analytic separation function of Eq. (4.44), we see that this absolutely prevents all propagators at a vertex going on-shell in massless perturbation theory. Since it is impossible for such soft momentum configurations to form it should be impossible for any IR divergences to develop in the region of integration. Thus were the analytic hard/soft separation function to fail at higher order in perturbation theory, this would not be disastrous since the analytic function is simply a tool for investigating the AIP. As mentioned previously, our ultimate goal is a numerical algorithm for computing cross-sections and in such cases the use of a theta-function split is actually desirable.

4.7   Asymptotic interaction propagators

4.7.1   Perturbative solutions

Despite the fact it is not possible to solve exactly for the asymptotic propagators, we can of course perturbatively expand the correlation function in terms of free fields. Using Eq. (4.45), with $N = 2$, for f_s we can determine the asymptotic propagator's behaviour as corrections to the free propagators, where the vertices have been supplemented with soft factors as depicted in Fig 4.5. We shall compute the corrections for both the fermion and the N_F dependent part of the gluon propagator. The splitting of the interaction will be shown to dynamically generate

a gluon mass, we shall then discuss the implications of this mass term.
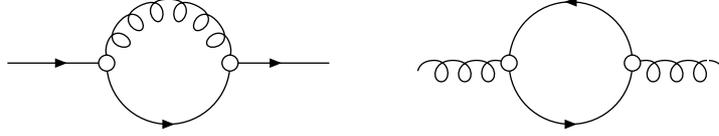
Figure 4.5: Feynman diagrams for lowest order corrections to the fermion and gluon asymptotic propagators, the open circles indicate soft vertex functions restricting the flow of hard momentum configurations.

4.7.2 The fermion propagator

Using the standard interaction picture the asymptotic fermionic propagator can be formally written as

$$
\begin{aligned}
S_\Xi(x_1 - x_2) &= \langle\Theta|\, T\{\Psi_A(x_1)\, \Psi_A(x_2)\}|\Theta\rangle \\
&= \frac{\langle 0|\, T\left\{\psi(x_1)\bar{\psi}(x_2)\, \exp\left(-i\int_{-\infty}^{\infty} d^4x\, \mathcal{L}_S(x)\right)\right\}|0\rangle}{\langle 0|\, T\left\{\exp\left(-i\int_{-\infty}^{\infty} d^4x\, \mathcal{L}_S(x)\right)\right\}|0\rangle}.
\end{aligned}
\tag{4.47}
$$

Evidently at zeroth order we obtain the free field propagator. By defining all higher order one-particle-irreducible diagrams (1PI) for this calculation as the self-energy Σ_Ξ, we can write the perturbative expansion as

$$
S_\Xi = S_\Xi^{(0)} + S_\Xi^{(0)}\, \Sigma_\Xi\, S_\Xi^{(0)} + S_\Xi^{(0)}\, \Sigma_\Xi\, S_\Xi^{(0)}\, \Sigma_\Xi\, S_\Xi^{(0)} + \dots
\tag{4.48}
$$

where $S_\Xi^{(0)}$ denotes the zeroth order correction (i.e order (0) in the coupling g) and therefore corresponds to the free propagator. Re-summing this geometric series allows us to obtain a solution to the fermion asymptotic propagator in terms of 1PI diagrams -

$$
S_\Xi = \frac{S_\Xi^{(0)}}{1 - S_\Xi^{(0)}\, \Sigma_\Xi}.
\tag{4.49}
$$

We can then compute the leading contribution to Σ_Ξ, which is given by

$$\Sigma_\Xi^{(2)} = - \frac{g^2 \, C_F \, \Delta^{12}}{(p^2 + \Delta)^4} \int \frac{d^4 k}{(2\pi)^4} \frac{\gamma_\mu (\not{p} + \not{k}) \gamma_\nu}{(p+k)^2 \, [(p+k)^2 + \Delta]^4} \frac{\left(g^{\mu\nu} - \xi_x \frac{k^\mu k^\nu}{k^2} \right)}{k^2 \, [k^2 + \Delta]^4}, \quad (4.50)$$

where the usual causality prescription is taken for each Feynman denominator and the external momentum p^μ is off-shell ($\xi_x = 1 - \xi$ for brevity). This integral is well-defined in four-dimensions and may therefore by directly evaluated using numerical integration or simplified to master integrals using some automated reduction routine (see Appendix C). The resulting expression is rather long and can be found in Appendix A, instead we substitute the result into Eq. (4.49) and examine the behaviour of the resummed propagator at large values of p^2, where we find

$$S_\Xi^{(2)} \to \frac{i \, \not{p}}{p^2} \left[1 - \left(\frac{\Delta}{p^2} \right)^9 \frac{C_F \, g^2 \, (-4 + \xi_x)}{96 \, \pi^2} + \cdots \right]. \quad (4.51)$$

This is an essentially negligible contribution, it is in correspondence with setting $\Delta = 0$ and recovering the free propagator. Since we are including only soft contributions to the propagator it can of course be argued that the coupling should be defined at the scale Δ and therefore an all orders determination of Σ_Ξ would be necessary to make statements about the behaviour of the two-point function. However, we intend to work entirely within the realms of perturbatively calculable observables, i.e. infrared safe, where a weak coupling expansion is justified and where the preceding statements can be made with some confidence. Similarly we can look at the region where the Δ becomes the large scale, in this limit the propagator behaves as

$$S_\Xi^{(2)} \to \frac{i \, \not{p}}{p^2} \left[1 - \frac{C_F \, g^2 \left(-223 + 328 \, \xi_x + 140 \, (-1 + \xi_x) \ln(\frac{p^2}{\Delta}) \right)}{2240 \, \pi^2} + \cdots \right]^{-1}. \quad (4.52)$$

Eq. (4.52) shows that while the infrared behaviour appears to be altered no mass term has been generated and the propagator is still singular at $p^2 = 0$. Numerically[10] the behaviour of the asymptotic fermion propagator appears to trace that of the free one for timelike p^μ; the spacelike behaviour is similar but carries some complicated structure associated with branch cuts of logarithms.

4.7.3 The gluon propagator

Following the same methodology for the asymptotic fermion propagator applied to the gluon propagator we can write

$$D_\Xi^{\mu\nu}(p) = D_{\Xi,0}^{\mu\nu}(p) + D_{\Xi,0}^{\mu\alpha}(p)\Pi_{\Xi\alpha\beta}(p)D_{\Xi,0}^{\beta\nu}(p) + \dots, \tag{4.53}$$

where $D_\Xi^{\mu\nu}(p)$ denotes the full gluon two-point function and $D_{\Xi,0}^{\mu\nu}(p)$ denotes the normal propagator of free field theory Eq. (2.4). Parameterising the self-energy as

$$\Pi_\Xi^{\mu\nu}(p) = A(p^2)\, p^2\, g^{\mu\nu} + B(p^2)\, p^\mu p^\nu, \tag{4.54}$$

we can write down a general form for Eq. (4.53) by substituting with Eqs. (4.54) and (2.4) to obtain an expression for the nth term of the expansion of the full two-point function as

$$\frac{(-i)^n}{p^2}\left(A(p^2)^{n-1}\left(g^{\mu\nu} - \frac{p^\mu p^\nu}{p^2}\right) + \xi^n\left(A(p^2) + B(p^2)\right)^{n-1}\frac{p^\mu p^\nu}{p^2}\right). \tag{4.55}$$

---

[10]Standard values for constants and couplings have been taken and ξ_x has been taken to range from -5 to 5.

We therefore have two geometric series, one describing the transverse part of the propagator the other describing the longitudinal part, they are resummed to give

$$D_\Xi^{\mu\nu}(p) = -\frac{i}{p^2}\left(\frac{T^{\mu\nu}}{1+i\,A(p^2)} + \frac{\xi\,L^{\mu\nu}}{1+i\,\xi\,(A(p^2)+B(p^2))}\right), \qquad (4.56)$$

where $T^{\mu\nu}$ and $L^{\mu\nu}$ respectively denote the transverse and longitudinal tensor structure displayed in Eq. (4.55). In the standard approach gauge invariance requires that $B(p^2) = -A(p^2)$ and the longitudinal part receives no radiative corrections to all orders in perturbation theory. We can write the lowest order correction to $\Pi_\Xi^{\mu\nu}(p)$ for the fermion loop as

$$\Pi_\Xi^{\mu\nu\,(2)} = -\frac{g^2\,N_F\,T_R\,\Delta^{12}\,\delta^{ab}}{(p^2+\Delta)^4}\int\frac{d^4k}{(2\pi)^4}\frac{tr(\gamma^\mu(\slashed{p}+\slashed{k})\gamma^\nu\slashed{k})}{k^2\,[k^2+\Delta]^2\,(p+k)^2\,[(p+k)^2+\Delta]^2}, \quad (4.57)$$

where N_F is the number of flavours running in the loop, T_R is the normalisation constant of the fundamental representation and δ^{ab} is the colour factor. The full result for this integral can also be found in Appendix A. Including only Eq. (4.57), the behaviour of the resummed gluon propagator, for the limit $p^2 \gg \Delta$ is given by

$$D_\Xi^{\mu\nu}(p) \to -\frac{i}{p^2}\left[T^{\mu\nu} + \xi\,L^{\mu\nu} + \left(\frac{\Delta}{p^2}\right)^9\frac{g^2\,N_F\,T_R}{12\,\pi^2}\left(2\,T^{\mu\nu} - 3\,\xi^2\,L^{\mu\nu}\right) + \cdots\right],$$
$$(4.58)$$

in correspondence with the soft interactions not altering the high energy behaviour of the propagator. If however we look in the soft region of the propagator, $\Delta \gg p^2$, we find that

$$\begin{aligned}
A(p^2) &\to \frac{i\,g^2\,N_F\,T_R}{56\,\pi^2}\left(\frac{\Delta}{p^2} + \frac{14}{3}\ln\frac{p^2}{\Delta} + \frac{1307}{270} + \cdots\right)\\
B(p^2) &\to \frac{i\,g^2\,N_F\,T_R}{12\,\pi^2}\left(-\ln\frac{p^2}{\Delta} - \frac{1937}{1260} + \cdots\right)
\end{aligned} \qquad (4.59)$$

indicating that propagator's pole has been shifted from $p^2 = 0$. Thus the effect of including soft interactions into the gluon propagator is to dynamically generate a gluon mass. This is in correspondence with the fact that our split of the Lagrangian violates gauge-invariance; the gluon's masslessness to all orders in normal perturbation is a direct consequence of this symmetry, so we expect a gluon mass to be generated for the asymptotic interaction picture. Solving for the gluon mass perturbatively we find that, to order α_s, the gluon's mass is given by

$$m_g^2 = \frac{g^2 N_F T_R \Delta}{56 \pi^2}. \tag{4.60}$$

Of course a full one-loop calculation necessarily requires the calculation of the gluon loops and the accompanying ghost correction, these additional calculations cannot change the above result in the sense that none of them are proportional to the colour structure N_F.

4.7.4   Perturbative calculations and transversality

We have shown that dressing the free gluon propagator appears to assign some inertia to it, this could be said to be in correspondence with confinement. Gluons afterall do not propagate over large distances, so when we attempt a more accurate solution to their equations of motion we might expect this to be confirmed by the dynamic generation of a mass term. However, from the viewpoint of free-field perturbative calculations, the asymptotic interaction picture's resummed propagators now introduce calculational difficulties.

It is basically impossible to take the one-loop resummed forms presented in the previous two sections and attempt to perform analytic perturbative calculations using them; ultimately we must use expanded forms for the resummed propagators. Using the expanded forms, as advocated in Section 4.4, has the immediate

advantage of linking straight back to standard perturbation theory. Thus, in the asymptotic interaction picture, to whatever order we calculate for some fully inclusive process, if we use expanded propagators and external states, then we must obtain the same results as compared to conventional perturbation theory.

$$\mathcal{A} \quad = \quad \mathcal{A}^\nu \, \frac{-i}{p^2} \left(g_{\nu\mu} + (1-\xi) \frac{p_\nu p_\mu}{p^2} \right) \, (-i \, \Pi^{\mu\alpha}) \, \varepsilon_\alpha$$

Figure 4.6: Depiction of the approach to computing the on-shell LSZ residue of the gauge boson propagator in perturbation theory.

Unfortunately, the way we split up the gluon self-energy violates the transverse structure of the perturbative gluon, it is no longer clear how we can compute the wave-function renormalisation necessary for the standard LSZ formalism. Consider the usual procedure for computing the on-shell residue of the external gauge boson field shown in Fig 4.6. Usually the orthogonality of the polarisation vector is sufficient to remove all tensor structures like $p^\mu p^\nu$, we are then left with the rest of the process denoted as $\mathcal{A}$ and the $g^{\mu\nu}$ part of the gluon self-energy multiplied by $1/p^2$. Depending on the order we are calculating at, the self-energy is given by the wave-function renormalisation constant of the gluon field and this is proportional to p^2, therefore the on-shell limit is regular. By violating transversality in the perturbatively expanded asymptotic interaction picture we instead find terms like $\Delta \, g^{\mu\nu}$ related to the generation of a gluon mass that are not regular in this limit and prevent a straightforward application of the LSZ formalism.

Such a predicament leaves us with the options of either modifying the LSZ or changing precisely how we split up the gluon propagator. The latter option represents a more pragmatic route to take since the split of the Lagrangian is rather ad

hoc anyway and it is quite possible that some choices may satisfy the separation requirements of Section 4.5.2 but lead to an ill-defined perturbative expansion. Indeed a simple modification as used in [74] maintains the transverse structure of the propagator. For the fermion one-loop diagram this is done by taking the standard expression for the gluon self-energy and adding a term that amounts to zero in dimensional regularisation. Having done this the transverse structure can be extracted completely from the integral; once this modification has been performed, then it is permissable to introduce hard and soft vertex factors. The masslessness of the gluon is maintained and perturbative calculations using standard methods may be applied.

4.7.5 Subtracting the quadratic divergence of the gluon propagator

In order to maintain the transverse structure of the propagator, we re-consider the one-loop calculation of the N_F part of the asymptotic propagator. Taking a different choice for the routing of momenta, we write the conventional perturbative expression as

$$\Pi^{\mu\nu\,(2)} = -g^2\,N_F\,T_R\,\delta^{ab} \int \frac{d^d k}{(2\pi)^d} \frac{tr(\gamma^\mu(\slashed{k} + \frac{\slashed{p}}{2})\gamma^\nu(\slashed{k} - \frac{\slashed{p}}{2}))}{(k + \frac{p}{2})^2\,(k - \frac{p}{2})^2}, \qquad (4.61)$$

where d denotes the space-time dimension. We then add to this expression, as suggested by [74], a term that evaluates to zero in dimensional regularisation

$$0 = -g^2\,N_F\,T_R\,\delta^{ab} \int \frac{d^d k}{(2\pi)^d} \times$$
$$\frac{-8\,(d-1)\,k^\mu k^\nu + 2\,p^\mu p^\nu + g^{\mu\nu}\,(\,4\,(d-1)\,k^2 + (d-3)\,p^2\,)}{(d-1)\,(k + \frac{p}{2})^2\,(k - \frac{p}{2})^2}. \qquad (4.62)$$

Adding Eq. (4.61) and Eq. (4.62) gives a scalar integral that ensures gauge invariance for loop corrections even when hard and soft factors are amended to the integral, the integral takes the form

$$\Pi^{\mu\nu\,(2)} = -g^2\,N_F\,T_R\,\delta^{ab} \int \frac{d^dk}{(2\pi)^d} \frac{2\,(d-2)(\,g^{\mu\nu}\,p^2 - p^\mu\,p^\nu\,)}{(d-1)\,(k+\frac{p}{2})^2\,(k-\frac{p}{2})^2}. \tag{4.63}$$

The full expression for this result is in Appendix A; expanding for $\Delta \gg p^2$ we obtain

$$A(p^2) = -B(p^2) \to \frac{i\,g^2\,N_F\,T_R}{12\,\pi^2} \left(\ln\frac{p^2}{\Delta} + \frac{223}{140} + \cdots \right), \tag{4.64}$$

thus no mass term is generated.

Chapter 5

Perturbative Calculations Using

IR-Finite QCD

5.1 Perturbative calculations

Now that we have defined an analytic separation of the QCD Lagrangian amenable to modern perturbative techniques, Eq. (4.45), the next step is to test the theory. As implied by Section 4.4 we take the pragmatic approach of computing all combinations of hard and soft vertices. That is we take the standard integrand defined by a particular Feynman diagram and multiply by appropriate hard and soft separation functions at each vertex.

In the calculations to be presented we shall avoid the additional difficulties associated with initial state radiation and only examine $e^+(l_1)e^-(l_2) \to$ hadrons in QCD. We shall aim for maximal simplicity of the method, so we leave the QED Lagrangian intact and take Feynman gauge for the photon propagator, the amplitude for some process can then be written as

$$\mathcal{A} = L^\mu(l_1, l_2) \frac{-ig^{\mu\sigma}}{s} H^\sigma(p_i), \tag{5.1}$$

where s denotes the centre of mass energy, $L^\mu(l_1, l_2)$ is the leptonic tensor and the hadronic tensor, $H^\nu(p_i)$, is a function of the final state momenta p_i. The amplitude-squared can then be written as

$$\left|\mathcal{A}\right|^2 = L^{\mu\nu}(l_1, l_2) H_{\mu\nu}(p_i), \tag{5.2}$$

where we have defined L to absorb the photon propagator and normalisation of the cross-section, $1/8s$, obtained by neglecting fermion masses and averaging over initial spins. We also define the integral over the final state momenta to be carried by the hadronic tensor $H^{\mu\nu}(p_i)$ (see Section 3.1.3 for representations of the final state phase-space). The leptonic part then involves a Dirac trace and can be written as

$$L^{\mu\nu}(l_1, l_2) = \frac{e^2}{2\,s^3} \left(\frac{s}{2}\, g^{\mu\nu} - l_1^\mu l_2^\nu - l_1^\nu l_2^\mu \right). \tag{5.3}$$

This expression can be further simplified by taking the average of the component matrix to obtain

$$L^{\mu\nu}(q) = \frac{e^2}{6\,s^3} \left(s\, g^{\mu\nu} - q^\mu q^\nu \right), \tag{5.4}$$

with $q = l_1 + l_2$. We further note that for any calculation corresponding to a physical observable, the hadronic tensor $H_{\mu\nu}(p_i)$ must conserve the electromagnetic current, therefore the second term of Eq. (5.4) may be neglected and it suffices to compute $H_\mu^\mu(q)$.

5.2 $e^+ e^- \rightarrow$ hadrons at $\mathcal{O}(\alpha_s)$

Before discussing the results of the calculation we shall consider how we expect to form the infrared finite amplitudes $|\{q_{p_1}\, \bar{q}_{p_2}\}\rangle$ and $|\{q_{p_1}\, \bar{q}_{p_2}\, g_{p_3}\}\rangle$ detailed in Section 4.4.2. At next-to-leading order (NLO), $|\{q_{p_1}\, \bar{q}_{p_2}\}\rangle$, consists of a free quark and an antiquark pair carrying momentum p_1 and p_2 respectively, plus an un-

resolved free gluon. This gluon may be unresolved because it corresponds to a virtual vertex correction or it is a soft real emission, the combination of these two possibilities leads directly to the cancellation of infrared poles and hence a finite four-dimensional amplitude. In the case of $|\{q_{p_1} \bar{q}_{p_2} g_{p_3}\}\rangle$ all three partons are resolved and, outside the limit of the two-parton phase-space, a one-to-one mapping exists between the asymptotic states and the free-states. This amplitude will contain vertices that are entirely hard and therefore will be finite in all regions of the massless three-parton phase-space.

5.2.1 The Born term

As discussed we are concerned with only the hadronic part of the amplitude and therefore we look at elements of the form $\gamma^* \to$ hadrons. At leading order (LO) the infrared finite amplitude matches the standard calculation and is given by

$$\mathcal{A}^{(0)}(q_{p_1}, \bar{q}_{p_2}) = \mathcal{A}^{(0)}(\{q_{p_1}, \bar{q}_{p_2}\}) = (-ie)\delta_{12}\langle p_1|\gamma^\mu|p_2\rangle \,, \tag{5.5}$$

where $\langle p_1|$ and $|p_2\rangle$ represent the spinors of massless fermions. The superscript (0) indicates the power of the strong coupling g, e is the QED coupling and δ_{12} is the colour factor.

5.2.2 The dressed three-parton amplitude

To obtain the three-parton dressed state amplitude, $\mathcal{A}^{(1)}(\{q_{p_1} \bar{q}_{p_2} g_{p_3}\})$, we multiply the conventional amplitude by hard factors at each QCD vertex. Using the hard

separation function defined by Eq. (4.45), with $N = 2$, we obtain

$$
\mathcal{A}^{(1)}(\{q_{p_1}, \bar{q}_{p_2}, g_{p_3}\}) = (ieg)T_{12}^3 \left(\frac{\langle p_1 | \not{\epsilon}(\not{p}_1 + \not{p}_3)\gamma^\mu | p_2 \rangle}{(\Delta + s_{13})^2} (2\Delta + s_{13}) - \right.
$$
$$
\left. \frac{\langle p_1 | \gamma^\mu (\not{p}_2 + \not{p}_3)\not{\epsilon} | p_2 \rangle}{(\Delta + s_{23})^2} (2\Delta + s_{23}) \right), (5.6)
$$

$\epsilon = \epsilon(p_3)$ denotes the polarisation vector of the gluon, T_{12}^3 denotes the colour matrix and $s_{ij} \equiv (p_i + p_j)^2$. The separation function will not generally maintain gauge invariance and we see that this symmetry is violated by terms suppressed by the soft scale

$$
q_\mu \, \mathcal{A}^{(1)}(\{q_{p_1}, \bar{q}_{p_2}, g_{p_3}\}) = (ieg)T_{12}^3 \, \langle p_1 | \not{\epsilon} | p_2 \rangle \left(\frac{\Delta^2}{(\Delta + s_{13})^2} - \frac{\Delta^2}{(\Delta + s_{23})^2} \right). \quad (5.7)
$$

In principle this means that the three-jet rate computed from $|\{q_{p_1} \, \bar{q}_{p_2} \, g_{p_3}\}\rangle$ is gauge-dependent. Such unphysical violations would clearly be disastrous for the theory were it not for the fact they are heavily suppressed and negligible. At higher-order in the strong coupling, such non-cancellations will become a problem, since they may be multiplied by factors containing poles in $\epsilon = \frac{4-d}{2}$, this will lead us to modifying the approach for calculating infra-red finite amplitudes.

5.2.3 Three-jet observables

Now that we have determined the dressed three-parton amplitude at LO we are at liberty to compute any infrared safe three-jet observable that could be obtained using conventional methods. The key point is that both infrared finite and conventional amplitudes should give the same results in regions of phase-space where perturbation theory is considered to be reliable i.e. where a hard scale is present. The only proviso to this is that the soft scale Δ should be smaller than the experimental resolution defined in the observable function, if this is not the case

then it will become possible to resolve this non-fundamental dressed construct. In the region where perturbation theory breaks down the results for observables are meaningless, the important difference between the conventional and infrared finite amplitudes is that the latter will give a meaningless, but finite, result.
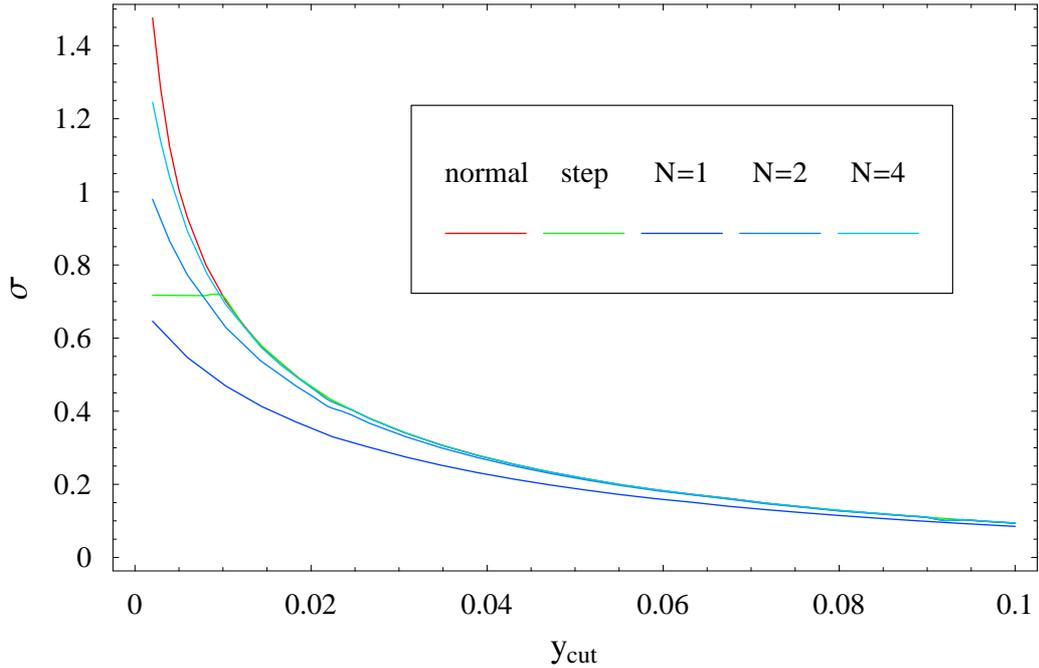
Figure 5.1: The three-jet rate as a function of the resolution parameter, $\Delta_s = 0.01$.

Thus using this amplitude we can easily calculate a simple observable like the three-jet cross-section. We do this by defining a three-jet event to be measured if $\min\{y_{ij}\} > y_{\mathrm{cut}}$, with $y_{ij} \equiv s_{ij}/s$ and y_{cut} defining some fraction of the total centre of mass energy. Indeed for this observable it is straightforward to test a variety of different soft-separation functions in order to compare the quality of hard/soft separation, Figure 5.1 for $\Delta_s = \Delta/s = 0.01$ depicts this. The red line denotes the standard perturbative result which diverges in the two-jet limit, $y_{\mathrm{cut}} \to 0$, the green line was computed using Eq. (4.44) and other lines show various values of N for Eq. (4.45). Crucially we see that the infrared finite amplitudes tend to finite values for $y_{\mathrm{cut}} \to 0$. Deviations from the standard red line should be

restricted to the region where perturbation theory breaks down, i.e where the three-jet rate exceeds the total cross-section and no line can be expected to agree with experiment.
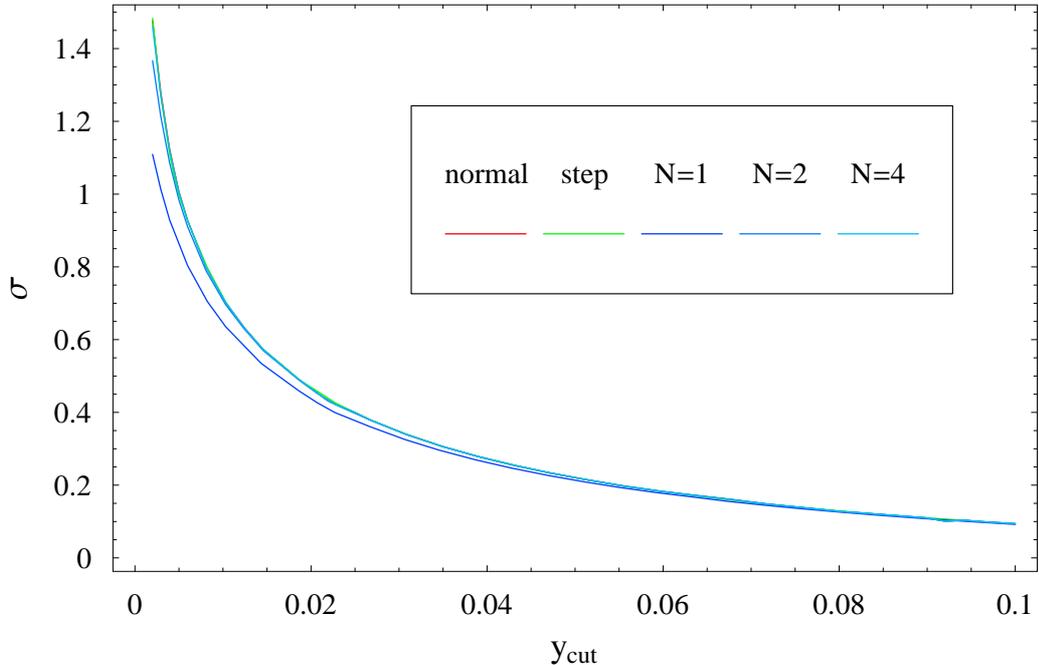
Figure 5.2: The three-jet rate as a function of the resolution parameter, $\Delta_s = 0.002$.

The dark blue $N = 1$ line also appears to disagree where perturbation theory is a valid approximation and therefore does not offer a suitable separation of hard and soft regions. For this reason we have chosen to evaluate amplitudes in the rest of this Section using $N = 2$, where the agreement with the conventional calculational method is improved over $N = 1$. The $N = 4$ curve is an even better approximation to the red curve and we may assume that this trend continues for larger N. However, larger N results in technically harder analytic calculations and since we actually want numerically (in addition to analytically) finite amplitudes in soft regions of phase-space, there is no apparent benefit from choosing larger values of N. Of course, whilst not amenable to analytic calculation, the theta-function split has the advantage of setting certain Feynman graphs to zero and

ensures infrared finiteness to all orders as previously discussed in Chapter 4.

If we lower the soft scale to $\Delta_s = 0.002$ (Figure 5.2), then we see a significant improvement for all analytic separation functions and this is a reflection of the resolution paramater being generally an order of magnitude larger than the soft-scale. From analysis of this simple example we can derive some confidence, at least to this order in perturbation theory, that the $N = 2$ choice of split will give a satisfactory separation of hard and soft regimes and that we can proceed to calculate using this choice.

5.2.4 The dressed two-parton amplitude
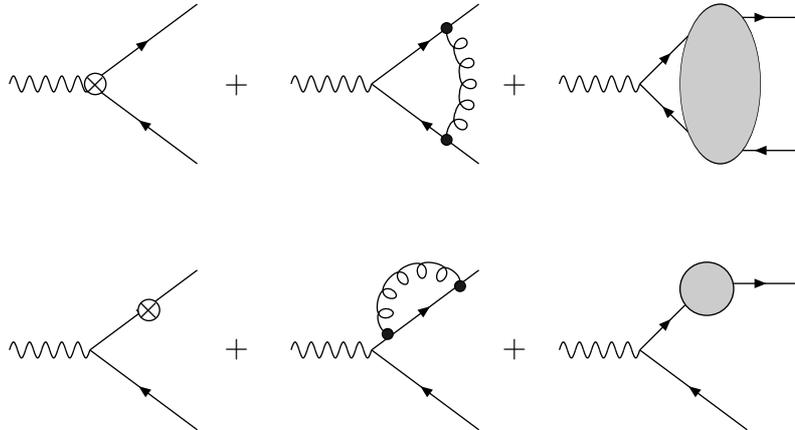
Figure 5.3: Schematic structure of the amplitude $\mathcal{A}^{(2)}\left(\{q_{p_1} \bar{q}_{p_2}\}\right)$. The conventional diagrams have their QCD vertices made hard (black circles), the usual UV counter-terms remain (crossed circles) and the grey blobs denote diagrams related to the modification of the LSZ formalism. A correction to the anti-quark leg must also be included.

To determine $\mathcal{A}^{(2)}(\{q_{p_1} \bar{q}_{p_2}\})$ we must consider contributions that come from the inherent modification to the LSZ formalism. First of all we have the contribution $\mathcal{A}_{\mathrm{H}}^{(2)}(\{q_{p_1} \bar{q}_{p_2}\})$ that comes from the hard scattering and requires renormalisation,

plus an additional piece $\mathcal{A}_{\mathrm{S}}^{(2)}(\{q_{p_1}\,\bar{q}_{p_2}\})$ due to modifications to the LSZ formalism, see Figure 5.3.

The hard vertex contribution is obtained by taking the standard loop integral, where the usual $+i0^+$ prescription is understood, and multiplying by the appropriate hard vertex factors

$$\mathcal{A}_{\mathrm{H}}^{(2)}(\{q_{p_1}\,\bar{q}_{p_2}\}) = \tag{5.8}$$
$$(ieg^2)\,C_F \int \frac{d^D k}{(2\pi)^D} \frac{\langle p_1|\gamma^\alpha(\slashed{p}_1 + \slashed{k})\gamma^\mu(\slashed{k} - \slashed{p}_2)\gamma^\beta|p_2\rangle}{k^2\,(k+p_1)^2\,(k-p_2)^2} \left(g_{\alpha\beta} - (1-\xi)\frac{k_\alpha k_\beta}{k^2}\right)$$
$$\times \left(1 - \frac{\Delta^4}{[k^2 + \Delta]^2\,[(k+p_1)^2 + \Delta]^2}\right)\left(1 - \frac{\Delta^4}{[k^2 + \Delta]^2\,[(k-p_2)^2 + \Delta]^2}\right).$$

C_F is the usual Casimir operator of QCD and ξ denotes the gauge parameter.

To compute this integral we take advantage of the linear dependence of Feynman denominators to reduce the problem to only three-point functions with propagators raised to some power, see Eq. (4.46). Davdychev tensor reduction [57] followed by Tarasov et al's scalar reduction algorithm [58] (see also Appendix C) is used to reduce the result to a simple set of massless and massive basis integrals, where the mass scale is $i\sqrt{\Delta}$ and all master integrals can be found in Appendix A.

Substituting the basis integrals, expanding in Δ_s and dropping suppressed contributions we obtain

$$\mathcal{A}_{\mathrm{H}}^{(2)}(\{q_{p_1}\,\bar{q}_{p_2}\}) = \mathcal{A}_{\mathrm{ct}}^{(2)}(\{q_{p_1}\,\bar{q}_{p_2}\}) + \mathcal{A}^{(0)}(\{q_{p_1}\,\bar{q}_{p_2}\})\,C_F\,c_\epsilon\,\frac{\alpha}{4\pi} \times \tag{5.9}$$
$$\left[\left(\frac{-s}{\mu^2}\right)^{-\epsilon}\frac{\xi}{\epsilon} - 2\ln^2\Delta_s + \frac{-1+11\xi}{3} - \frac{2\pi^2}{3} + \mathcal{O}(\Delta_s)\right],$$

where $c_\epsilon = (4\pi)^\epsilon e^{\epsilon\gamma_E}$. Only an ultra-violet pole remains in this expression and this is cancelled exactly by the standard $\overline{MS}$ counter-term diagram, $\mathcal{A}_{\mathrm{ct}}^{(2)}(\{q_{p_1},\bar{q}_{p_2}\})$.

Similarly, due to the presence of the hard factors, the wave-function graph of the

quark propagator is infrared-finite and will give an overall constant once renormalised. This is in contrast to the normal perturbative calculation where the corresponding integral vanishes in dimensional regularisation and is therefore left with an infrared pole once the $\overline{MS}$ wave function-renormalisation counter-term has been added. Thus the hard asymptotic wave function constant for the external quark field, before renormalisation, is found to be

$$Z_{\mathrm{A}} = 1 - \frac{\alpha}{4\pi}\, C_F\, c_\epsilon \left(\frac{-\Delta}{\mu^2}\right)^{-\epsilon} \left[\frac{\xi}{\epsilon} - \frac{3}{4} - \frac{383\xi}{210}\right]. \tag{5.10}$$

Combining both $\overline{MS}$ renormalised contributions gives

$$\mathcal{A}_{\mathrm{H}}^{(2)}(\{q_{p_1}\,\bar{q}_{p_2}\}) = \mathcal{A}^{(0)}(\{q_{p_1}\,\bar{q}_{p_2}\})\, C_F\, \frac{\alpha}{4\pi} \tag{5.11}$$
$$\times\ \left[-2\ln^2\Delta_s + \xi\ln\Delta_s + \frac{5}{12} + \frac{129\xi}{70} - \frac{2\pi^2}{3} + \mathcal{O}(\Delta_s)\right].$$
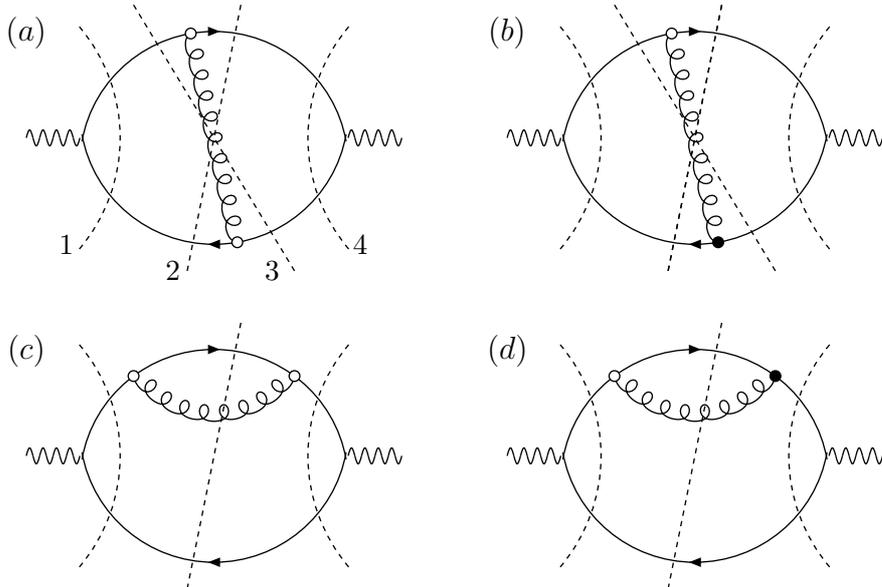
Figure 5.4: Cut diagrams contributing to the amplitude squared for the final state $|\{q\,\bar{q}\}\rangle$. Additional diagrams obtained through symmetry are understood.

What is left now is to compute the contributions due to modification of the LSZ

formalism $\mathcal{A}_{\mathrm{S}}^{(2)}(\{q_{p_1}\,\bar{q}_{p_2}\})$, this consists of the Feynman diagrams shown Figure 5.4. As a consequence of *the cutting rules* [75] and unitarity, each sum-over-cuts is guaranteed to be finite provided the gluon polarisation sum is treated identically to the gluon propagator, this amounts to taking Feynman gauge, $\xi = 1$. Failure to treat the polarisation sum and propagators the same will instead lead to poles in ϵ that cancel only once both topologies of Fig 5.4 have been combined.

Construction of finite amplitudes proceeds by taking, for example, the real cuts 2 and 3 and dividing their contributions between the virtual cut 4 and its conjugate cut 1. This amounts to re-writing terms with $\ln s$ and $\ln^2 s$ as $\ln s = 1/2(\ln(-s) + \ln^*(-s))$ and $\ln^2 s = 1/2(\ln^2(-s) + \pi^2) + 1/2(\ln^2(-s) + \pi^2)^*$, then assigning the first term of each equality to cut 4 and the second term to the conjugate cut 1. Using this division of the soft real diagrams it is possible to write down finite amplitudes. An explicit example is the sum of Eq. (5.12) and Eq. (5.13)

$$
\begin{aligned}
\mathcal{A}_{(a)\,4}^{(2)} \;=\; & \mathcal{A}^{(0)}(q_{p_1}\,\bar{q}_{p_2})\,C_F\,c_\epsilon\,\frac{\alpha}{4\pi}\left(\frac{-s}{\mu^2}\right)^{-\epsilon} \times \\
& \left(-\frac{2}{\epsilon^2} + \frac{-3-\xi+4\ln\Delta_s}{\epsilon} - 4\ln^2\Delta_s + 2(3+\xi)\ln\Delta_s - 2\xi - \frac{2\pi^2}{3} + \mathcal{O}(\Delta_s)\right)
\end{aligned}
\tag{5.12}
$$

$$
\begin{aligned}
\mathcal{A}_{(a)\,2\&3}^{(2)} \;=\; & \mathcal{A}^{(0)}(q_{p_1}\,\bar{q}_{p_2})\,C_F\,c_\epsilon\,\frac{\alpha}{4\pi}\left(\frac{-s}{\mu^2}\right)^{-\epsilon} \times \\
& \left(\frac{2}{\epsilon^2} + \frac{4\,(1-\ln\Delta_s)}{\epsilon} + 4\ln^2\Delta_s - 8\ln\Delta_s + \frac{5\,\pi^2}{3} + 2 + \mathcal{O}(\Delta_s)\right),
\end{aligned}
\tag{5.13}
$$

where the poles cancel provided $\xi = 1$.

Using Feynman gauge and summing over the cuts of diagrams a, b, c and d in

Figure 5.4, we obtain

$$
\mathcal{A}^{(2)}_{(a)}(\{q_{p_1}\,\bar{q}_{p_2}\}) \;=\; \mathcal{A}^{(0)}(q_{p_1}\,\bar{q}_{p_2})\,C_F\,\frac{\alpha}{4\pi}\left(\pi^2 + \mathcal{O}(\Delta_s)\right) \tag{5.14}
$$

$$
\mathcal{A}^{(2)}_{(b)}(\{q_{p_1}\,\bar{q}_{p_2}\}) \;=\; \mathcal{A}^{(0)}(q_{p_1}\,\bar{q}_{p_2})\,C_F\,\frac{\alpha}{4\pi}\left(-\frac{2}{3} + \mathcal{O}(\Delta_s)\right) \tag{5.15}
$$

$$
\mathcal{A}^{(2)}_{(c)}(\{q_{p_1}\,\bar{q}_{p_2}\}) \;=\; \mathcal{A}^{(0)}(q_{p_1}\,\bar{q}_{p_2})\,C_F\,\frac{\alpha}{4\pi}\left(-\frac{101}{840} + \mathcal{O}(\Delta_s)\right) \tag{5.16}
$$

$$
\mathcal{A}^{(2)}_{(d)}(\{q_{p_1}\,\bar{q}_{p_2}\}) \;=\; \mathcal{A}^{(0)}(q_{p_1}\,\bar{q}_{p_2})\,C_F\,\frac{\alpha}{4\pi}\left(\frac{31}{840} + \mathcal{O}(\Delta_s)\right). \tag{5.17}
$$

Including the contributions of all diagrams obtained through symmetry operations we find

$$
\mathcal{A}^{(2)}_{\mathrm{S}}(\{q_{p_1}\,\bar{q}_{p_2}\}) = \mathcal{A}^{(0)}(q_{p_1}\,\bar{q}_{p_2})\,C_F\,\frac{\alpha}{4\pi}\left(-\frac{599}{420} + \pi^2 + \mathcal{O}(\Delta_s)\right). \tag{5.18}
$$

Finally, combining Eq. (5.11) with Eq. (5.18) and not dropping terms suppressed by Δ_s we obtain the infrared-finite amplitude

$$
\begin{aligned}
\mathcal{A}^{(2)}(\{q_{p_1}\,\bar{q}_{p_2}\}) \;=\;\; & \mathcal{A}^{(0)}(q_{p_1}\,\bar{q}_{p_2})\,C_F\,\frac{\alpha}{4\pi}\times \\[4pt]
& \left[\Delta_s^2 - 2\Delta_s + \frac{(1+\pi^2)}{3} - 2\left(\ln^2\frac{\Delta_s}{1+2\Delta_s} + 2\,\mathrm{Li}_2\frac{\Delta_s}{1+2\Delta_s}\right) + \cdots \right. \\[4pt]
& \left. + \frac{1}{2(1+\Delta_s)} + \frac{(1 - 2\Delta_s - 6\Delta_s^2 - 2\Delta_s^3 + 2\Delta_s^4)}{1+2\Delta_s}\ln\left(\frac{\Delta_s}{1+\Delta_s}\right)\right].
\end{aligned} \tag{5.19}
$$

As can be seen, Eq. (5.19) is explicitly finite and well defined in four dimensions. Again, like the case of the three-parton dressed amplitude, it is now possible to go ahead and compute any two-jet observable. We obtain a prediction for the cross-section by computing the amplitude-squared, obtained by contracting the NLO state $|\{q_{p_1}\,\bar{q}_{p_2}\}\rangle$ with its LO companion, and then integrating over the two-parton phase-space.

Using this amplitude we choose to compute the two-jet rate as shown in Figure 5.5, where $y_{\mathrm{cut}} = 0.1$ and the rate has been plotted as a function of Δ_s. The red line
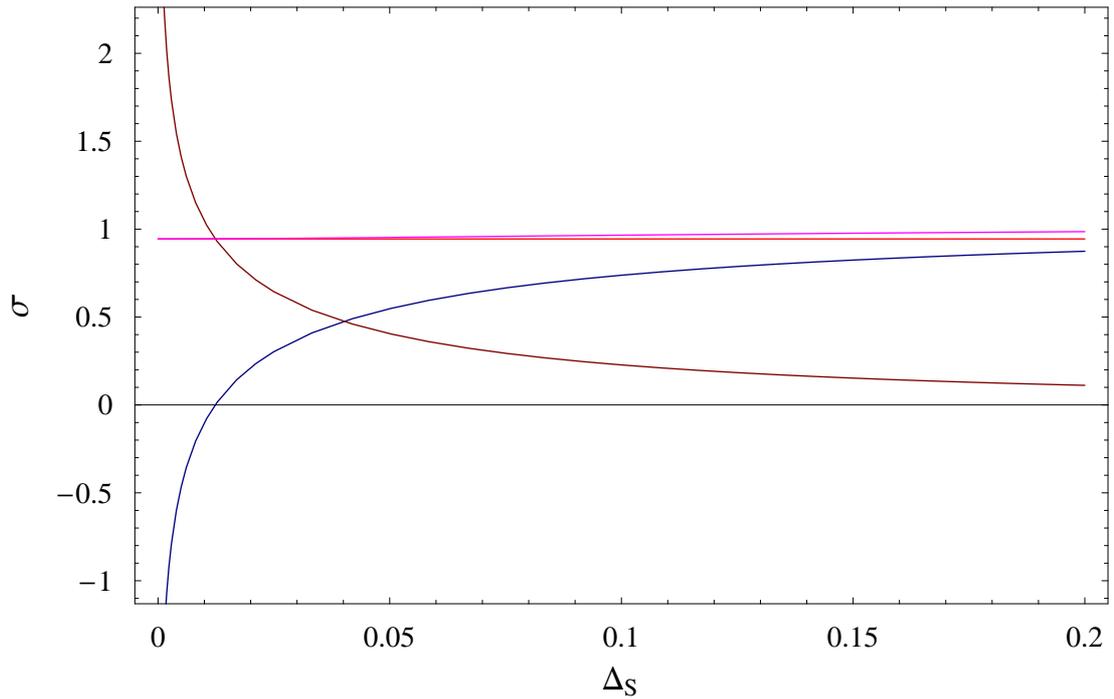
Figure 5.5: The two-jet rate as a function of Δ_s ($y_{cut} = 0.1$), red line displays the standard perturbative result, pink curve the sum of the contributions from $|\{q_{p_1} \bar{q}_{p_2}\}\rangle$ (dark blue) and $|\{q_{p_1} \bar{q}_{p_2} g\}\rangle$ (dark red).

displays the standard perturbative result with the approaching pink curve the sum of the contributions from $|\{q_{p_1} \bar{q}_{p_2}\}\rangle$ (dark blue) and $|\{q_{p_1} \bar{q}_{p_2} g\}\rangle$ (dark red). Yet again we see the benefit of using infrared finite amplitudes. In the standard approach we add the divergent contributions from the two-parton and three-parton final states to give the finite result that is the red line. In contrast the dressed-state rates are individually finite and therefore manageable by a numerical integration routine. It should be stressed that, despite the contributions from the two states being finite, they have no individual physical interpretation and only their sum is relevent. We note that for a range of Δ_s, from approximately $\Delta_s = 0.02$ to $\Delta_s = 0.07$, the dressed-state rates have similar sized contributions and therefore do not lead to issues of numerical rounding error associated with the adding of large terms of different sign.

From this example we conclude that AIP formalism may well be applicable to

the numerical evaluation of perturbative corrections. Of course many more aspects of the analytic theory should be first be investigated before an numerical implementation is attempted. Technically speaking, the biggest difficulty for an entirely numerical algorithm would be the computation of the sum over cuts of Figure 5.4. However, it may be possible to take advantage of the inclusive nature of the gluon's phase-space integral to match that of the loop integral. Assuming such an alignment of integration variables between real and virtual contributions can be achieved, then integration would be possible in four-dimensions, and a Monte-Carlo approach would ultimately be successful. Work along these lines has already been published by Soper et al [17], where one-loop integrals, after contour integration in the energy variable, are re-written as phase-space integrals.

5.3 $e^+e^- \rightarrow$ hadrons, the N_F part at $\mathcal{O}(\alpha_s^2)$

Having successfully implemented the infrared finite formalism for the simplest of QCD observables we shall now describe results for Feynman diagrams proportional to N_F at the next order in the strong coupling. For the remainder of the calculations in this section Feynman gauge will be used throughout. We do this in order to treat the tensor structure of the polarisation sum and the gauge-boson propagator the same and facilitate IR cancellations at the level of individual topologies. Throughout this section we will use the $N = 2$ analytic split for Eq. (4.45). We shall show that gauge boson's tensor structure leads us to further problems and forces us to modify our procedure for computing infrared finite amplitudes.

5.3.1   The N_F part of $|\{q_{p_1} q_{p_2} q_{p_3} q_{p_4}\}\rangle$ at LO

The N_F dependent part of the dressed four parton amplitude is obtained simply by calculating in standard massless QCD with each quark-gluon vertex assigned a

hard factor. At this order we have two hard vertices preventing the possibility of any soft momentum configurations developing in the amplitude. Note that if we were to use the non-analytic separation function defined by Eq. (4.44) then it would be sufficient to place a single hard vertex at the secondary pair of quarks. This is because, as explained in Section 4.5.3, the requirement that the gluon propagator has an invariant mass $> \Delta$ ensures that subsequent real emissions down the chain must also be hard. However, in the case of the analytic split this argument breaks down and it is necessary to explicitly place hard factors at every QCD vertex.
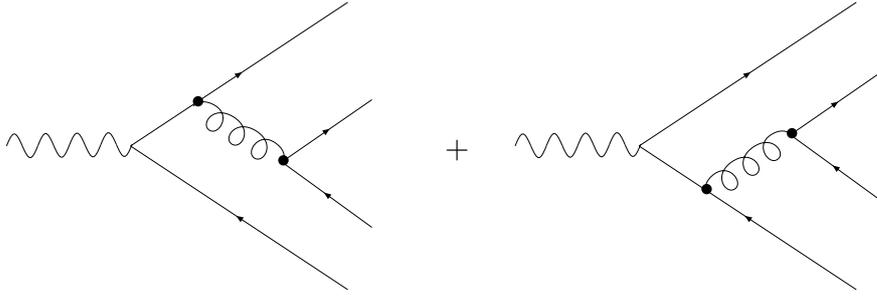
Figure 5.6: Contributions to the dressed-four-jet amplitude $\mathcal{A}^{(2)}(\{q_{p_1} q_{p_2} q_{p_3}, q_{p_4}\})$, additional diagrams are obtained by permuting the quark labels.

Using Feynman gauge the amplitude for the hadronic matrix element corresponding to the first Feynman graph of Figure 5.6 takes the form

$$
\mathcal{A}^{(2)}(\{q_{p_1} q_{p_2} q_{p_3} q_{p_4}\}) = (ieg^2) \, T_{12}^A T_{34}^A \, \langle p_1 | \gamma^\alpha (\not{p}_1 + \not{p}_3) \gamma^\mu | p_2 \rangle \langle p_3 | \gamma_\alpha | p_4 \rangle \times
$$
$$
\left(\frac{2\,\Delta + s_{34}}{(\Delta + s_{34})^4} \right) \left\{ \frac{s_{34}\,(2\,\Delta + s_{34})}{s_{134}} + \frac{\Delta^2}{s_{134} + \Delta} + \frac{\Delta^3}{(s_{134} + \Delta)^2} \right\}, \quad (5.20)
$$

where we see that the limit $\Delta \to 0$ reproduces the standard result. Using this amplitude, plus the seven other Feynman graphs obtained via permutation of the quark labels and the external leg from which the gluon is emitted, the squared

result reproduces exactly that found in [76] except that the potential singular denominators are regulated by hard factors as in Eq. (5.20).

5.3.2 The N_F part of $|\{q_{p_1} q_{p_2} q_{p_3}\}\rangle$ at NLO
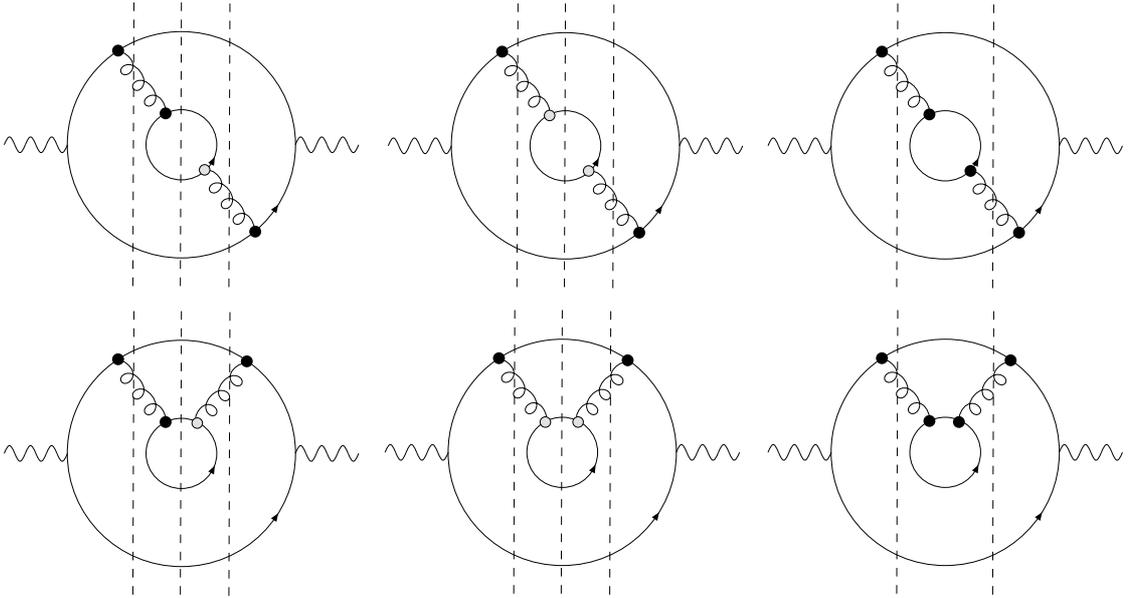
Figure 5.7: Various cuts of the N_F topologies contributing to $\mathcal{A}^{(3)}(\{q_{p_1} q_{p_2} q_{p_3}\})$. Contributions to $\mathcal{A}_S$ come from the four diagrams to the left with the remaining two diagrams contributing to $\mathcal{A}_H$. Additional diagrams obtained through symmetry are understood.

To compute the three-parton dressed state it is helpful to consider the cuts of the different topologies that contribute to the N_F part as depicted in Figure 5.7. It is clear that placing a soft factor at either, or both, of the two "inner" vertices can only enforce the momenta of the two internal quarks to coalesce, if the other vertices are hard then this must be a three-parton dressed state. Soft "outer" vertices we attribute solely to NNLO corrections to $\mathcal{A}_S(\{q_{p_1} q_{p_2}\})$, as any possible contribution to the three-parton dressed state would be heavily suppressed.

Were we to use theta-functions to separate hard and soft as in Eq. (4.44), we would find that several of the Feynman graphs for this amplitude are set to zero. This

happens because, due to the symmetry of the graph, the self-energy bubble cannot have a hard momentum entering it with a soft momentum leaving. The only non-vanishing contributions in this case come from the all hard diagrams of Figure 5.7 plus contributions due to modification of the LSZ coming from the diagrams where the self-energy bubble is completely soft.

In principle the cuts involving wave-function renormalisation with differing hard and soft factors should be calculated separately as in the $\mathcal{O}(\alpha_s)$ calculation of the previous section. However, as we are only really interested in their sum it is simpler to add these diagrams immediately, giving us the standard N_F part of the gluon wave-function renormalisation constant of massless QCD [50] multiplying the $\mathcal{O}(\alpha_s)$ dressed-three-jet Eq. (5.6).

The real cuts require an integration over the unresolved phase space of the "inner" external quarks. This integral can be performed using standard factorisation formula for collinear momentum configurations [15] and will generate poles that cancel against the aforementioned virtual cuts. By virtue of the soft factors, the four-parton phase-space, PS_4, can be factorised into a three-parton phase-space, PS_3, times an integral over the invariant mass of the collinear composite, given as

$$PS_4 \to PS_3 \times \int_0^x \frac{(4\,\pi)^{\epsilon-2}\Gamma(1-\epsilon)}{\Gamma(2-2\,\epsilon)} \, s_{34}^{-\epsilon} \, ds_{34}. \tag{5.21}$$

In calculating the integral over the unresolved phase space of the internal quark line composite there is a degree of arbitrariness as to what energy scale, x in Eq. (5.21), to integrate up to. However, since the integrand has been constructed such that it only contributes in the region where the energy of the composite is small, integrating up to large energies effectively makes no difference to the resulting amplitude for the dressed three-parton amplitude-squared. Empirically we find that the integrand is only non-vanishing below 2Δ and so we integrate up

to this squared-energy scale.

5.3.3 Problems with gauge invariance

Applying the prescription for infrared finite amplitudes as outlined at lowest order presents us with a problem. In the standard calculation the real cuts of the two topologies have terms with infrared s_{34}^{-2} singularities, such divergences have no physical interpretation and always cancel due to gauge invariance [51]. However, this cancellation occurs only at the level of a gauge invariant sum of diagrams and not for an individual topology, thus the sums over the cut diagrams in Figure 5.7 are not separately finite. In fact, by virtue of the "external" hard factors, there are also additional suppressed but un-cancelled poles that come from terms related to the $q^\mu q^\nu$ part of the Leptonic tensor.

In short, the approach of using soft separation functions breaks down unless the sum-over-cuts of each Feynman diagram is finite. For gauge theories such as massless QCD and QED this constraint is not satisfied for standard $\overline{MS}$ renormalisation. We can see an example of this by considering the full-form of the photon propagator in standard perturbation theory

$$\text{\raisebox{-1ex}{\includegraphics{}}} \quad = \quad \frac{-i}{q^2(1 - \Pi(q^2))}\left(g_{\alpha\beta} - \frac{q_\alpha q_\beta}{q^2}\right) + \frac{-i}{q^2}\left(\frac{q_\alpha q_\beta}{q^2}\right). \tag{5.22}$$

Usually the Ward identity is used to remove terms in Eq. (5.22) proportional to $q_\alpha q_\beta$, this leaves the propagator with a simple pole the residue of which can be interpreted as Z_3. Since gauge invariance is manifest in all physical observables this approach is perfectly adequate for performing analytic perturbative calculations. However, it is also clear that making use of gauge invariance in Eq. (5.22) implies that renormalisation of the photon propagator occurs in a global sense - Z_3 counter-

terms associated with a particular cut-diagram do not necessarily contain the correct UV sub-divergences. As a result the sum-over-cuts will not be finite in general for any diagram containing charge renormalisation [9].

To get around this problem we take the more pragmatic approach of discarding the terms that disrupt the sum-over-cuts and then inserting hard and soft factors; this amounts to applying the full symmetries of the theory. Thus we take our Leptonic tensor to be proportional to $g^{\mu\nu}$ enforcing charge conservation and we require that terms that cancel at the integrand level in normal perturbation theory are allowed to do so before hard and soft factors are introduced. Effectively we are now splitting the Lagrangian in a manner that respects gauge invariance allowing for finite computations at the level of individual topologies.

5.3.4 The amplitude $\mathcal{A}^{(3)}(\{q_{p_1}\, q_{p_2}\, g_{p_3}\})$

Applying this modified procedure and performing the sum of the cut diagrams for the two topologies of Figure 5.7 (taking into account the symmetries) we obtain the hadronic part of the infrared finite dressed-three-parton amplitude-squared given as

$$2\left|\mathcal{A}^{(3)}(\{q_{p_1}\, q_{p_2}\, g_{p_3}\})\, \mathcal{A}^{(1)}(\{q_{p_1}\, q_{p_2}\, g_{p_3}\})\right| = \tag{5.23}$$

$$|\mathcal{A}^{(0)}(\{q_{p_1}\, q_{p_2}\})|^2\, N_F\, C_F\, T_R \left(\frac{\alpha}{4\pi}\right)^2 \left(\frac{256\,\pi^3}{243\, s}\right) \frac{(y_{13} + 2\Delta_s)(y_{23} + 2\Delta_s)}{(y_{13} + \Delta_s)^2 (y_{23} + \Delta_s)^2}$$

$$\left\{ 162\ln(3)\Delta_s^2 - 118\Delta_s^2 + 82\Delta_s + (1 - y_{13} - y_{23})\left(82\Delta_s + 81\ln\left[\frac{2\Delta_s}{3}\right] - 127\right) \right.$$

$$\left. + \frac{(y_{23} + \Delta_s)^2\,(y_{13} + 2\Delta_s)}{(y_{23} + 2\Delta_s)\,(y_{13} + \Delta_s)^2}\left(\frac{y_{13}y_{23}}{2\Delta}\left(81\ln\left[\frac{2\Delta_s}{3}\right] - 127\right) - 82\Delta\right) \right\} + \{1 \Leftrightarrow 2\}.$$

Having obtained this result we can now use it, together with the dressed-four-jet amplitude-squared, to compute the N_F part of any multi-final-state observable at $\mathcal{O}(\alpha_s^2)$.

Working backwards it is also straightforward to infer that the dressed-three-jet amplitude at NLO is given by

$$
\mathcal{A}^{(3)}(\{q_{p_1}, q_{p_2}, g_{p_3}\}) = ieg^3 T_{12}^A \, T_R \, C_F \, N_F \, s^2 \frac{(s_{13} + 2\Delta)}{972\pi^2 \, s_{13} \, s_{23} \, (s_{13} + \Delta)^2} \times
$$

$$
\left\{ \langle p_1 | \gamma^\alpha (\not{p}_1 + \not{p}_3) \gamma^\mu | p_2 \rangle \left(\frac{82\Delta}{s} - \frac{\left(81 \ln\left(\frac{2\Delta}{3s}\right) - 127 \right) s_{13} \, s_{23}}{s^2} \right) \right.
$$

$$
+ \langle p_1 | \gamma^\alpha \not{p}_1 \gamma^\mu | p_2 \rangle \frac{2\,\Delta}{s^2} \left(\frac{\Delta(-59 + 81\ln(3))\, s_{13}\, s_{23}}{(s - s_{23})\,(s - s_{13} - s_{23})} + \dots \right.
$$

$$
\left. \left. + 41 \left(\frac{s\,(s - s_{13})}{s - s_{13} - s_{23}} - s_{13} + \frac{s\, s_{13}}{s - s_{23}} \right) \right) \right\}. \tag{5.24}
$$

5.3.5   Calculation of the C-parameter

The C-parameter defines a global event shape parameter independent of the jet axis [76]. If the external partons are massless then, in terms of Lorentz invariants, it is given by

$$
C = 3 - \frac{3}{2} \sum_{i,j} \frac{(p_i \cdot p_j)^2}{(p_i \cdot q)\,(p_j \cdot q)} \,, \tag{5.25}
$$

where p_i is the four–momentum of the i–th particle and q is the total four momentum of the centre of mass system. The C parameter varies in the range $0 \leq C \leq 1$. $C = 0$ corresponds to a perfect two–jet event, while $C = 1$ characterises a spherical event. Planar events are distributed in the range $0 \leq C \leq 3/4$; in particular the $\mathcal{O}(\alpha_s)$ perturbative result is entirely planar in nature.

In order to compute the C-parameter, standard methods for integration over the phase space of multi-particle final states are employed. To keep the evaluation as technically simple as possible we choose to avoid using the method of sequentially boosting two-parton phase spaces [77] and use the RAMBO [78] algorithm which generates a flat phase space for massless particles. We use the basic integration routine of VEGAS [79] to obtain our results. No attempt has been made to

optimise the integration and since the amplitudes are explicitly finite no constraints have been placed on what points in the integration space VEGAS may go. Results are obtained by first simulating dressed-three-jet events and binning the computed values for the C-parameter and then repeating this procedure for the dressed-four-jet contribution.
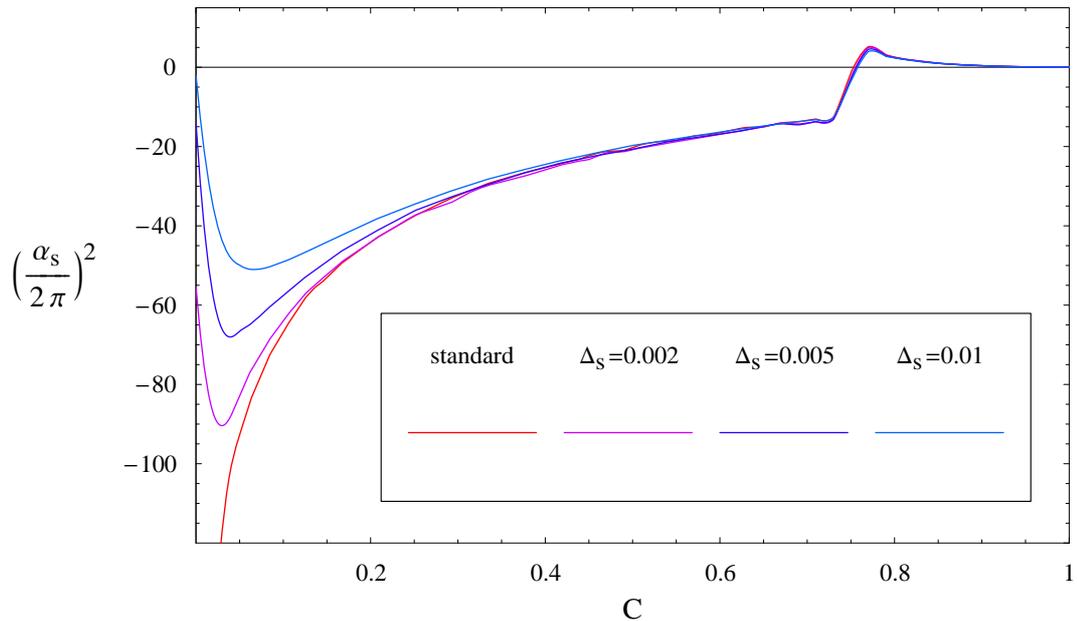
Figure 5.8: Part of the $\mathcal{O}(\alpha_s^2)$ correction to $\frac{C\,d\sigma}{\sigma\,dC}$ containing the Casimirs $C_F T_R$ is plotted in units of $\left(\frac{\alpha_s}{2\pi}\right)^2$ against the variable C, $N_F = 5$.

Figure 5.8 displays the infrared finite cross-sections compared with the standard calculation using dipole subtraction [13] (data for the standard rate obtained from the EVENT2 program). The number of points required to reach an accuracy of approximately 0.1% on the total integral varies greatly with the value of Δ_s chosen, for larger values of Δ_s convergence is fast, typically $1,000,000$ integration points are needed. This corresponds to the fact VEGAS converges faster the smoother the integrand. For $\Delta_s = 0.002$ (pink curve), which closely follows the data points obtained with EVENT2, $100,000,000$ integration points where required.

For all three infrared finite curves we see that the general trend is to only diverge from the standard perturbative result in the region where perturbation theory itself becomes unreliable, in this region none of these curves can be expected to give accurate physical predictions since they have all been constructed exclusively using finite-order perturbation theory. In the standard approach the divergence at $C = 0$ would be cancelled by contributions from the two-parton final state and large logarithms that spoil the convergence of the perturbation series would have to be resummed. For the infrared finite amplitudes the divergence at $C = 0$ has already been shifted into the dressed-two-jet by virtue of the hard factors at the "outer" vertices. The problem of resummation of large logarithms still remains for the infrared finite approach. It is conceivable that these all order resummations can be included consistently in the asymptotic propagator of the theory. For the purposes of this thesis we have taken a perturbative expansion of the asymptotic propagator in terms of free fields but in principle a non-perturbative form for the propagator could be used. Indeed a phenomenological study of the correct form for the propagator could be undertaken in this way, but is beyond the scope of this thesis.

5.4 Extension to more complex processes

A logical next step would be the calculation of the Feynman diagrams, at $\mathcal{O}(\alpha_s^2)$, contributing to the Casimir combinations of $C_F N_C$ and C_F^2. This is a formidable task. First we require a systematic method for identifying all terms that cancel across topologies due to gauge invariance and then removing them. Secondly we need a method for identifying whether a given set of hard soft vertices constitutes part of the dressed-two, three or four jet. Clearly a dressed-four-jet contribution is obtained when all the vertices are hard, however it is not completely clear how

to allocate between dressed-two and dressed-three jets. Lastly we need to reduce the associated amplitudes to basis integrals. For scalar four-point functions the reduction turns out to generate very large algebraic expressions and this problem alone makes serious demands on computer resources.

Another possible route is the examination of the singularity structure for cut diagrams contributing to the fully inclusive computation of the N_F part at $\mathcal{O}(\alpha^2)$ that contains the NNLO correction to the dressed-two-jet. We should note that, since we already have dressed state amplitudes for four and three partons, the dressed two-parton amplitude can be obtained by fully integrating over the phase-space of these two amplitude-squared and subtracting them from the total cross-section. However, from the point of view of developing the AIP, it will be instructive to construct the infrared finite, dressed two-parton amplitude by directly assembling the diagrams that contribute to this. We shall examine part of this calculation in Chapter 7.

Ultimately the cross-topology cancellations of poles is a result of failing to treat the polarisation sum for external gluons *exactly* the same as for the internal propagators and this is related to the degeneracy in the choice of the gauge parameter ξ. For the simple leading order correction to the hadronic cross-section it was sufficient to take Feynman gauge, $\xi = 1$, and treat the polarisation sum with the corresponding metric tensor, however this naive approach will breakdown for more complicated processes. For gauge theories we therefore need to construct a new way of treating the gauge bosons.

Sidestepping this problem for the moment we can instead investigate the Asymptotic Interaction Picture applied to ϕ^3 theory. The advantage of using this set of Feynman rules is that the renormalised sum-over-cuts of a given topology is guaranteed to be finite since there is no gauge structure and therefore no ambiguity associated with fixing the gauge. Also from a technical point of view, calculations

will be considerably simpler as there are no tensor structures. The results from these calculations will also allow us to validate the general approach of the asymptotic interaction picture at higher order and help us to identify what type of jet a set of hard and soft vertex factors belongs to, so this shall be investigated in the following section.

Chapter 6

Perturbative Calculations Using IR-Finite ϕ^3

6.1 Working in massless ϕ^3 theory

As discussed in Section 5.4, the standard approach for perturbative calculations for gauge theories involves the cancellation of infrared divergences across various topologies and this is intimately related to the gauge structure of the theory. Such cross topology cancellations will break down when hard and soft factors are used and it is therefore necessary to develop a new way of treating the gauge bosons. For now we want to avoid this additional complication and look at higher-order corrections in field theory, a suitable candidate for investigation is ϕ^3 theory. Using this theory as a toy model, we can investigate the divergent behaviour of higher-order corrections without the complications outlined for gauge theories with tensor structure. We shall generally neglect the finite parts of the calculations since they cannot be compared to any experiment.

In order to mimic the infrared structure of QCD as closely as possible we would wish to explore the asymptotic interaction picture applied to massless ϕ^3 in four

space-time dimensions. However, if we look at the form of the resummed propagator we see that higher-order contributions will, in general, introduce a radiative correction to the mass of the ϕ field. As a result the massless Lagrangian is not renormalisable, save for the case of six space-time dimensions where we find that the propagator remains massless to all orders in perturbation theory. Therefore to avoid massive fields we choose to perform the calculations in six space-time dimensions. It would of course still be enlightening to look at the massive theory in four-dimensions, where infrared poles in ϵ would be replaced by logarithms of the mass parameter, however the calculations would be technically much harder to perform. That said, we note that for graphs in ϕ^3 in four dimensions without self-energy insertions, the mass of the external ϕ field and the internal propagators can be taken to be zero [16]. Later we shall exploit this fact to look at the infrared divergent structure of a ϕ^3 graph in four space-time dimensions.

Changing to a larger space-time dimension alters the nature of the infrared singularities present. In six dimensions only collinear singularities remain and therefore there is a clear difference between the divergences when compared to QCD [32], specifically there are no double poles associated with overlapping soft and collinear configurations, so we expect at most one inverse power of ϵ for every order of perturbation theory. However, the separation function's form is independent of space-time dimension and these calculations therefore provide some insight into the method applied to four-dimensional gauge theory and give useful tests for a future numerical implementation. Throughout this section we shall use the soft separation factor as defined in 4.45, we shall take $N = 1$ as this is technically simpler.

The coupling constant α will be defined as

$$\alpha = \frac{\lambda^2}{(4\,\pi)^3},$$

(6.1)

89

where λ denotes the coupling of the theory as defined in the Feynman rules of ϕ^3 theory [9, 80].

6.2 Wave function renormalisation and residues

For practical perturbative calculations of correlation functions, the LSZ formalism requires the calculation of on-shell residues for external particles.

6.2.1 Residues at one-loop

$$-i\,\Sigma^{(2)}(0) = \qquad \underbrace{}_{i} \qquad + \qquad \underbrace{\otimes}_{ii}$$

Figure 6.1: The renormalised one-loop computation of the on-shell residue of the scalar field amounts to the calculation of the pole-scheme wave function renormalisation constant plus counter-term.

Fig 6.1 describes the one-loop contribution to the on-shell residue of the scalar field ϕ. For massless perturbation theory Feynman graph i is zero since the integral is devoid of scale, whereas contribution ii corresponds to the counter-term, defined in some appropriate renormalisation scheme, and is the subtraction of the ultraviolet divergence of graph i, plus some finite part. Taking the $\overline{MS}$ prescription, as given in Eq. (2.6), the counter-term for the one-loop wave function renormalisation constant is given by

$$\delta Z \sim \frac{\partial\,\Sigma^{(2)}(p^2)}{\partial p^2} \sim -\frac{\alpha}{12\,\bar{\epsilon}_{UV}}, \tag{6.2}$$

where $\sim$ denotes that the poles structures are the same. Correspondingly

$$Z_p = 1 + \left.\frac{\partial\,\Sigma^{(2)}(p^2)}{\partial p^2}\right|_{p^2=0} - \delta Z = 1 + \frac{\alpha}{12\,\bar{\epsilon}_{IR}}, \tag{6.3}$$

90

where Z_p denotes the renormalised on-shell residue of the two-point function to $\mathcal{O}(\alpha)$.

The insertion of soft factors at the vertices of Fig 6.1, alters the calculation considerably. First we recognise that diagram i with a soft factor is no longer scaleless and is ultra-violet finite. A naive argument would then set the counter-term diagram ii to zero since there is no longer any high-energy behaviour to be accounted for, however this is not necessarily correct. It can be argued that the soft separation function may cut up the counterterm such that it gives a finite contribution to diagrams that are themselves UV finite. It is certainly possible to pick an integral representation for the constant defined in Eq. (6.2), for example

$$\delta Z \approx \frac{-i\,\lambda^2\,\mu^{2\epsilon}}{6} \int \frac{d^{6-2\epsilon}k}{(2\,\pi)^{6-2\epsilon}} \frac{1}{(k^2 - \mu^2)^3}, \tag{6.4}$$

where μ is the renormalisation scale, will integrate to give δZ to $\mathcal{O}(\epsilon)$. Applying soft factors to Eq. (6.4) will then give us finite renormalisation constants. As there is apparently some ambiguity as to how to treat the diagram ii we shall *choose* to cut up the counter-term such that all of it is contained only in the diagram with both vertices hard. We shall come back to this point when we discuss a more involved calculation in Section 6.3.

For graph i we give the results for the calculation with a single soft factor at one of the vertices, Z_p^s, and two soft factors, Z_p^{ss}, these two results can then be combined to obtain the result for any combination of hard and soft vertices for the on-shell one-loop self-energy. Note that the two vertices are symmetric and therefore their soft factors are the same, we obtain

$$Z_p^s = 1 + \frac{\alpha}{12\,\bar{\epsilon}} - \frac{\alpha}{12}\left(\ln(-\Delta_\mu) - 4\right) \tag{6.5}$$

$$Z_p^{ss} = 1 + \frac{\alpha}{12\,\bar{\epsilon}} - \frac{\alpha}{5040}\left(420\ln(-\Delta_\mu) - 1999\right), \tag{6.6}$$

with $\Delta_\mu \equiv \frac{\Delta}{\mu}$ (where μ is the renormalisation scale and not a Lorentz index!). A simple check on these two results is that the sum of all diagrams with soft factors should reproduce the same infrared poles as Z_p, thus we have

$$Z_p^{sh} + Z_p^{hs} + Z_p^{ss} = 2\,Z_p^s - Z_p^{ss} = 1 + \frac{\alpha}{12\,\bar\epsilon} - \frac{\alpha}{36}\,(\,3\ln(-\Delta_\mu) - 7\,), \qquad (6.7)$$

giving us the correct divergence. The fact that Eqs. (6.5) and (6.6) also have the correct infrared structure is a direct consequence of Z_p^{hs} being both UV and IR finite.

6.2.2 Residues at two-loop

$$-i\,\Sigma^{(4)}(0) =$$

Figure 6.2: Part of the two-loop computation of the on-shell residue of the scalar field.

Moving on to two loop we can investigate the pole-scheme wave-function renormalisation of Fig 6.2, here we consider only part of the two loop correction necessary for the topologies that we will consider in the following subsections. As in the previous calculation diagrams i and ii now constitute scaleless integrals and therefore evaluate to zero. The two loop $\overline{MS}$ counterterm, diagram iii, obtained by computing the diagrams of i and ii off-shell, gives

$$\delta Z = -\frac{\alpha^2}{144\,\bar\epsilon^2} + \frac{11\,\alpha^2}{864\,\bar\epsilon}\,. \qquad (6.8)$$

Again we proceed in a similar manner to the one loop calculation and compute diagram i now with some soft vertices. We start by investigating the effect of

placing a soft separation factor at one or both of the external field lines, we obtain the unrenormalised residues of

$$
\delta Z_p^s = -\frac{\alpha^2}{144\,\bar{\epsilon}^2} + \frac{\alpha^2}{864\,\bar{\epsilon}} \left(12\ln(-\Delta_\mu) - 49 \right) + \cdots
$$
$$
- \frac{\alpha^2}{5184} \left(72\ln^2(-\Delta_\mu) - 588\ln(-\Delta_\mu) + 18\,\pi^2 + 1303 \right) \quad (6.9)
$$

with one soft vertex and

$$
\delta Z_p^{ss} = -\frac{\alpha^2}{144\,\bar{\epsilon}^2} + \frac{\alpha^2}{864\,\bar{\epsilon}} \left(12\ln(-\Delta_\mu) - 59 \right) + \cdots
$$
$$
- \frac{\alpha^2}{5184} \left(72\ln^2(-\Delta_\mu) - 708\ln(-\Delta_\mu) + 18\,\pi^2 + 1817 \right) \quad (6.10)
$$

with two soft vertices. To renormalise we add diagram ii; with one soft vertex the one-loop counterterm diagram corresponds to Eq. (6.5) multiplied by Eq. (6.2), giving

$$
\delta Z_p^{s,ct} = \frac{\alpha^2}{72\,\bar{\epsilon}^2} - \frac{\alpha^2}{432\,\bar{\epsilon}} \left(6\ln(-\Delta_\mu) - 19 \right) + \cdots
$$
$$
+ \frac{\alpha^2}{2592} \left(18\ln^2(-\Delta_\mu) - 114\ln(-\Delta_\mu) + 3\,\pi^2 + 193 \right) \quad (6.11)
$$

and

$$
\delta Z_p^{ss,ct} = \frac{\alpha^2}{72\,\bar{\epsilon}^2} - \frac{\alpha^2}{432\,\bar{\epsilon}} \left(\ln(-\Delta_\mu) - 4 \right) + \cdots
$$
$$
+ \frac{\alpha^2}{864} \left(6\ln^2(-\Delta_\mu) - 48\ln(-\Delta_\mu) + \pi^2 + 98 \right). \quad (6.12)
$$

It is clear that diagram iii will be zero (or at least finite) when a soft vertex is placed at the vertices involving external fields, since in that case the only source of UV divergence is contained in the internal loop and counter-term diagram ii will completely negate this. Taking Eqs. (6.9),(6.10),(6.11) and (6.12) we can sum all

$\delta Z_{p\,hh}^{hh}$	$\dfrac{-119529-20720\,\Upsilon+39420\,\pi^2+540\ln(-\Delta_\mu)\,(-25+3\ln(-\Delta_\mu))}{233280}$
$\delta Z_{p\,hs}^{hh}$	$\dfrac{20457+13840\,\Upsilon-17280\,\pi^2}{116640}$
$\delta Z_{p\,ss}^{hh}$	$\dfrac{32463-17320\,\Upsilon+15120\,\pi^2}{116640}$
$\delta Z_{p\,hh}^{hs}$	$-\dfrac{5}{36\,\bar\epsilon}+\dfrac{9279+3760\,\Upsilon-8460\,\pi^2+10350\ln(-\Delta_\mu)}{38880}$
$\delta Z_{p\,hs}^{hs}$	$\dfrac{1}{18\,\bar\epsilon}+\dfrac{5187-2480\,\Upsilon+2580\,\pi^2-1440\ln(-\Delta_\mu)}{12960}$
$\delta Z_{p\,ss}^{hs}$	$\dfrac{1}{36\,\bar\epsilon}+\dfrac{-38061+11120\,\Upsilon-7020\,\pi^2-2160\ln(-\Delta_\mu)}{38880}$
$\delta Z_{p\,hh}^{ss}$	$\dfrac{109+5\ln(-\Delta_\mu)}{360\,\bar\epsilon}+\dfrac{152163-61900\,\Upsilon+155925\,\pi^2-320760\ln(-\Delta_\mu)-12150\ln(-\Delta_\mu)^2}{583200}$
$\delta Z_{p\,hs}^{ss}$	$-\dfrac{49}{360\,\bar\epsilon}+\dfrac{-702063+163000\,\Upsilon-145800\,\pi^2+158760\ln(-\Delta_\mu)}{583200}$
$\delta Z_{p\,ss}^{ss}$	$\dfrac{1}{144\,\bar\epsilon^2}-\dfrac{187+60\ln(-\Delta_\mu)}{4320\,\bar\epsilon}+\dfrac{2227401-528200\,\Upsilon+268650\,\pi^2+100980\ln(-\Delta_\mu)+16200\ln(-\Delta_\mu)^2}{1166400}$

Table 6.1: Table showing all renormalised combinations of hard and soft vertices applied to the two loop self-energy of Figure 6.2 with symmetric amplitudes omitted. The coupling has been set to one and Υ is defined in Eq. (6.14).

combinations of hard and soft vertices except both hard, as in Eq. (6.7), to obtain

$$\delta Z_p^{sh} + \delta Z_p^{hs} + \delta Z_p^{ss} = \frac{\alpha^2}{144\,\bar\epsilon^2} - \frac{11\,\alpha^2}{864\,\bar\epsilon} + \cdots$$
$$- \frac{\alpha^2}{5184}\left(36\ln^2(-\Delta_\mu) - 300\ln(-\Delta_\mu) + 12\,\pi^2 + 605 \right). \quad (6.13)$$

Comparing with Eq. (6.8) we see that Eq. (6.13) has precisely the IR poles of the standard calculation, this is expected since all diagrams with soft vertices have been included and renormalisation has been performed.

6.2.3 Ultra-violet finite residues at two loop

In the previous section we discussed only the addition of soft factors at the outer vertices of Figure 6.2, in order to determine all combinations of hard and soft vertices it suffices to calculate the remaining combinations of soft factors placed
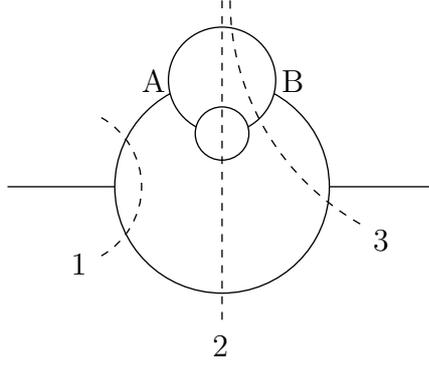
Figure 6.3: Investigation of the sum-over cuts of a three-loop self-energy type topology with soft factors inserted at vertices A and B.

on the inner and outer loops. Using power-counting, diagrams with soft factors on the inner loop are UV finite, therefore we set the counterterm diagrams, *ii* and *iii*, to zero. This leaves us needing to compute the on-shell diagram *i* of Figure 6.2; integrals defined in Appendix A and hypergeometric reduction identities (see for example [81]) were necessary to reduce the problem to a small set of basis functions on which an expansion in ϵ could be applied. Table 6.1 details all combinations of hard and soft vertices, with the upper labels referring to factors on the external vertices and the lower labels referring to the inner loop's vertices. Note that α has been set to 1 in this table and for convenience we make the definition

$$
\Upsilon \equiv \sqrt{3}\,\pi\ln(4) - \psi'\left(\frac{1}{3}\right) + \psi'\left(\frac{2}{3}\right) + \cdots
$$
$$
i\,6\sqrt{3}\left(\mathrm{Li}_2\left[\frac{1 - i\,\sqrt{3}}{4}\right] - \mathrm{Li}_2\left[\frac{1 + i\,\sqrt{3}}{4}\right]\right). \quad (6.14)
$$

From Table 6.1 we see that both of the external vertices need to be hard for infrared divergences to be avoided.

6.3 The three-loop self-energy topology

Having obtained residues for wave function renormalisation, we shall now investigate the sum-over-cuts of the topology shown in Figure 6.3. We shall show that infrared cancellation due to KLN [7,10] is maintained in the presence of soft/hard vertices at A and B and that we can construct amplitudes that correspond to dressed two, three and four parton final states.

6.3.1 Checking KLN with soft factors present

As a first step we calculate the three cuts with soft and hard factors on vertices A and B. We shall also show that the results given in this section, plus their accompanying finite parts, are sufficient to construct the dressed final states - in other words we will not need to consider placing soft factors at the vertices of the innermost loop. We note that for the purposes of displaying this section's results we have absorbed a factor of s^ϵ into σ and omitted the finite parts of cuts 2 and 3 owing to their large size.

Cut 1 of Figure 6.3, with the appropriate normalisation, is obtained simply by multiplying the renormalised residues computed in Section 6.2 with the six dimensional two-parton phase-space, the results are given below in Table 6.2.

$\sigma_1{}^{hh}$	$\dfrac{\pi\,s\,\alpha^3\left(605+12\,\pi^2-300\ln(-\Delta_\mu)+36\ln(-\Delta_\mu)^2\right)}{15552}$
$\sigma_1{}^{hs}$	$\dfrac{\pi\,s\,\alpha^3\left(26-5\ln(-\Delta_\mu)\right)}{1296}$
$\sigma_1{}^{ss}$	$\dfrac{\pi\,s\,\alpha^3}{432\,\epsilon^2}+\dfrac{5\,\pi\,s\,\alpha^3}{2592\,\epsilon}-\dfrac{\pi\,s\,\alpha^3\left(7\left(57+\pi^2\right)+4\ln(-\Delta_\mu)\left(-35+3\ln(-\Delta_\mu)\right)\right)}{5184}$

Table 6.2: Table showing the inclusive calculation of cut 1 of Figure 6.3 with different combinations of hard and soft factors at vertices A and B where s is the centre-of-mass energy and a factor of s^ϵ has been absorbed into σ.

Cut 2 requires integration over the four-parton phase-space, this can be calculated

by applying plus-distributions to the representation of [21] or using Mellin-Barnes transformations [67] to obtain a form amenable to the algorithm of [22]. We obtain results given in Table 6.3, the analytic form for the finite part is too large to display but will be included in the construction of the dressed states.

$\sigma_2{}^{hh}$	$\dfrac{\pi\,s\,\alpha^3\left(17+42\,\Delta_s+24\,\Delta_s{}^2+6\ln\left[\frac{\Delta_s}{1+\Delta_s}\right](1+\Delta_s)^2\,(1+4\,\Delta_s)\right)}{648\,\bar{\epsilon}}$
$\sigma_2{}^{hs}$	$-\dfrac{\left(\pi\,s\,\alpha^3\left(2+9\,\Delta_s+6\,\Delta_s{}^2+6\ln\left[\frac{\Delta_s}{1+\Delta_s}\right]\Delta_s\,(1+\Delta_s)^2\right)\right)}{216\,\bar{\epsilon}}$
$\sigma_2{}^{ss}$	$\dfrac{\pi\,s\,\alpha^3}{216\,\bar{\epsilon}^2}+\dfrac{\pi\,s\,\alpha^3\left(71-12\ln(s)+24\,\Delta_s\,(1+\Delta_s)-12\ln\left[\frac{\Delta_s}{1+\Delta_s}\right](1+\Delta_s)^2\,(1-2\,\Delta_s)\right)}{1296\,\bar{\epsilon}}$

Table 6.3: Table showing the inclusive calculation of cut 2 of Figure 6.3 with different combinations of hard and soft factors at vertices A and B where s is the centre-of-mass energy and a factor of s^ϵ has been absorbed into σ.

Similarly cut 3 can be obtained either by using plus-distributions or by direct integration followed by multiplication of the standard wave function renormalisation factor of Eq. (6.2). As can be seen in Table 6.4, σ_3^{AB} gives precisely the poles necessary to cancel those of $1/2\,\sigma_2^{AB}+\sigma_1^{AB}$ where A or B can be either a hard or soft separation factor.

$\sigma_3{}^{hh}$	$-\dfrac{\pi\,s\,\alpha^3\left(17+42\,\Delta_s+24\,\Delta_s{}^2+6\ln\left[\frac{\Delta_s}{1+\Delta_s}\right](1+\Delta_s)^2\,(1+4\,\Delta_s)\right)}{1296\,\bar{\epsilon}}$
$\sigma_3{}^{hs}$	$\dfrac{\pi\,s\,\alpha^3\left(2+9\,\Delta_s+6\,\Delta_s{}^2+6\ln\left[\frac{\Delta_s}{1+\Delta_s}\right]\Delta_s\,(1+\Delta_s)^2\right)}{432\,\bar{\epsilon}}$
$\sigma_3{}^{ss}$	$-\dfrac{\pi\,s\,\alpha^3}{216\,\bar{\epsilon}^2}+\dfrac{\pi\,s\,\alpha^3\left(-19+3\ln(s_\mu)-6\,\Delta_s\,(1+\Delta_s)+3\ln\left[\frac{\Delta_s}{1+\Delta_s}\right](1+\Delta_s)^2\,(1-2\,\Delta_s)\right)}{648\,\bar{\epsilon}}$

Table 6.4: Table showing the inclusive calculation of cut 3 of Figure 6.3 with different combinations of hard and soft factors at vertices A and B where s is the centre-of-mass energy and a factor of s^ϵ has been absorbed into σ.

To extend this check on KLN further we should also compute the results for hard and soft factors at the vertices of the inner loop. However as discussed in Sections 6.2.1, within the approach of $\overline{MS}$ renormalisation, there is a problem with the inherent ambiguity associated with finite counterterms. In the calculations

presented so far any contributions from finite counterterms could only alter the finite part of the amplitude and not the pole structure, this is no longer the case when hard and soft factors are inserted at the inner-loop vertices. For example, for cut 3 we may have a divergent three-parton phase-space multiplying a UV-finite residue with an ill-defined finite part. In this case taking the contribution from the finite counter-term to be zero fails to give the necessary pole structure to satisfy KLN theorem.

Rather than this result being a general breakdown of the asymptotic interaction approach it really is related to how we chose to renormalise our theory. Although technically more complicated, using BPHZ renormalisation [9] we may write down an expression for the above computation that is explicitly UV finite at the integrand level. It is clear that there is no longer any ambiguity with regard to the finite part of the propagator's residue and with this approach we expect KLN theorem to survive for all combinations of hard and soft vertices. However, in the next section we shall see that, for the purposes of constructing dressed states from this topology, it is not necessary to change the renormalisation scheme.

6.3.2 Constructing dressed final states

To determine what combinations of hard and soft vertices go into the dressed two-jet amplitude it is enough to consider Table 6.1 and the singularity structure of the four-jet cross-section given in Table 6.3. First we recognise that the following relationships are satisfied

$$\sigma_2{}^{hh} \sim \sigma_2{}^{hh}_{ss} \qquad \sigma_2{}^{hs} \sim \sigma_2{}^{hs}_{ss} \qquad \sigma_2{}^{ss} \sim \sigma_2{}^{ss}_{ss} \qquad (6.15)$$

where $\sim$ denotes that the two terms have the same pole structure. We see this is true by realising that, when the four-jet cross-section is in a region of phase space

that might simulate a three-jet or two-jet event, a hard factor on the inner-loop will suppress the amplitude. Note that this argument is true only if we working in a six dimensional phase-space - the hard factor contributes a factor of the invariant mass of the particles that make-up the inner loop, while the phase-space also contributes a power of the invariant mass. If we were to work in four-dimensions then taking $N = 2$ for Eq. (4.45) would be required for this argument to hold and this is precisely what is done in the previous chapter[1].

If we then take this result and combine it with what is known about the pole structure of cut 1, we see that generally cut 3 must be included in order to cancel all the remaining singularities. From Table 6.1 we see that all three cuts contribute to the dressed two-jet if a soft factor is placed at either vertex A or B of Figure 6.3.

The dressed three-jet can now be assembled by taking both vertices A and B hard and combining cuts 2 and 3 summing over all soft/hard permutations on the inner-loop. The only cut that need be excluded from this sum is cut 2 with all vertices hard, this should be associated with the dressed four-jet amplitude. It may also be argued that since contributions like $\sigma_{2\,hs}^{\,hh}$ are finite they can be attributed to either the dressed four or three-jet amplitude. Whilst this is true we find that such contributions, which would be zero using the theta-function split, are heavily suppressed by larger powers of the ratio Δ_s and are therefore negligible.

Below we display the infrared finite amplitudes of Figure 6.3. The final analytic form for the dressed two-jet is too complicated to be displayed here and so we expand it to order Δ_s^2.

$$\mathcal{A}^{(3)}(\{\phi_{p_1}\,\phi_{p_2}\,\phi_{p_3}\,\phi_{p_4}\}) = \frac{\lambda^3\,(y_{123}\,\Delta_s + y_{13}\,(y_{123} + \Delta_s))}{s^2\,y_{123}\,(y_{13} + \Delta_s)^2\,(y_{123} + \Delta_s)} \tag{6.16}$$

---

[1]The easiest way to see this explicitly is to take the four-parton phase-space of [76] and make the substitution $\epsilon \to -1$ to obtain the six dimensional phase-space.

$$\mathcal{A}^{(4)}(\{\phi_{p_1}\,\phi_{p_2}\,\phi_{p_3}\}) = \mathcal{A}^{(2)}(\{\phi_{p_1}, \phi_{p_2}, \phi_{p_3}\})\left(\frac{\alpha}{72}\right)\left\{+6\ln\left[\frac{s_\mu\,y_{13}\,y_{23}\,\Delta_s}{y_{13}\,y_{23}+\Delta_s}\right]+\cdots\right.$$

$$\left.+10+\frac{6\,(1-3\,y_{13})\,\Delta_s}{y_{13}\,y_{23}+\Delta_s}+\frac{(6-5\,y_{13})\,y_{13}\,\Delta_s{}^2}{(y_{13}\,y_{23}+\Delta_s)^2}+\frac{2\,y_{13}{}^2\,\Delta_s{}^3}{(y_{13}\,y_{23}+\Delta_s)^3}\right\} \quad (6.17)$$

$$\mathcal{A}^{(5)}(\{\phi_{p_1}\,\phi_{p_2}\}) = \mathcal{A}^{(1)}(\{\phi_{p_1}, \phi_{p_2}\})\left(\frac{\alpha^2}{144}\right)\left\{-\ln(-s_\mu)^2-\ln(\Delta_s)^2\,(1-12\,\Delta_s)+\right.$$

$$+\ln(-s_\mu)\left(\frac{31}{3}+12\,\Delta_s-\ln(\Delta_s)\,(2-12\,\Delta_s)\right)+\cdots$$

$$\left.+\ln(\Delta_s)\left(\frac{31}{3}-20\,\Delta_s\right)-\frac{310}{9}+26\,\Delta_s+\pi^2\left(\frac{5}{12}+4\,\Delta_s\right)+\mathcal{O}(\Delta_s^2)\right\} \quad (6.18)$$

6.4 The three-loop vertex topology
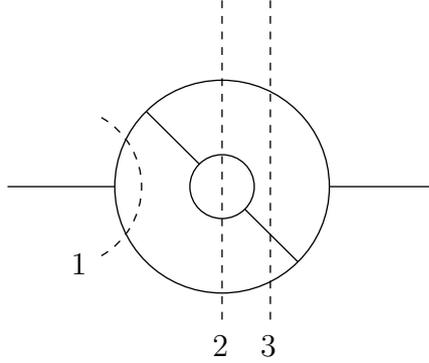
Figure 6.4: Investigation of the sum-over cuts of a three-loop vertex type topology with soft factors.

Another topology that is related to the QCD calculation of the N_F part at $\mathcal{O}(\alpha^2)$ is displayed in Figure 6.4. In four dimensions cut 1 represents a complex mix of UV and IR divergences, however in six dimensions we find that this cut is in fact IR finite. Thus the cancellation of infrared divergences occurs only in the sum of cuts 2 and 3 where the particles in the inner loop become collinear. The corresponding calculations are relatively straight-forward however since the soft factors placed on the vertices of the inner loop are irrelevant to the infrared structure as they tend

always to one in the three-jet region of phase-space. As a result it is easy to show that the presence of a hard factor on the inner loop prevents collinear divergences and renders the cut in question infrared finite. This is commensurate with the fact that the soft residues computed at one loop, Eqs. (6.5) and (6.6), give the same infrared poles as the standard result. Therefore the only non-trivial check of the soft factors occurs for the vertices of the outer loop. Yet again we find the cancellation is exact and therefore we give only the pole structure of cut 3 with one soft factor on an outer vertex

$$\sigma_3{}^s = -\frac{\pi\, s\, \alpha^3\, \Delta_s\, (3 + 2\, \Delta_s)}{144\, \bar{\epsilon}} - \frac{\pi\, s\, \alpha^3\, \Delta_s\, (1 + \Delta_s)^2 \ln(\frac{\Delta_s}{1 + \Delta_s})}{72\, \pi^2\, \bar{\epsilon}}, \qquad (6.19)$$

and also $\sigma_3{}^{ss}$ denoting two soft vertices

$$\sigma_3{}^{ss} = \frac{\pi\, s\, \alpha^3\, \Delta_s{}^2}{18\, \pi^2\, \bar{\epsilon}} + \frac{\pi\, s\, \alpha^3\, \Delta_s{}^2\, (1 + 2\, \Delta_s)}{36\, \bar{\epsilon}} \left(\text{Li}_2 \left[\frac{\Delta_s}{1 + 2\, \Delta_s} \right] - \text{Li}_2 \left[\frac{1 + \Delta_s}{1 + 2\, \Delta_s} \right] \right)$$
$$+ \frac{\pi\, s\, \alpha^3\, \Delta_s{}^2}{36\, \bar{\epsilon}} \ln \left[\frac{\Delta_s}{1 + \Delta_s} \right] \left(2\, (1 + \Delta_s) + (1 + 2\, \Delta_s) \ln \left[\frac{\Delta_s}{1 + 2\, \Delta_s} \right] \right), \quad (6.20)$$

using these two results the pole structure of any combination of hard and soft factors for any cut in Figure 6.4 may be determined. As in the previous topology we can combine those three and four parton cuts (minus the all hard four-parton cut) with hard factors on the outer loop to obtain the dressed three-jet amplitude for this topology given as

$$\mathcal{A}^{(4)}(\{\phi_{p_1}, \phi_{p_2}, \phi_{p_3}\}) = \mathcal{A}^{(2)}(\{\phi_{p_1}, \phi_{p_2}, \phi_{p_3}\}) \left(\frac{8\, \alpha}{9} \right) \left\{ 6 \ln \left[\frac{s_\mu\, y_{13}\, y_{23}\, \Delta_s}{y_{13}\, y_{23} + \Delta_s} \right] - 10 + \cdots \right.$$
$$\frac{5\, \Delta_s{}^2 - 6\, \Delta_s}{y_{13}\, y_{23} + \Delta_s} + \frac{3\, (y_{13} + y_{23})\, \Delta_s\, (3\, y_{13}\, y_{23} + 2\, \Delta_s) - 7\, \Delta_s{}^3}{(y_{13}\, y_{23} + \Delta_s)^2} + \left. \frac{2\, \Delta_s{}^4}{(y_{13}\, y_{23} + \Delta_s)^3} \right\}.$$
$$(6.21)$$

Comparing Eq. (6.21) and Eq. (6.17) it is clear that NLO corrections to the LO

dressed three-parton amplitude will be dependent on the conjugate cut. For the N_F part of the QCD dressed three parton final state it was possible to write down a form for the NLO correction that would give the correct amplitude-squared when contracted with either of the two LO conjugate three-parton cuts. The possibility to do this exploited the tensor structure of the amplitude, since this is absent for scalar field theory such a construction is not possible. In general a higher-order correction to a dressed amplitude will therefore have a conjugate cut associated to it and it should be defined to only give a non-zero contribution when the amplitude-squared is formed with this conjugate cut.

6.5 UV finite massless ϕ^3 in four-dimensions

We have seen that using a theory without gauge structure, namely ϕ^3 in six dimensions, we can construct dressed states and successfully compute on-shell UV-finite residues required by the LSZ formalism. We have also seen potential ambiguities associated with $\overline{MS}$ renormalisation and have advocated the use of a prescription, such as BPHZ, that renders amplitudes finite at the level of the integrand. However, by working in six dimensions we limit ourselves to collinear divergences only. In four spacetime dimensions, despite the fact that the external state of ϕ^3 are necessarily massive, we can from a technical viewpoint perform massless calculations provided we work only with diagrams that have no self-energy insertions. In the next sub-section we shall look at one such diagram and check that the soft separation functions perform as expected. Another advantage of such calculations is that the vertex is ultra-violet finite so we no longer need to perform any renormalisation.
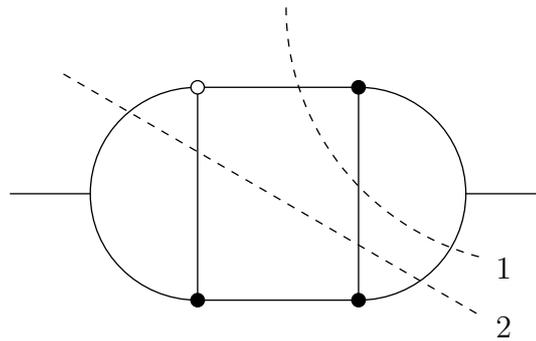
Figure 6.5: A check on the soft function - in the three-jet region of phase-space the singular behaviour of cuts 1 and 2 must cancel.

6.5.1 An uncrossed topology

Observing Figure 6.5 we see that the in the three-jet region of phase-space the IR divergences of cuts 1 and 2 have to cancel. To check this we can consider all other cuts that might possibly give divergences in the three-jet region of phase-space. Looking at all other three parton cuts, we first realise that the two cuts which involve all hard vertices in the loop integral cannot have any IR divergences. The remaining three parton cut is obtained by reflecting cut 1 in the central x-axis of Figure 6.5 and corresponds to the loop integral shown in Figure 6.6
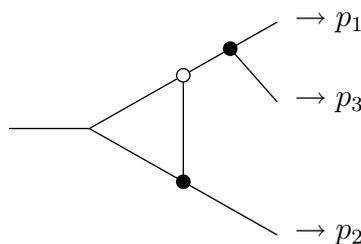
Figure 6.6: This configuration of hard and soft vertices should give no IR singularities in the loop integral.

Figure 6.6 should have no IR divergences. The loop integral corresponds to a three-point function with two off-shell legs, the presence of the soft factor is incompatible with this and the theta-function split would send this graph to zero. Alternatively

you can argue that the lowermost hard vertex alone prevents singular momentum configurations. For analytic separations we would therefore expect only a finite contribution and this is precisely what is found.

There are two four final state cuts, the partner of cut 2 describes the hard real emission of a particle followed by a soft emission from loer down the same leg. In the language of the theta-function split this would also be set to zero, since all successive emissions must be hard. Using the analytic split we can also clearly see that there are no divergences in the three-parton region of phase-space, this implies that the IR divergences of cuts 1 and 2 must cancel.

Using the program TIRA (see Appendix C) we compute the loop integral of cut 1 and we find that the pole structure of the conventional calculation is modified to

$$
\frac{-1}{16\,\pi^2\,\bar\epsilon}\,\frac{\ln\!\left(\frac{s_{12}}{s}\right)}{s_{12}\,s_{23}\,(s_{13}+s_{23})} \;\to\; \frac{-1}{16\,\pi^2\,\bar\epsilon}\,\frac{\Delta\ln\!\left(\frac{\Delta+s_{12}}{s+\Delta}\right)+\ln\!\left(\frac{s_{12}}{s}\right)s_{12}}{(\Delta+s_{12})^2\,(\Delta+s_{23})\,(s_{13}+s_{23})}, \qquad (6.22)
$$

where the external momentum are described by Figure 6.6. The pole structure of cut 2 can be computed using Eq. (5.21) and simply applying a plus-distribution; we find that the pole structure is identical to Eq. (6.22) up to a minus sign.

Chapter 7

A Two Loop Calculation in QCD

7.1   Back to QCD

Having successfully implemented the asymptotic interaction picture in ϕ^3 theory we shall go back to QCD and test KLN at two loop for a gauge theory. Here we present the first step in the calculation of the inclusive N_F part of e^+e^- to hadrons at $\mathcal{O}(\alpha_s^2)$ and therefore to the construction of the NNLO correction to the dressed two-parton amplitude. Since we already know the form for the dressed three and four parton amplitudes we could of course obtain the dressed two-parton amplitude by integrating over the phase-space of these squared amplitudes and then subtracting the result from the total cross-section. Instead we are interested in the process of directly constructing the amplitude without reference to the total cross-section.

We start by examining the effect of adding a single soft factor at the vertices shown in Figure 7.1. The advantage of this is that $\overline{MS}$ renormalisation can still be used and because the form for the soft factor is common to both topologies this modification should not destroy the finiteness of their sum. We will denote

the vertex topology as $T1$ and the self-energy type topology of Figure 7.1 as $T2$. Feynman gauge is used throughout.
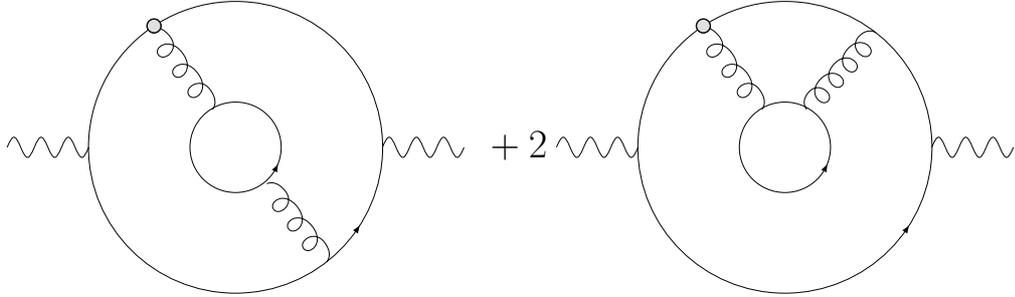
Figure 7.1: Investigation of the sum-over-cuts of the three-loop diagrams contributing to the N_F part of the total hadronic cross-section with a single soft factor.

7.2   Renormalisation

Before discussing the technical details of the calculation, it is worth mentioning that at least two different views of renormalisation can be adopted when applied to the LSZ formalism. One approach is to compute renormalised on-shell residues in some scheme (typically $\overline{MS}$) by including the necessary counter-terms to render the connected amputated Green's function UV finite. From this viewpoint the residues of the on-shell two-point functions are finite or IR divergent if massless particles are present in higher-order corrections. Alternatively the pole-scheme (on-shell) residues can be used un-renormalised and therefore counter-terms for external lines must also be included in the calculation. Clearly both views give identical results, though the former is possibly more transparent. Following the methodology of the previous chapter we take the first view and write the $\mathcal{O}(\alpha^2)$ renormalised pole-scheme fermion propagator as shown in Figure 7.2. For massless QCD the first two terms are of course zero, however this will not be true when the vertices are separated into hard and soft parts.
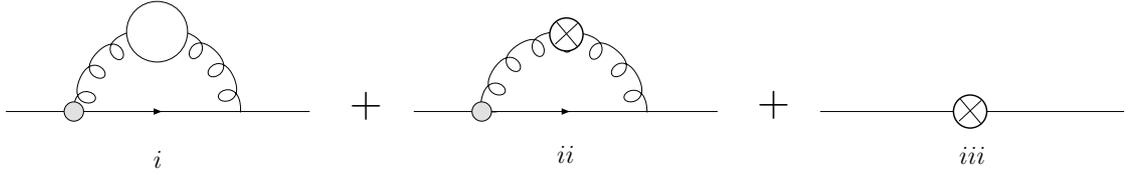
Figure 7.2: Calculation of the two-loop residue of the N_F part of the fermion propagator in the pole-scheme.

7.2.1 Computation of the N_F part of the fermion pole-scheme residue

Whilst the soft vertex gives a proliferation of non-zero contributions, the N_F part is made simpler since it occurs only at $\mathcal{O}(\alpha^2)$. Diagram ii of Figure 7.2 is nothing but the corresponding $\mathcal{O}(\alpha)$ diagram multiplied by $(1 - Z_3)$ to the order we are working. The remaining two diagrams constitute the on-shell and off-shell computations (with only the UV pole of the off-shell calculation required for $\overline{MS}$ renormalisation) of the same Feynman integral. However, by virtue of the soft factor, this integral only has a UV sub-divergence due to the fermion loop, hence the two-loop counter-term is zero (or at least is finite) and this is borne out by calculation (see Appendix A for required loop integrals). The on-shell calculation of diagram i gives

$$\delta Z_2{}^s = \left(\frac{\alpha}{\pi}\right)^2 \left(\frac{\mu^2}{-\Delta}\right)^{2\,\epsilon} c_\epsilon{}^2 C_F \, N_F \, T_R \left(\frac{1}{16\,\epsilon} + \frac{37}{96}\right), \qquad (7.1)$$

where $c_\epsilon = (4\pi)^\epsilon e^{-\epsilon\gamma_E}$, combining this with contribution ii gives a soft renormalised pole-scheme residue of

$$Z_2{}^s_p = 1 + \left(\frac{\alpha}{\pi}\right)^2 \left(\frac{\mu^2}{-\Delta}\right)^{\epsilon} c_\epsilon{}^2 C_F \, N_F \, T_R \left(\frac{1}{12\,\epsilon^2} + \frac{25}{144\,\epsilon} - \frac{2+\pi^2}{144}\right). \qquad (7.2)$$

The $\mathcal{O}(\alpha)$ renormalised residue of the gluon propagator, without a soft factor, is also required for this calculation

$$Z_{3\,p} = 1 + \left(\frac{\alpha}{\pi}\right)^2 c_\epsilon C_F \, N_F \, T_R \left(\frac{1}{3\,\epsilon}\right). \tag{7.3}$$

7.3 Fully inclusive contributions to N_F at $\mathcal{O}(\alpha^2)$

Using the renormalised pole-scheme, we need to compute all the cut diagrams, suggested by Figure 7.1, that contribute to the S-matrix and the real cuts of the corresponding $\mathcal{O}(\alpha)$ diagrams multiplied by $\sqrt{Z_{3\,p}}$ (or in fact $\frac{Z_{3\,p}^{(2)}}{2}$). In addition we need the graph corresponding to the $\overline{MS}$ renormalisation of the gluon propagator as well as the N_F part of the two loop vertex counter-term and the $\mathcal{O}(\alpha^2)$ residue of the quark propagator. The results for each cut represent contributions to the total cross-section, they include any symmetry factors and are normalised by the factor $N = \left(\frac{\alpha}{\pi}\right)^2 c_\epsilon^2 \, C_F \, N_F \, T_R$, $\Delta_s = \frac{\Delta}{s}$.

7.3.1 The single real contributions

The two single real emission diagrams can be easily evaluated using the three-parton phase-space as given in Eq. (3.8). Using this representation, plus-distributions can be applied or the integrals can be evaluated directly in terms of $_2F_1$ hypergeometric functions. The results for the two topologies are

$$
\begin{aligned}
\frac{\sigma_{T1}^{SR}}{\sigma_0 N} &= \left(\frac{\mu^2}{s}\right)^\epsilon \left\{ \frac{1}{3\,\epsilon^3} + \frac{2 - \ln(\frac{\Delta_s}{1+\Delta_s})}{3\,\epsilon^2} + \frac{36 - 7\,\pi^2}{36\,\epsilon} \right. \\
&\qquad \left. - \frac{\mathrm{Li}_2(-\Delta_s^{-1})}{\epsilon} - \frac{\ln(\frac{\Delta_s}{1+\Delta_s})^2}{3\,\epsilon} - \frac{\ln(\frac{\Delta_s}{1+\Delta_s})\,(2 + 3\,\Delta_s)}{3\,\epsilon} \right\} \\
\frac{\sigma_{T2}^{SR}}{\sigma_0 N} &= \left(\frac{\mu^2}{s}\right)^\epsilon \left\{ -\frac{1}{12\,\epsilon^2} - \frac{2 + \Delta_s - \ln(\frac{\Delta_s}{1+\Delta_s})\,\left(1 - \Delta_s^{\,2}\right)}{12\,\epsilon} \right\}.
\end{aligned}
\tag{7.4}
$$

7.3.2 The double real contributions

To evaluate these two cut diagrams the four-parton phase-space is parameterised as given by Eq. (3.10), with this implemented the Mellin-Barnes identity [67] can be used to repose the problem as contour integrals over gamma functions. This transformation allows the automated analytic continuation of the integral representation to be performed and hence a series expansion in ϵ can be obtained using [22]. The coefficients of the poles can then be evaluated analytically using Barne's Lemmas and summation identities. A good check of the analytic results is obtained by applying sector-decomposition instead of Mellin-Barnes identities and numerically integrating the coefficients using a Monte-Carlo routine. Both the integrals' contour integral representations and sector decomposed forms can be found in Appendix B, here we simply quote the results.

$$
\begin{aligned}
\frac{\sigma_{T1}^{DR}}{\sigma_0 N} &= \left(\frac{\mu^2}{s}\right)^{2\epsilon} \left\{ -\frac{1}{12\,\epsilon^3} + \frac{-7 + 3\ln(\frac{\Delta_s}{1+\Delta_s})}{18\,\epsilon^2} + \frac{-308 + 33\,\pi^2 - 36\,\Delta_s}{216\,\epsilon} \right. \\
&\qquad \left. + \frac{5\,\mathrm{Li}_2(-\Delta_s^{-1})}{6\,\epsilon} + \frac{\ln(\frac{\Delta_s}{1+\Delta_s})^2}{4\,\epsilon} + \frac{\ln(\frac{\Delta_s}{1+\Delta_s})\left(14 + 9\,\Delta_s - 3\,\Delta_s^2\right)}{18\,\epsilon} \right\} \\
\frac{\sigma_{T2}^{DR}}{\sigma_0 N} &= \left(\frac{\mu^2}{s}\right)^{2\epsilon} \left\{ \frac{1}{16\,\epsilon} + \frac{1 + 2\,\Delta_s + 2\ln(\frac{\Delta_s}{1+\Delta_s})\,\Delta_s\,(1+\Delta_s)}{12\,\epsilon} \right\}
\end{aligned}
\tag{7.5}
$$

7.3.3 The two loop contribution

Only topology $T1$ has a contribution to the S-matrix. Automated Mellin-Barnes and standard reduction loop integral methods can be used with both methods

giving the same analytic result

$$
\frac{\sigma_{T1}^{DV}}{\sigma_0 N} = \left(\frac{\mu^2}{s}\right)^{2\epsilon} \left\{ \frac{1}{12\,\epsilon^3} + \frac{7 - 3\ln(\frac{\Delta_s}{1+\Delta_s})}{18\,\epsilon^2} + \frac{266 - 27\,\pi^2 + 108\,\Delta_s - 72\,\Delta_s^2}{216\,\epsilon} \right.
$$
$$
- \frac{\ln(\frac{\Delta_s}{1+\Delta_s})^2}{4\,\epsilon} + \frac{\ln(\frac{\Delta_s}{1+\Delta_s})\left(-11 + 3\,\Delta_s + 6\,\Delta_s^2 - 6\,\Delta_s^3\right)}{18\,\epsilon}
$$
$$
+ \frac{\ln(\Delta_s)\left(-2 + \ln(\Delta_s) + 4\ln(\frac{\Delta_s}{1+\Delta_s}) - 4\,\Delta_s\right)}{12\,\epsilon}
$$
$$
\left. + \frac{\mathrm{Li}_2(-\Delta_s)}{6\,\epsilon} - \frac{\left(\mathrm{Li}_2(1 - \Delta_s) - \mathrm{Li}_2(-\Delta_s)\right)\left(1 - \Delta_s^2\right)}{3\,\epsilon} \right\}. \tag{7.6}
$$

It should be noted that the results presented are contributions to the cross-section and are therefore real as the conjugate cut has been included. Due to the soft factor, the renormalisation of this virtual cut requires only the N_F part of Z_3 multiplying the $\mathcal{O}(\alpha)$ diagram, it is

$$
\frac{\sigma_{T1}^{CT}}{\sigma_0 N} = \left(\frac{\mu^2}{s}\right)^{\epsilon} \left\{ -\frac{1}{3\,\epsilon^3} + \frac{-2 + \ln(\frac{\Delta_s}{1+\Delta_s})}{3\,\epsilon^2} + \frac{-240 + 30\,\pi^2 - 108\,\Delta_s + 72\,\Delta_s^2}{216\,\epsilon} \right.
$$
$$
+ \frac{\ln(\frac{\Delta_s}{1+\Delta_s})^2}{6\,\epsilon} + \frac{\ln(\frac{\Delta_s}{1+\Delta_s})\left(1 - \Delta_s^2 + \Delta_s^3\right)}{3\,\epsilon}
$$
$$
+ \frac{\ln(\Delta_s)\left(1 - \ln(\Delta_s) + \Delta_s\right)}{3\,\epsilon} + \frac{\ln(1 + \Delta_s)^2}{6\,\epsilon}
$$
$$
\left. - \frac{\mathrm{Li}_2(-\Delta_s)}{3\,\epsilon} + \frac{\left(\mathrm{Li}_2(1 - \Delta_s) - \mathrm{Li}_2(-\Delta_s)\right)\left(1 - \Delta_s^2\right)}{3\,\epsilon} \right\}. \tag{7.7}
$$

The two loop counter-term does not contribute to the pole structure of topology $T1$ and is zero for the purposes of this calculation. This is because the overall divergence of the two-loop cut is also zero; only an ultra-violet sub-divergence, coming from the inner fermion loop, requires subtraction.

7.4   Adding up the poles

Despite the involved nature of the calculation we find that summing up all the contributions to the total cross-section does lead to a complete cancellation of the IR poles. Thus, aside from the problems associated with the gauge dependence of the amplitudes and the need to modify the method of renormalisation, we find that, for this topology, it should be possible to construct infrared finite amplitudes at NNLO in QCD. We have shown that the origin of all IR divergences in the amplitude appear to be understood and therefore the main obstacle to doing so is the sheer complexity of the calculation.

Chapter 8

Conclusions and Outlook

8.1 Summary of results

We have outlined a new approach to the calculation of observables in field theory. To begin with we considered precisely how one might construct a new perturbation series based in the asymptotic interaction picture. We found that the necessary modifications to the LSZ, as described by Eq. (4.41), were beyond our capacity to compute directly. For the same reasons the propagators of the theory had to be expanded perturbatively on the free-state basis of states, see Eq. (4.40). This led to a more pragmatic interpretation of the AIP where we reverted to conventional perturbation theory, but used hard and soft factors to change the way amplitudes are defined.

Instead of the usual approach where states are defined by the number of external particles, our dressed states are effectively defined by the number of "resolved" particles. Taking a conventional amplitude we thus constrain each vertex to be hard and then add to it amplitudes with greater external particle content, where the additional particles are constrained by vertex factors to be soft. Due to the soft interacting nature of these states we found that dressed states could only

really be defined from calculations performed at the level of the amplitude-squared (discussed more fully in Section 4.4). A result of this is that the S-matrix, living on a basis of Fock states, is really still ill-defined. However, this does not mean that the new method for constructing infrared finite amplitudes does not offer benefits over the conventional approach.

In Sections 5, 6 and 7 we implemented practical checks of the new theory, constructing infrared finite amplitudes and their corresponding cross-sections. For QCD at NLO the method appears to work well for the limited number of observables we have tested. The apparent finiteness of the amplitudes means that a numerical algorithm could successfully evaluate these observables. Further investigations at higher orders in the coupling highlighted two key problems with the method. The first difficulty stems from the method used for renormalisation. In the $\overline{MS}$ prescription ambiguities develop over the finite contributions obtained when soft factors are applied to counter-terms of the theory. However this is evidently a technical problem that can be overcome by ensuring that renormalisation is performed consistently at the level of the integrand, using BPHZ renormalisation for example.

A more serious problem for gauge theories is that the need to fix the gauge in order to form the boson propagator introduces an apparent inconsistency over how the polarisation sum and internal lines are treated and this leads to cross topology cancellations of IR poles. Thus for gauge theories only a gauge invariant infrared safe sum of renormalised topologies can be shown to be finite. We saw in Section 6 that such problems were indeed constrained to gauge theories and found that infrared finite amplitudes could be constructed in ϕ^3 without the need to modify the theory. For calculating the N_F part of $e^+e^- \rightarrow$ hadrons at $\mathcal{O}(\alpha_s)$ we negotiated this problem by altering the way we split up the conventional amplitudes with hard and soft factors. This was achieved by invoking the gauge symmetries of the theory

before applying hard and soft factors. In this way it was possible to compute the NLO contribution to the dressed three-parton state and the LO contribution to the dressed four-parton state.

Section 7 represents the application of the modified AIP to the first steps in the direct construction of the dressed two-parton state at NNLO for $e^+e^- \to$ hadrons. We have shown that the two loop IR singularity structure for this example is under control and it is therefore hopeful that this method may eventually be used to compute NNLO corrections to observables. However there are still problems to be overcome.

8.2 Outlook

There are many issues still to be addressed by this formalism. The most pressing is the need to develop a method of systematically removing cross-topology cancellations. It seems impossible to construct a perturbation theory without fixing the gauge, thus the first step to dealing with cross-topology cancellations is to identify which groups of topologies add to make a gauge invariant sum [82, 83]. The question then remains how to systematically remove all terms that cancel across topologies. A successful algorithm for doing this would then make the application of hard and soft factors as straightforward as in scalar field theory. A possible alternative to this approach is described by Sterman [72, 73], where a complex non-covariant choice of gauge fixing may be chosen such that all IR divergences cancel at the level of individual topologies. Losing covariance would of course complicate renormalisation and make analytic calculations technically more difficult.

Additionally we need a way of systematically identifying what dressed amplitude-squared a particular cut diagram, with various hard and soft factors, belongs to. For the case of the non-analytic theta cut, this will be simpler to achieve, however

for complicated topologies ambiguities remain and it appears that only a direct calculation can shed light on the problem. Evidently non-analytic investigations using the theta function split are basically impossible, whilst for the analytic split they are just very hard using perturbative methods. Thus until a better understanding of the effect of hard and soft factors on cut diagrams is achieved the analytic methods used in this thesis cannot be abandoned in favour of non-analytic methods.

Another development that is of key importance is how to develop a successful numerical implementation of this theory. Assuming the previous two problems are addressed, we are left with computing contributions that give a finite total answer but have separately divergent parts. What is absolutely necessary is that we parameterise these divergent parts in *exactly* the same manner. Once this is achieved then a Monte-Carlo integration routine would be stable and able to evaluate such infrared finite amplitudes-squared. The advantage of this approach, in comparison to semi-analytic approaches, being that no further algebraic reduction of the integrand would be necessary.

Work along these line has been presented by Soper for NLO corrections [84] where, after a contour integral over the energy, the virtual term is rewritten as a phase-space integral with identical singular regions of phase-space to the corresponding real graphs. This method appears viable but also requires careful consideration of the singularities present in the region of integration in order that a stable sampling of integration points may be made. If hard soft separation functions were to be used it would also require the use of an analytic separation function, at least in the energy, in order that the contour integral might be performed. Instead, since the application of soft factors allows for a completely inclusive integration in the soft regions of phase space, we advocate a method of re-writing the soft real phase-space integral as a loop integral. Assuming this could be achieved then

the assumption is that some form of Feynman parameterisation might be used to cancel the divergences directly at the level of the integrand.

A problem that has yet to be considered is initial state radiation. This opens up a host of problems that need to be investigated. It is clear that relying on the usual PDFs would mean that we would not be able to define infrared finite amplitudes using the standard conventional methods of perturbation theory. Using the usual bare PDFs would mean that some of the IR divergences present in the perturbative calculation would have to be removed using IR subtractions similar to conventional subtraction methods. If we wish to avoid this then we will ultimately need to appeal to KLN theorem and look at ways of including different initial state diagrams such that all IR divergences are cancelled. The formulation for doing this is currently far from clear and fundamental questions remain over IR cancellations involving initial state radiation [11]. Assuming this problem could be surmounted we would also be left with the problem of having to redefine exactly what is meant by a PDF and then recalculate them. This new definition would of course be attractive in the sense it would not lead to divergent PDFs and would correspond directly to the probability of picking out some parton in a bound state.

8.3 Conclusion

In this thesis we have, through example, described the usefulness of the modified asymptotic interaction picture, which essentially involves a new way of grouping terms in conventional perturbation theory. This new approach opens up the possibility of taking fully inclusive integrations over the soft phase-space of real emission diagrams and converting them effectively to the status of loop corrections to conventional contributions with external particle content reduced. In this way infrared finite amplitudes, or at least amplitudes-squared, can be formed.

We have attempted to extend the validity of the theory to higher-order corrections and have discovered that gauge theories introduce additional obstructions to the method that stem from the procedure of gauge fixing. For the cases considered we described how to get around these problems and discussed how hard and soft factors can be used to classify the effective external particle content of a cut-diagram. We have highlighted the need to develop algorithms that can identify cross-topology cancellations and determine the contributions of cut-diagrams to dressed states.

Aside from these problems, we have shown that this method appears to work for NNLO corrections and there appears to be no further obstruction to its application at even higher orders. This method, without the additional complication of initial state radiation, therefore offers an alternative approach to conventional subtraction methods and may eventually offer a competitive alternative when the era of the ILC beckons.

Appendix A

Full Expressions and Basis Integrals

Asymptotic propagator corrections

The two-point basis integrals

The two-point basis integrals for the reduction of the asymptotic propagators are given below in Eq. (A.1). Note that the integrals have been expanded in $4 - 2\epsilon$ dimensions and that the poles are defined in the usual $\overline{MS}$ fashion carring the attendant factor of $c_\epsilon = (4\pi)^\epsilon e^{\epsilon \gamma_E}$. Note also that $\omega \equiv \frac{\Delta}{p^2}$, where Δ is the soft scale and can be interpreted as the square of an imaginary mass.

$$\int \frac{d^d k}{i\,\pi^{d/2}} \frac{1}{k^2 + \Delta} = -\frac{\Delta}{\bar{\epsilon}} - \Delta + \Delta \ln(-\Delta) \tag{A.1}$$

$$\int \frac{d^d k}{i\,\pi^{d/2}} \frac{1}{k^2\,(k+p)^2} = \frac{1}{\bar{\epsilon}} + 2 - \ln(-p^2)$$

$$\int \frac{d^d k}{i\,\pi^{d/2}} \frac{1}{k^2\,[(k+p)^2 + \Delta]} = \frac{1}{\bar{\epsilon}} + 2 - \ln(-\Delta) + (1+\omega)\,\ln\left(\frac{\omega}{1+\omega}\right)$$

$$\int \frac{d^d k}{i\,\pi^{d/2}} \frac{1}{[k^2 + \Delta]\,[(k+p)^2 + \Delta]} = \frac{1}{\bar{\epsilon}} + 2 - \ln(-\Delta) + \sqrt{1+4\,\omega}\,\ln\left(\frac{\sqrt{1+4\,\omega}-1}{\sqrt{1+4\,\omega}+1}\right)$$

The fermion propagator

The full form for the calculation of Eq. (4.50) in Section 4.7.2 is given by

$$\Sigma_{\Xi}^{(2)} = -i\,\slashed{p}\,\frac{g^2\,C_F}{16\,\pi^2}\left[\frac{\omega}{1+\omega}\right]^4 \left\{ \frac{(\omega - \xi_x\,(2+\omega))\,(2\ln(1+\omega) - \ln(\omega))}{\omega} + \cdots \right.$$
$$\left. - \frac{\omega\,(C_1 + C_2\,\xi_x)}{6\,(1+\omega)^2\,(1+4\,\omega)^5} - \frac{(C_3 + C_4\,\xi_x)\,\ln\left(\frac{\sqrt{1+4\,\omega}-1}{\sqrt{1+4\,\omega}+1}\right)}{\omega\,(1+4\,\omega)^{\frac{11}{2}}} \right\} \tag{A.2}$$

$$C_1 = 12\,\omega + 228\,\omega^2 + 1722\,\omega^3 + 6464\,\omega^4 + 12092\,\omega^5 + \cdots$$
$$+ 8760\,\omega^6 + 1796\,\omega^7 + 896\,\omega^8 + 240\,\omega^9$$

$$C_2 = -24 - 468\,\omega - 3672\,\omega^2 - 14658\,\omega^3 - 30835\,\omega^4 - 31711\,\omega^5 + \cdots$$
$$- 12906\,\omega^6 - 130\,\omega^7 + 584\,\omega^8 + 600\,\omega^9$$

$$C_3 = -\omega - 22\,\omega^2 - 198\,\omega^3 - 924\,\omega^4 - 2310\,\omega^5 + \cdots$$
$$- 2772\,\omega^6 - 924\,\omega^7 + 264\,\omega^8 + 152\,\omega^9 + 80\,\omega^{10}$$

$$C_4 = 2 + 45\,\omega + 418\,\omega^2 + 2046\,\omega^3 + 5544\,\omega^4 + 7854\,\omega^5 + \cdots$$
$$+ 4620\,\omega^6 + 396\,\omega^7 + 132\,\omega^8 - 172\,\omega^9 + 200\,\omega^{10} \tag{A.3}$$

The gluon propagator

The full form for the calculation of Eq. (4.57) in Section 4.7.2 is given by

$$\Pi_{\Xi}^{\mu\nu\,(2)} = -i\,\frac{g^2\,N_F\,T_R}{12\,\pi^2}\,\left[\frac{\omega}{1+\omega}\right]^4\,\left\{\,(2\ln(1+\omega)-\ln(\omega))\,\left(g^{\mu\nu}\,p^2 - p^\mu p^\nu\right) + \cdots\right.$$
$$\left. -\,\frac{\omega^2\,(A_1\,p^2 g^{\mu\nu} - B_1\,p^{\mu\nu})}{3\,(1+\omega)^2\,(1+4\,\omega)^5} + \frac{(A_2\,p^2 g^{\mu\nu} - B_2\,p^{\mu\nu})\,\ln(\frac{\sqrt{1+4\,\omega}-1}{\sqrt{1+4\,\omega}+1})}{(1+4\,\omega)^{\frac{11}{2}}}\,\right\} \quad \text{(A.4)}$$

$$
\begin{aligned}
A_1 =\ & 6 + 108\,\omega + 753\,\omega^2 + 2481\,\omega^3 + 3605\,\omega^4 + \cdots \\
& +\ 1104\,\omega^5 + 378\,\omega^6 + 920\,\omega^7 + 600\,\omega^8 \\
B_1 =\ & 6 + 108\,\omega + 753\,\omega^2 + 2481\,\omega^3 + 3596\,\omega^4 + \cdots \\
& -\ 852\,\omega^5 + 1224\,\omega^6 + 2360\,\omega^7 + 1680\,\omega^8 \\
A_2 =\ & 1 + 22\,\omega + 198\,\omega^2 + 924\,\omega^3 + 2310\,\omega^4 + 2772\,\omega^5 + \cdots \\
& +\ 924\,\omega^6 - 264\,\omega^7 - 72\,\omega^8 - 280\,\omega^9 - 400\,\omega^{10} \\
B_2 =\ & 1 + 22\,\omega + 198\,\omega^2 + 924\,\omega^3 + 2310\,\omega^4 + 2772\,\omega^5 + \cdots \\
& +\ 924\,\omega^6 - 264\,\omega^7 - 432\,\omega^8 - 640\,\omega^9 - 1120\,\omega^{10} \quad \text{(A.5)}
\end{aligned}
$$

For the calculation of Eq. (4.63), where quadratic subtraction is used, the coefficients take the form

$$A_1 = B_1 = \; 6 + 114\,\omega + 861\,\omega^2 + 3232\,\omega^3 + 6046\,\omega^4 + \cdots$$

$$+ \; 4380\,\omega^5 + 898\,\omega^6 + 448\,\omega^7 + 120\,\omega^8$$

$$A_2 = B_2 = \; 1 + 22\,\omega + 198\,\omega^2 + 924\,\omega^3 + 2310\,\omega^4 + 2772\,\omega^5 + \cdots$$

$$+ \; 924\,\omega^6 - 264\,\omega^7 - 152\,\omega^8 - 80\,\omega^9 \qquad (A.6)$$

Three-point function integrals

Here we define three-point integrals used in the loop calculations of Chapter 5 and Chapter 6. The external momentum are on-shell with $p_1^2 = p_2^2 = 0$ and the invariant mass is given by $(p_1 + p_2)^2 = s_{12}$.

$$\int \frac{d^d k}{i\,\pi^{d/2}} \frac{s_{12}}{k^2\,(k-p_1)^2\,[(k-p_1-p_2)^2 + \Delta]} = -\frac{1}{\epsilon} \ln\left[\frac{\Delta}{\Delta + s_{12}}\right] + \cdots$$
$$-\frac{\pi^2}{6} - \mathrm{Li}_2\left[-\frac{\Delta}{s_{12}}\right] - \frac{1}{2}\ln^2\left[\frac{\Delta}{s_{12}}\right] - \ln\left[\frac{\Delta}{\Delta + s_{12}}\right]\ln\left[(-s_{12})\left(1 + \frac{\Delta}{s_{12}}\right)\right]$$

$$\int \frac{d^d k}{i\,\pi^{d/2}} \frac{s_{12}}{k^2\,[(k-p_1)^2 + \Delta]\,(k-p_1-p_2)^2} = \frac{\pi^2}{6} + \mathrm{Li}_2\left[1 - \frac{\Delta}{s_{12}}\right] + \frac{1}{2}\ln^2\left[\frac{\Delta}{s_{12}}\right]$$

$$\int \frac{d^d k}{i\,\pi^{d/2}} \frac{s_{12}}{k^2\,[(k-p_1)^2 + \Delta]\,[(k-p_1-p_2)^2 + \Delta]} = \frac{\pi^2}{6} + \mathrm{Li}_2\left[-\frac{\Delta}{s_{12}}\right] + \frac{1}{2}\ln^2\left[\frac{\Delta}{s_{12}}\right]$$

$$\int \frac{d^d k}{i\,\pi^{d/2}} \frac{s_{12}}{[k^2 + \Delta]\,(k-p_1)^2\,[(k-p_1-p_2)^2 + \Delta]} = 4\ln^2\left[\frac{1}{2}\left(\sqrt{4 + \frac{s_{12}}{\Delta}} + \sqrt{\frac{s_{12}}{\Delta}}\right)\right]$$

$$\int \frac{d^d k}{i\,\pi^{d/2}} \frac{s_{12}}{[k^2 + \Delta]\,[(k-p_1)^2 + \Delta]\,[(k-p_1-p_2)^2 + \Delta]} =$$
$$- \mathrm{Li}_2\left[\frac{2}{1 + \sqrt{4\frac{s_{12}}{\Delta} + 1}}\right] - \mathrm{Li}_2\left[\frac{2}{1 - \sqrt{4\frac{s_{12}}{\Delta} + 1}}\right] \quad (A.7)$$

Two loop propagator integrals

In Chapter 6 most of the on-shell two loop propagator integrals are straightforward to evaluated using known one-loop integrals computed in terms of gamma functions. The all massive two-loop integral is less straightforward and is given by

$$
\iint \frac{d^d l}{i\,\pi^{d/2}} \frac{d^d k}{i\,\pi^{d/2}} \frac{1}{[k^2+\Delta]^{n_1}\,[(k-l)^2+\Delta]^{n_2}\,[l^2+\Delta]^{n_3}} = -(-1)^{n_{123}}\,(-\Delta)^{d-n_{123}} \times
$$

$$
\left\{ \Gamma\left[\begin{matrix} n_1-\frac{d}{2}, n_{23}-\frac{d}{2} \\ n_1, n_{23} \end{matrix}\right] {}_4F_3\left[\begin{matrix} \frac{d}{2}, n_2, n_3, n_{23}-\frac{d}{2} \\ 1+\frac{d}{2}-n_1, \frac{n_{23}}{2}, \frac{1}{2}+\frac{n_{23}}{2} \end{matrix};\, \frac{1}{4}\right] + \cdots \right.
$$

$$
\left. \Gamma\left[\begin{matrix} \frac{d}{2}-n_1, n_{12}-\frac{d}{2}, n_{13}-\frac{d}{2}, n_{123}-d \\ \frac{d}{2}, n_2, n_3, 2\,n_{123}-d \end{matrix}\right] {}_4F_3\left[\begin{matrix} n_1, n_{12}-\frac{d}{2}, n_{13}-\frac{d}{2}, n_{123}-d \\ 1-\frac{d}{2}+n_1, \frac{n_1+n_{123}-d}{2}, \frac{1-d+n_1+n_{123}}{2} \end{matrix};\, \frac{1}{4}\right] \right\},
$$

where $n_{ij}=n_i+n_j$, $n_{ijk}=n_i+n_j+n_k$ and $\Gamma\left[\begin{matrix} a,\cdots,b \\ c,\cdots,d \end{matrix}\right] = \frac{\Gamma(a)\cdots\Gamma(b)}{\Gamma(c)\cdots\Gamma(d)}$.

For the six-dimensional self-energy in ϕ^3 theory, the methods described in [81] were used to reduce all hypergeometric functions to two basis functions. Necessary expansions in ϵ are given below

$$
{}_2F_1\left[\begin{matrix} 1, 1+\epsilon \\ \frac{3}{2} \end{matrix};\, \frac{1}{4}\right] = \frac{\sqrt{3}\,\pi}{3} - \frac{2\,\epsilon}{9}\left(\sqrt{3}\,\pi\ln(3) - \psi'\left(\frac{1}{3}\right) + \psi'\left(\frac{2}{3}\right)\right)
$$

$$
{}_2F_1\left[\begin{matrix} 1, 1+2\,\epsilon \\ \frac{3}{2}+\epsilon \end{matrix};\, \frac{1}{4}\right] = \frac{\sqrt{3}\,\pi}{3} - \frac{2\,\epsilon}{9}\left(\sqrt{3}\,\pi\,(\ln(12)-2) - 2\,\psi'\left(\frac{1}{3}\right) + 2\,\psi'\left(\frac{2}{3}\right)\right)
$$

$$
\cdots + i\,6\sqrt{3}\,\epsilon\left(\mathrm{Li}_2\left[\frac{1-i\,\sqrt{3}}{4}\right] - \mathrm{Li}_2\left[\frac{1+i\,\sqrt{3}}{4}\right]\right). \quad (\mathrm{A.8})
$$

Integrals for two loop QCD calculation

For the two loop vertex diagram of Section 7 the analytic evaluation can be achieved using the following integrals

$$\int \frac{d^d k}{i\,\pi^{d/2}} \frac{1}{[k^2]^{n_1}\,[k^2 + \Delta]\,(k - p_1)^2\,(k - p_2)^2} = (-1)^{n_1 + 1}\,(-\Delta)^{-1}\,\times$$

$$\frac{(-s)^{-2 + \frac{d}{2} - n_1}\,\Gamma(-1 + \frac{d}{2} - n_1)^2\,\Gamma(2 - \frac{d}{2} + n_1)}{\Gamma(-2 + d - n_1)}\,{}_2F_1\left[\begin{array}{c} 1, \frac{d}{2} - 1 - n_1 \\ d - 2 - n_1 \end{array}; \frac{s}{\Delta}\right]$$

$$\cdots + (-\Delta)^{-2 + \frac{d}{2} - n_1}\,\Gamma(\tfrac{d}{2})\,\Gamma(\tfrac{d}{2} - n_1)\,\Gamma(1 - \tfrac{d}{2} + n_1)\,{}_2F_1\left[\begin{array}{c} 1, 1 \\ \frac{d}{2} \end{array}; \frac{s}{\Delta}\right]$$

$$\int \frac{d^d k}{i\,\pi^{d/2}} \frac{1}{[k^2]^{n_1}\,[k^2 + \Delta]^{n_2}\,[(k - p_1)^2]^{n_3}\,(k - p_2)^2} = (-1)^{n_{123}}\,(-\Delta)^{-1 + \frac{d}{2} - n_{123}}\,\times$$

$$\frac{\Gamma(\frac{d}{2} - n_1)\,\Gamma(1 - \frac{d}{2} + n_{123})}{\Gamma(\frac{d}{2})\,\Gamma(n_{23})\,\left(1 - \frac{d}{2} + n_1\right)}\,{}_3F_2\left[\begin{array}{c} 1, n_3, 1 - \frac{d}{2} + n_{123} \\ \frac{d}{2}, n_{23} \end{array}; -\frac{s}{\Delta}\right]. \quad (A.9)$$

The hypergeometric functions generated in the calculation of the soft two loop vertex give functions that can be expanded in ϵ using [85]. An analytic check of this calculation was performed using the technique of automated Mellin-Barnes [22].

Appendix B

Mellin-Barnes and Sector-Decomposed Representations

During the computation of more difficult Feynman diagrams, particularly at two loop, Mellin-Barnes and Sector-Decomposition techniques were used to analytically and numerically evaluate the integrals. This appendix presents the forms of the integrand used to obtain the results quoted in the main body of the thesis for the four-parton phase-space diagrams of Section 7.3.2.

The integrands of the fully inclusive four-parton final state graphs are given below for the two topologies, an overall factor of $\left(\frac{\mu^2}{s}\right)^{2\epsilon} \left(\frac{\alpha}{\pi}\right)^2 C_F N_F T_R$ is missing. The variables of integration are the λ_i's, with the region of integration being the unit

cube.

$T1 =$

$$-\left(\frac{16^\epsilon \, \pi^{2\,\epsilon} \, (-1+\epsilon)^2 \, \lambda_1^{-1-2\,\epsilon} \, \lambda_2^{-2-\epsilon} (1-\lambda_1)^{2-2\,\epsilon} \, (1-\lambda_2)^{2-2\,\epsilon} \, (1-\lambda_3)^{-\epsilon} \, \lambda_3^{-\epsilon} \, \Delta_s^4}{\Gamma(4-2\,\epsilon) \, (\lambda_2 + (1-\lambda_1) \, (1-\lambda_2) \, \lambda_3) \, (\Delta_s + \lambda_1)^2 \, (\Delta_s + \lambda_1 \, \lambda_2)^2}\right)$$

$$\left(-(\lambda_2 \, (1+2\,\lambda_1\,\lambda_2)) + \left(1 + \lambda_1 \, \left(-1 + \lambda_2 + 2\,\epsilon\,\lambda_2 + 2\,\lambda_2^2\right)\right)\lambda_3 - (1-\lambda_1) \, (1-\lambda_2) \, \lambda_3^2\right)$$

$T2 =$

$$-\left(\frac{16^\epsilon \, \pi^{2\,\epsilon} \, (-1+\epsilon)^2 \, \lambda_1^{-1-2\,\epsilon} \, \lambda_2^{-2-\epsilon} (1-\lambda_1)^{2-2\,\epsilon} \, (1-\lambda_2)^{2-2\,\epsilon} \, (1-\lambda_3)^{-\epsilon} \, \lambda_3^{-\epsilon} \, \Delta_s^4}{2\,\Gamma(4-2\,\epsilon) \, (\Delta_s + \lambda_1)^2 \, (\Delta_s + \lambda_1 \, \lambda_2)^2}\right)$$

$$(-1 + \lambda_3 - 2\,\lambda_2\,\lambda_3 + 2\,\epsilon\,\lambda_2\,\lambda_3) \tag{B.1}$$

These two expressions, re-cast as contour integrals, have terms of the form

$T1_i =$

$$-\prod_{j=1}^{3} \oint_{c_j-i\infty}^{c_j+i\infty} dz_j \, \frac{16^\epsilon \, \pi^{2\,\epsilon} \, \Gamma(-z_1) \, \Gamma(1+z_1) \, \Gamma(-z_2) \, \Gamma(2+z_2) \, \Gamma(-z_3) \, \Gamma(2+z_3) \, \Delta_s^{4+z_2+z_3}}{(2\,\pi i)^3 \, \Gamma(4-2\,\epsilon)}$$

$$\frac{\Gamma(1-\epsilon+n_3) \, \Gamma(1-\epsilon+m_3+z_1) \, \Gamma(1-2\,\epsilon+n_1+z_1) \, \Gamma(1-2\,\epsilon+n_2+z_1)}{\Gamma(2-2\,\epsilon+m_3+n_3+z_1) \, \Gamma(-1-3\,\epsilon+m_2+n_2-z_3)} \tag{B.2}$$

$$\frac{\Gamma(-2-\epsilon+m_2-z_1-z_3) \, \Gamma(-3-2\,\epsilon+m_1-z_2-z_3)}{\Gamma(-2-4\,\epsilon+m_1+n_1+z_1-z_2-z_3)}$$

$T2_i =$

$$-\prod_{j=2}^{3} \oint_{c_j-i\infty}^{c_j+i\infty} dz_j \, \frac{16^\epsilon \, \pi^{2\,\epsilon} \, \Gamma(-z_2) \, \Gamma(2+z_2) \, \Gamma(-z_3) \, \Gamma(2+z_3) \, \Delta_s^{4+z_2+z_3}}{(2\,\pi i)^2 \, \Gamma(4-2\,\epsilon)}$$

$$\frac{\Gamma(3-2\,\epsilon) \, \Gamma(1-\epsilon) \, \Gamma(2-\epsilon) \, \Gamma(-3-\epsilon-z_3) \, \Gamma(-4-2\,\epsilon-z_2-z_3)}{2\,\Gamma(-3\,\epsilon-z_3) \, \Gamma(-1-4\,\epsilon-z_2-z_3)}, \tag{B.3}$$

where m_i and n_i correspond to the integer powers $(1-z_i)$ and z_i are respectively raised. To compute the contour integrals M.Czakon's *Mathematica* algorithm [22] is used to analytically continue the integrals and then expand about $\epsilon = 0$. The analytic forms for the poles can then be obtained using Barnes lemmas and summation identities. A strong check on the analytical results is obtained by using

sector-decomposition techniques,

$T1 =$

$$-\frac{2^{3+3\,\epsilon}\,F(1-\frac{\lambda_1\lambda_2}{2},\frac{\lambda_2\lambda_3}{2},\lambda_3)\,\lambda_2{}^{-2-3\,\epsilon}\,\lambda_3{}^{-2-2\,\epsilon}\,\lambda_1{}^{-2\,\epsilon}\,(1-\lambda_3)^{-\epsilon}}{\left(1-\frac{\lambda_1\lambda_2}{2}\right)^{2\,\epsilon}(-2+\lambda_1\,\lambda_2)\left(1-\frac{\lambda_2\lambda_3}{2}\right)^{2\,\epsilon}(-2-2\,\lambda_1+\lambda_1\,\lambda_2\,\lambda_3)}$$

$$-\frac{2^{3+3\,\epsilon}\,F(1-\frac{\lambda_1}{2},\frac{\lambda_1\lambda_2\lambda_3}{2},\lambda_3)\,\lambda_1{}^{-2-3\,\epsilon}\,\lambda_2{}^{-2-\epsilon}\,\lambda_3{}^{-2-2\,\epsilon}\,(1-\lambda_3)^{-\epsilon}}{\left(1-\frac{\lambda_1}{2}\right)^{2\,\epsilon}(-2+\lambda_1)\left(1-\frac{\lambda_1\lambda_2\lambda_3}{2}\right)^{2\,\epsilon}(-2-2\,\lambda_2+\lambda_1\,\lambda_2\,\lambda_3)}$$

$$-\frac{2^{3+3\,\epsilon}\,F(1-\frac{\lambda_1}{2},\frac{\lambda_2}{2},\lambda_2\,\lambda_3)\,\lambda_2{}^{-2-2\,\epsilon}\,\lambda_1{}^{-2\,\epsilon}\,\lambda_3{}^{-\epsilon}}{\left(1-\frac{\lambda_1}{2}\right)^{2\,\epsilon}(-2+\lambda_1)\left(1-\frac{\lambda_2}{2}\right)^{2\,\epsilon}(1-\lambda_2\,\lambda_3)^{\epsilon}(-2-2\,\lambda_1\,\lambda_3+\lambda_1\,\lambda_2\,\lambda_3)}$$

$$-\frac{2^{3+3\,\epsilon}\,F(\frac{\lambda_1}{2},\frac{\lambda_2\lambda_3}{2},\lambda_3)\,\lambda_1{}^{-1-2\,\epsilon}\,\lambda_2{}^{-2-\epsilon}\,\lambda_3{}^{-2-2\,\epsilon}\,(1-\lambda_3)^{-\epsilon}}{\left(1-\frac{\lambda_1}{2}\right)^{2\,\epsilon}\left(1-\frac{\lambda_2\lambda_3}{2}\right)^{2\,\epsilon}(4-2\,\lambda_1+2\,\lambda_2-2\,\lambda_2\,\lambda_3+\lambda_1\,\lambda_2\,\lambda_3)}$$

$$-\frac{2^{3+3\,\epsilon}\,F(\frac{\lambda_1}{2},\frac{\lambda_2}{2},\lambda_2\,\lambda_3)\,\lambda_1{}^{-1-2\,\epsilon}\,\lambda_2{}^{-2-2\,\epsilon}\,\lambda_3{}^{-\epsilon}}{\left(1-\frac{\lambda_1}{2}\right)^{2\,\epsilon}\left(1-\frac{\lambda_2}{2}\right)^{2\,\epsilon}(1-\lambda_2\,\lambda_3)^{\epsilon}(2+4\,\lambda_3-2\,\lambda_1\,\lambda_3-2\,\lambda_2\,\lambda_3+\lambda_1\,\lambda_2\,\lambda_3)}$$

$$+\frac{2^{3+4\,\epsilon}\,F(1-\frac{\lambda_1}{2},1-\frac{\lambda_2}{2},\lambda_2\,\lambda_3)\,\lambda_2{}^{1-3\,\epsilon}\,\lambda_1{}^{-2\,\epsilon}\,\lambda_3{}^{\epsilon}}{\left(1-\frac{\lambda_1}{2}\right)^{2\,\epsilon}(-2+\lambda_1)\left(1-\frac{\lambda_2}{2}\right)^{\epsilon}(-2+\lambda_2)^2\,(1-\lambda_2\,\lambda_3)^{\epsilon}\left(4-2\,\lambda_2+\lambda_1\,\lambda_2{}^2\,\lambda_3\right)}$$

$$+\frac{2^{3+4\,\epsilon}\,F(\frac{\lambda_1}{2},1-\frac{\lambda_2}{2},\lambda_2\,\lambda_3)\,\lambda_1{}^{-1-2\,\epsilon}\,\lambda_2{}^{1-3\,\epsilon}\,\lambda_3{}^{-\epsilon}}{\left(1-\frac{\lambda_1}{2}\right)^{2\,\epsilon}\left(1-\frac{\lambda_2}{2}\right)^{\epsilon}(-2+\lambda_2)^2\,(1-\lambda_2\,\lambda_3)^{\epsilon}\left(-4+2\,\lambda_2-2\,\lambda_2{}^2\,\lambda_3+\lambda_1\,\lambda_2{}^2\,\lambda_3\right)}$$

$$+\frac{2^{3+4\,\epsilon}\,F(1-\frac{\lambda_1}{2},1-\frac{\lambda_2\lambda_3}{2},\lambda_3)\,\lambda_3{}^{1-3\,\epsilon}\,\lambda_1{}^{-2\,\epsilon}\,\lambda_2{}^{-2\,\epsilon}\,(1-\lambda_3)^{-\epsilon}}{\left(1-\frac{\lambda_1}{2}\right)^{2\,\epsilon}(-2+\lambda_1)\left(1-\frac{\lambda_2\lambda_3}{2}\right)^{\epsilon}(-2+\lambda_2\,\lambda_3)^2\,\left(4-2\,\lambda_2\,\lambda_3+\lambda_1\,\lambda_2\,\lambda_3{}^2\right)}$$

$$+\frac{2^{3+4\,\epsilon}\,F(\frac{\lambda_1}{2},1-\frac{\lambda_2\lambda_3}{2},\lambda_3)\,\lambda_1{}^{-1-2\,\epsilon}\,\lambda_3{}^{1-3\,\epsilon}\,\lambda_2{}^{-2\,\epsilon}\,(1-\lambda_3)^{-\epsilon}}{\left(1-\frac{\lambda_1}{2}\right)^{2\,\epsilon}\left(1-\frac{\lambda_2\lambda_3}{2}\right)^{\epsilon}(-2+\lambda_2\,\lambda_3)^2\,\left(-4+2\,\lambda_2\,\lambda_3-2\,\lambda_2\,\lambda_3{}^2+\lambda_1\,\lambda_2\,\lambda_3{}^2\right)},\quad\text{(B.4)}$$

here the finite function F before sector decomposition takes on the form $F(\lambda_1,\lambda_2,\lambda_3)$. Numerical evaluation proceeds by applying plus-distributions, inserting the correct form for the finite function F and simply integrating the result using VEGAS [79, 86]. The $T2$ topology can be evaluated directly using plus distributions since it has no overlapping singularities.

Appendix C

TIRA - An Interactive One-Loop Reduction Algorithm

Program summary

Title of program: TIRA

Version: 1.0

Available at: http:www.ippp.dur.ac.uk/˜dph3gb/main.html

Programming Language: Mathematica 5.0

Nature of problem: Reduction of Feynman Integrals at one-loop with upto four denominators (raised to any integer power) and a tensor rank of three.

Dependencies: Requires the installation of FeynCalc for tensor algebra.

Program notes

In these program notes we describe how to use a simple deterministic one-loop reduction algorithm. The algorithm will reduce one-loop integrals with upto four Feynman denominators raised to any integer power and with a tensor rank of no more than three. The tensor reduction is achieved by implementing Davdychev's solution of rewriting tensor integrals as scalar integrals in higher dimensions with propagators raised by some power [57]. Such scalar integrals can naturally be reduced using recurrence relations and integration-by-parts as described in [58].

The purpose of this program is to provide users with an easy to use calculational tool for quick reduction of small to medium sized one-loop calculations. It is written in *Mathematica* and is not intended for large one-loop reduction problems, such situations require the building of integral reduction tables (see for example AIR [87]). The program should be viewed as an alternative to the OneLoop reduction program found in FeynCalc. Compared to OneLoop it offers a more complete reduction for arbitrary kinematics; the reduction algorithm adapts as required if either the Gram or Cayley determinants vanish. TIRA also improves over OneLoop in that it can deal with propagators raised to higher integer powers and Feynman integrals defined in dimensions different from $4 - 2\epsilon$. It should be noted that reduction times for scalar integrals grows exponentially with the powers of the propagators and therefore computing resources quickly become an issue. For example TIRA will not be able to reduce a four-denominator Feynman integral where the powers of the propagators have all been raised to, say, four or more. In such cases *Mathematica* will most likely run out of memory on modern desktop computers.

In principle it is straightforward to reduce higher ranked tensors; the algorithm may also be extended to a greater number of denominators. However as previously discussed this is a move towards more serious one-loop calculations and is outside the scope of this program.

Description of TIRA

The *Mathematica* package is loaded simply via the command $\ll$ TIRA.m whereupon Feyncalc will also be automatically loaded. The basic scalar integral is defined as given in equation C.1 and the functions available are

$$\int \frac{d^d k}{(2\,\pi)^d} \prod_{i=1}^{4} [(k + p_i)^2 - m_i^2]^{-n_i} \tag{C.1}$$

- SetGlobalMomentum[{ p_1, p_2, p_3, p_4 }] - Function takes a four element list that defines the external momenta entering into the scalar integral defined in equation C.1.

- SetGlobalMasses[{ m_1^2, m_2^2, m_3^2, m_4^2 }] - Function takes a four element list that defines the propagator masses-squared entering into the scalar integral defined in equation C.1.

- SetKinematicInvariant[p_a, p_b, $p_a \cdot p_b$] - Function takes the symbolic names of two external four-vectors as the first two arguments and sets their dot-product to be equal to the third argument. This is of critical importance since the reduction of associated scalar integrals will change as the calculation of Gram and Cayley determinants depends directly of the value of the kinematic invariants.

- SI[dim , { n_1, n_2, n_3, n_4 }] - First argument defines the dimension of a the scalar integral you wish to reduce, the second argument is a list defining

the powers of the propagators. Note that the dimension must be an integer, an associated -2ϵ is necessarily assumed. This function will return an expression for this integral in terms of a reduction to basis scalar integrals, BSI's. The reduction algorithm will work based on the global definitions for external four-momenta and masses. The BSI function is defined as

$$\mathrm{BSI}\left(\begin{bmatrix} p_1 & m_1^2 \\ \vdots & \vdots \\ \vdots & \vdots \\ p_n & m_n^2 \end{bmatrix}\right) = \int \frac{d^{4-2\epsilon}k}{(2\pi)^{4-2\epsilon}} \prod_{i=1}^{n} [(k+p_i)^2 - m_i^2]^{-1}. \qquad (\mathrm{C.2})$$

- TI[dim , rank , { n_1, n_2, n_3, n_4 }] - This will write out the Davdychev tensor reduction using the global four-momenta definitions. tensor rank can take on the values 1, 2 or 3. The scalar integrals returned take the form SI[dim , { n_1, n_2, n_3, n_4 } , { 1, 2, 3, 4 }], the third argument is a list used by the internal scalar reduction algorithm.

- ReduceSI[expression] - Function will apply the scalar reduction algorithm to any scalar integrals found in expression (format as given by the TI function). The algorithm relies on global definitions of momentum and masses.

- SI[VEC, MASS, dim , { n_1, n_2, n_3, n_4 }] - This is the same as the previously defined SI function except that the external four-momenta and masses are defined by two four-entry lists that defines local values.

- TI[VEC, MASS, dim , rank, { n_1, n_2, n_3, n_4 }] - This is the same as the previously defined TI function except that the external four-momenta and masses are defined by two four-entry lists that defines local values.

- ReduceSI[VEC, MASS, expression] - This is the same as the previously defined TI function except that the external four-momenta and masses are defined by two four-entry lists that defines local values.

Bibliography

[1] E. P. Wigner, "On unitary representations of the inhomogeneous Lorentz group," *Annals Math.* **40** (1939) 149–204.

[2] F. Bloch and A. Nordsieck, "Note on the radiation field of the electron," *Phys. Rev.* **52** (1937) 54–59.

[3] E. Bagan, M. Lavelle, and D. McMullan, "Electrons and photons: Fact not fiction," *Phys. Lett.* **B477** (2000) 396–400, `hep-th/0003087`.

[4] M. E. Peskin and D. V. Schroeder, *An Introduction To Quantum Field Theory*. Perseus Books, 1995.

[5] C. Itzykson and J. Zuber, *Quantum Field Theory*. McGraw-Hill, 1980.

[6] D. Zwanziger, "Scattering theory for Quantum Electrodynamics. 1. Infrared renormalization and asymptotic fields," *Phys. Rev.* **D11** (1975) 3481.

[7] T. Kinoshita, "Mass singularities of Feynman amplitudes," *J. Math. Phys.* **3** (1962) 650–677.

[8] B. Schroer, "Infraparticles in quantum field theory," *Fortsch. Phys.* **11** (1963) 1–31.

[9] J. Collins, *Renormalization*. Cambridge University Press, 1984.

BIBLIOGRAPHY

[10] T. D. Lee and M. Nauenberg, "Degenerate systems and mass singularities," *Phys. Rev.* **133** (1964) B1549–B1562.

[11] M. Lavelle and D. McMullan, "Collinearity, convergence and cancelling infrared divergences," *JHEP* **03** (2006) 026, `hep-ph/0511314`.

[12] G. 't Hooft and M. J. G. Veltman, "Regularization and renormalization of gauge fields," *Nucl. Phys.* **B44** (1972) 189–213.

[13] S. Catani and M. H. Seymour, "A general algorithm for calculating jet cross sections in NLO QCD," *Nucl. Phys.* **B485** (1997) 291–419, `hep-ph/9605323`.

[14] S. Frixione, Z. Kunszt, and A. Signer, "Three-jet cross sections to next-to-leading order," *Nucl. Phys.* **B467** (1996) 399–442, `hep-ph/9512328`.

[15] W. T. Giele and E. W. N. Glover, "Higher order corrections to jet cross-sections in e+ e- annihilation," *Phys. Rev.* **D46** (1992) 1980–2010.

[16] D. E. Soper, "Techniques for QCD calculations by numerical integration," *Phys. Rev.* **D62** (2000) 014009, `hep-ph/9910292`.

[17] D. E. Soper, "Letting real-virtual cancellations happen by themselves in QCD calculations," `hep-ph/0102031`.

[18] S. Weinzierl, "Status of jet cross sections to NNLO," *Nucl. Phys. Proc. Suppl.* **160** (2006) 126–130, `hep-ph/0606301`.

[19] A. G.-D. Ridder, T. Gehrmann, E. W. N. Glover, and G. Heinrich, "Infrared structure of e+ e- → 3jets at NNLO: QED-type contributions," *Nucl. Phys. Proc. Suppl.* **160** (2006) 190–194, `hep-ph/0607042`.

[20] T. Binoth and G. Heinrich, "An automatized algorithm to compute infrared divergent multi-loop integrals," *Nucl. Phys.* **B585** (2000) 741–759, `hep-ph/0004013`.

BIBLIOGRAPHY

[21] C. Anastasiou, K. Melnikov, and F. Petriello, "A new method for real radiation at NNLO," *Phys. Rev.* **D69** (2004) 076010, `hep-ph/0311311`.

[22] M. Czakon, "Automatized analytic continuation of Mellin-Barnes integrals," *Comput. Phys. Commun.* **175** (2006) 559–571, `hep-ph/0511200`.

[23] C. Anastasiou and A. Daleo, "Numerical evaluation of loop integrals," `hep-ph/0511176`.

[24] T. Gehrmann and E. Remiddi, "Progress on two-loop non-propagator integrals," `hep-ph/0101147`.

[25] P. Mastrolia and E. Remiddi, "Analytic evaluation of Feynman graph integrals," *Nucl. Phys. Proc. Suppl.* **116** (2003) 412–416, `hep-ph/0211210`.

[26] V. A. Smirnov, "Evaluating multiloop Feynman integrals by Mellin-Barnes representation," *Nucl. Phys. Proc. Suppl.* **135** (2004) 252–256, `hep-ph/0406052`.

[27] P. P. Kulish and L. D. Faddeev, "Asymptotic conditions and infrared divergences in quantum electrodynamics," *Theor. Math. Phys.* **4** (1970) 745.

[28] J. D. Dollard, "Asymptotic Convergence and the Coulomb Interaction," *J. Math. Phys.* **5** (1964) 729–738.

[29] R. Horan, M. Lavelle, and D. McMullan, "Asymptotic dynamics in quantum field theory," *J. Math. Phys.* **41** (2000) 4437–4451, `hep-th/9909044`.

[30] V. Chung, "Infrared Divergence in Quantum Electrodynamics," *Phys. Rev.* **140** (1965) B1110.

[31] T. W. B. Kibble, "Coherent soft-photon states and infrared divergences. i. Classical Currents," *J. Math. Phys.* **9** (1968) 315–324.

BIBLIOGRAPHY

[32] V. Del Duca, L. Magnea, and G. Sterman, "Collinear infrared factorisation and asymptotic evolution," *Nucl. Phys.* **B324** (1989) 391.

[33] M. Greco, F. Palumbo, G. Pancheri-Srivastava, and Y. Srivastava, "Coherent state approach to the infrared behavior of nonabelian gauge theories," *Phys. Lett.* **B77** (1978) 282.

[34] D. R. Butler and C. A. Nelson, "Nonabelian structure of Yang-Mills theory and infrared finite asymptotic states," *Phys. Rev.* **D18** (1978) 1196.

[35] C. A. Nelson, "Origin of cancellation of infrared divergences in coherent state approach: forward process q q → q q gluon," *Nucl. Phys.* **B181** (1981) 141.

[36] C. A. Nelson, "Avoidance of counter example to nonabelian Bloch-Nordsieck conjecture by using coherent state approach," *Nucl. Phys.* **B186** (1981) 187.

[37] M. Ciafaloni, "The QCD coherent state from asymptotic dynamics," *Phys. Lett.* **B150** (1985) 379.

[38] S. Catani, M. Ciafaloni, and G. Marchesini, "Asymptotic coherent states and color screening," *Phys. Lett.* **B168** (1986) 284.

[39] S. Catani, M. Ciafaloni, and G. Marchesini, "Noncancelling infrared divergences in QCD coherent state," *Nucl. Phys.* **B264** (1986) 588–620.

[40] S. Catani and M. Ciafaloni, "Generalized coherent state for soft gluon emission," *Nucl. Phys.* **B249** (1985) 301.

[41] D. Zwanziger, "Reduction formulas for charged particles and coherent states in quantum electrodynamics," *Phys. Rev.* **D7** (1973) 1082–1099.

[42] H. F. Contopanagos and M. B. Einhorn, "Theory of the asymptotic S matrix for massless particles," *Phys. Rev.* **D45** (1992) 1291–1321.

BIBLIOGRAPHY

[43] L. V. Prokhorov, "Infrared and collinear divergences in gauge theories," *Phys. Usp.* **42** (1999) 1099–1120.

[44] M. Lavelle and D. McMullan, "Constituent quarks from QCD," *Phys. Rept.* **279** (1997) 1–65, `hep-ph/9509344`.

[45] E. Bagan, M. Lavelle, and D. McMullan, "Charges from dressed matter: Physics and renormalisation," *Annals Phys.* **282** (2000) 503–540, `hep-ph/9909262`.

[46] D. A. Forde and A. Signer, "Infrared-finite amplitudes for massless gauge theories," *Nucl. Phys.* **B684** (2004) 125–161, `hep-ph/0311059`.

[47] J. Frenkel, J. G. M. Gatheral, and J. C. Taylor, "Asymptotic states and infrared divergences in nonabelian theories," *Nucl. Phys.* **B194** (1982) 172.

[48] D. Forde, *Infrared Finite Amplitudes*. PhD thesis, University of Durham, August, 2004.

[49] M. Morley-Fletcher, *Covariant Infrared Finite Amplitudes*. PhD thesis, University of Durham, November, 2005.

[50] T. Muta, *Foundations of Quantum Chromodynamics*. World Scientific, 2000.

[51] G. Sterman, *An Introduction to Quantum Field Theory*. CUP, 1993.

[52] R. K. Ellis, W. J. Stirling, and B. R. Webber, *QCD and Collider Physics*. CUP, 1996.

[53] T. Binoth and G. Heinrich, "Numerical evaluation of multi-loop integrals by sector decomposition," *Nucl. Phys.* **B680** (2004) 375–388, `hep-ph/0305234`.

[54] O. V. Tarasov, "Connection between Feynman integrals having different values of the space-time dimension," *Phys. Rev.* **D54** (1996) 6479–6490, `hep-th/9606018`.

BIBLIOGRAPHY

[55] G. Passarino and M. J. G. Veltman, "One loop corrections for e+ e-annihilation to mu+ mu- in the Weinberg model," *Nucl. Phys.* **B160** (1979) 151.

[56] S. Weinzierl, "The art of computing loop integrals," `hep-ph/0604068`.

[57] A. I. Davydychev, "A Simple formula for reducing Feynman diagrams to scalar integrals," *Phys. Lett.* **B263** (1991) 107–111.

[58] J. Fleischer, F. Jegerlehner, and O. V. Tarasov, "Algebraic reduction of one-loop Feynman graph amplitudes," *Nucl. Phys.* **B566** (2000) 423–440, `hep-ph/9907327`.

[59] C. Anastasiou and K. Melnikov, "Higgs boson production at hadron colliders in NNLO QCD," *Nucl. Phys.* **B646** (2002) 220–256, `hep-ph/0207004`.

[60] K. G. Chetyrkin and F. V. Tkachov, "Integration by parts: The algorithm to calculate the Beta functions in 4 loops," *Nucl. Phys.* **B192** (1981) 159–204.

[61] T. Gehrmann and E. Remiddi, "Differential equations for two-loop four-point functions," *Nucl. Phys.* **B580** (2000) 485–518, `hep-ph/9912329`.

[62] S. Laporta, "High-precision calculation of multi-loop Feynman integrals by difference equations," *Int. J. Mod. Phys.* **A15** (2000) 5087–5159, `hep-ph/0102033`.

[63] R. Mertig and R. Scharf, "TARCER: A mathematica program for the reduction of two-loop propagator integrals," *Comput. Phys. Commun.* **111** (1998) 265–273, `hep-ph/9801383`.

[64] J. Kublbeck, H. Eck, and R. Mertig, "Computeralgebraic generation and calculation of Feynman graphs using FeynArts and FeynCalc," *Nucl. Phys. Proc. Suppl.* **29A** (1992) 204–208.

[65] G. 't Hooft and M. J. G. Veltman, "Diagrammar,". In *Louvain 1973, Particle Interactions At Very High Energies, Part B*, New York 1973, 177-322 and CERN Geneva - CERN 73-9 (73,REC.OCT) 114p.

[66] G. 't Hooft and M. J. G. Veltman, "Scalar one loop integrals," *Nucl. Phys.* **B153** (1979) 365–401.

[67] E. E. Boos and A. I. Davydychev, "A Method of evaluating massive Feynman integrals," *Theor. Math. Phys.* **89** (1991) 1052–1063.

[68] V. A. Smirnov, "Analytical result for dimensionally regularized massless on-shell double box," *Phys. Lett.* **B460** (1999) 397–404, `hep-ph/9905323`.

[69] J. B. Tausk, "Non-planar massless two-loop Feynman diagrams with four on- shell legs," *Phys. Lett.* **B469** (1999) 225–234, `hep-ph/9909506`.

[70] J. Fleischer, A. V. Kotikov, and O. L. Veretin, "Analytic two-loop results for selfenergy- and vertex-type diagrams with one non-zero mass," *Nucl. Phys.* **B547** (1999) 343–374, `hep-ph/9808242`.

[71] S. Moch, P. Uwer, and S. Weinzierl, "Nested sums, expansion of transcendental functions and multi-scale multi-loop integrals," *J. Math. Phys.* **43** (2002) 3363–3386, `hep-ph/0110083`.

[72] G. Sterman, "Mass divergences in annihilation processes. 1. Origin and nature of divergences in cut vacuum polarization diagrams," *Phys. Rev.* **D17** (1978) 2773.

[73] S. B. Libby and G. Sterman, "Mass divergences in two particle inelastic scattering," *Phys. Rev.* **D18** (1978) 4737.

[74] Z. Nagy and D. E. Soper, "General subtraction method for numerical calculation of one-loop QCD matrix elements," *JHEP* **09** (2003) 055, `hep-ph/0308127`.

[75] R. E. Cutkosky, "Singularities and discontinuities of Feynman amplitudes," *J. Math. Phys.* **1** (1960) 429–433.

[76] R. K. Ellis, D. A. Ross, and A. E. Terrano, "The perturbative calculation of jet structure in e+ e- annihilation," *Nucl. Phys.* **B178** (1981) 421.

[77] S. Weinzierl, "Introduction to Monte Carlo methods," `hep-ph/0006269`.

[78] R. Kleiss, W. J. Stirling, and S. D. Ellis, "A new Monte-Carlo treatment of multiparticle phase space at high-energies," *Comput. Phys. Commun.* **40** (1986) 359.

[79] G. P. Lepage, "VEGAS: An adaptive multidimensional integration program,". CLNS-80/447.

[80] M. Srednicki, *Notes on Quantum Field Theory.* UCSB, 1993.

[81] M. Y. Kalmykov, "Gauss hypergeometric function: Reduction, epsilon-expansion for integer / half-integer parameters and Feynman diagrams," *JHEP* **04** (2006) 056, `hep-th/0602028`.

[82] Z. Bern, L. J. Dixon, and D. A. Kosower, "One loop corrections to two quark three gluon amplitudes," *Nucl. Phys.* **B437** (1995) 259–304, `hep-ph/9409393`.

[83] E. Boos and T. Ohl, "Minimal gauge invariant classes of tree diagrams in gauge theories," *Phys. Rev. Lett.* **83** (1999) 480–483, `hep-ph/9903357`.

[84] D. E. Soper, "Choosing integration points for QCD calculations by numerical integration," *Phys. Rev.* **D64** (2001) 034018, `hep-ph/0103262`.

[85] T. Huber and D. Maitre, "HypExp, a Mathematica package for expanding hypergeometric functions around integer-valued parameters," *Comput. Phys. Commun.* **175** (2006) 122–144, `hep-ph/0507094`.

[86] T. Hahn, "CUBA: A library for multidimensional numerical integration," *Comput. Phys. Commun.* **168** (2005) 78–95, `hep-ph/0404043`.

[87] C. Anastasiou and A. Lazopoulos, "Automatic integral reduction for higher order perturbative calculations," *JHEP* **07** (2004) 046, `hep-ph/0404258`.